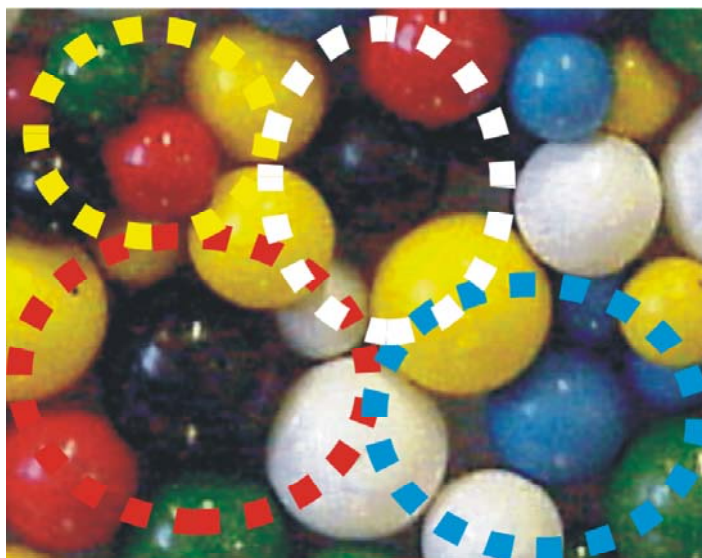


# **A New Combinatorial Approach to the Synthesis and Isolation of Ferromagnetic and Superconducting Oxides Materials**

Inauguraldissertation  
der Philosophisch-naturwissenschaftlichen Fakultät  
der Universität Bern



Presented by

**Muhammad Aslam Awan**

From Pakistan

Supervisor

Prof. Dr. Jürg Hulliger

Department of Chemistry and Biochemistry, University Berne, Switzerland.

**A New Combinatorial Approach to the Synthesis and Isolation of  
Ferromagnetic and Superconducting Oxides Materials**

Inauguraldissertation  
der Philosophisch-naturwissenschaftlichen Fakultät  
der Universität Bern

Presented by

**Muhammad Aslam Awan**

From Lahore (Pakistan)

Supervisor

Prof. Dr. Jürg Hulliger

Department of Chemistry and Biochemistry, University Berne, Switzerland

Accepted by the Philosophisch-naturwissenschaftlichen Fakultät

Berne, 2005

**The Dean  
Prof. Dr. P. Messerli**

بِسْمِ اللَّهِ الرَّحْمَنِ الرَّحِيمِ

*"In the name of Allah, the Gracious, the Merciful"*



**"God"**

*Is the Creator, the Maker, the Fashioner,*

*His Names are Most Beautiful.*

*All that is in the Heavens and the Earth Glorifies Him*

*He is the Mighty, the Wise.*

*Thanks of "God" he is providing us life, health, mind & knowledge ...*

## Acknowledgments

It's my pleasure to avail the opportunity of challenging research project under the supervision of Prof. J. Hulliger as a new "combinatorial approach" that is a promising technique, which hopefully will progress in forward direction to synthesize new solid-state materials. Prof. J. Hulliger has been given me best scientific ideas and fruitful discussion. I give him credit of thanks with the hopes : Human life should take scientific advantages from scientific personality.

I am thankful to Prof. Dr. W. F. Maier (Chair for Chemical Engineering University of Saarland, Germany), as a co-examiner to give his valuable time to read my thesis. I am also thankful to Prof. Hans-Ulrich Güdel for the kindness of chairing of my defence and attentively reading of my thesis and his useful suggestions.

I am thankful to Dr. R. Kremer (group of Prof. Simon, MPI for solid-state research, Stuttgart) for scientific useful discussion about superconductivity and related measurements. Thanks to Dr. L. Kienle, B. Frey and Dr. K. Krämer for X-rays powder diffraction and microscopic analysis. I am also thankful to PD. Dr. T. Phillips for EPR (solid-state) analysis and related scientific discussion. Thanks to Prof. S. Decourtins for the use of SQUID equipment. Thanks to G. Annina to work with us (diploma student in 2001) on combinatorial approach by considering superconducting materials.

I am thankful to B. Trusch for technical assistance; U. Kindler and G. Baumann for magnetic separators construction, and thanks to R. Schraner, K. Escher to solve the electric problems, i.e. cryostat, magnetic separators etc.

I am very thankful to Dr. R. Mariaca, Dr. T. Wüst, Dr. R. Nusrat and of my brother Dr. M. Azhar Awan for giving me useful suggestions. Thanks to T. A. Samtleben for a literature survey and other colleagues in the group of Prof. J. Hulliger for useful discussions during group seminars as well as providing a pleasant friendship atmosphere of collaboration. I am also thankful to all my teachers educating me up to now.

I am deeply thankful to all those remember me in "prays", especially thanks to my Khaliph, my mother, my father, my sisters and brothers and my wife and our children. Thanks to my little smiling daughter who always waits for me during lunch and dinner to

play and provides me fresh bright mind, and thanks to my friends specially J. Iqbal, M. Zarulla, R. Reddy, M. Syed and all others those I forget.

At the end, I would like to thanks to Department of Chemistry and Biochemistry, University of Berne, for providing me all research facilities related to this work and Portland Cements for chemical financial supports as well as “Government of Switzerland” (BFF, Kanton Bern department of Immigration) for providing me permission of stay etc.

## Contents

	Page No.
<b>Summary</b>	1
<b>1. Combinatorial Chemistry</b>	2
1.1. Introduction	2
1.2. Solution Phase Combinatorial Synthesis	3
1.3. Solid Phase Combinatorial Synthesis	4
1.4. Combinatorial Synthesis for Solid-State Materials	5
1.5. References	9
<b>2. Challenges and the “Single-Sample Concept” (SSC) :</b>	
<b>A New Combinatorial Approach to Synthesize Solid-State Materials</b>	11
2.1. Introduction	11
2.2. Combinatorial Synthesis for Ferromagnetic Oxides	17
2.3. Magnetic Isolation of Product Phases	19
2.3.1. Magnetic Column Separator	20
2.3.2. Magnetic Horizontal Separator	22
2.4. Property Search through EDX Analysis	23
2.5. References	31
<b>3. A “Single Sample Concept” (SSC) : New Approach to Combinatorial Chemistry of Inorganic Material</b>	32
J. Hulliger, M. A. Awan, <i>Chem. Eur. J.</i> 2004, 10, 4694 - 4702.	
3.1. Abstract	32
3.2. Introduction	33
3.3. Results and Discussion	38
3.3.1. Isolation of Product Phases by Magnetic Separation	38
3.3.2. Results for Magnetic Oxides	42
3.4. Conclusions	53
3.5. Acknowledgments	54
3.6. References	55

<b>4. “Single Sample Concept” (SSC) : Theoretical Model for a New Combinatorial Approach to Solid-State Inorganic Materials</b>	<b>58</b>
J. Hulliger, M. A. Awan, <i>J. Comb. Chem.</i> <b>2005</b> , 7, 73 - 77.	
4.1. Abstract	58
4.2. Introduction	58
4.3. The SSC : Assumptions and Basic Ideas	61
4.4. Combinatorial Model	62
4.5. Conclusions	68
4.6. Nomenclature	69
4.7. Acknowledgements	69
4.8. References	70
<b>5. Chemical Diversity in View of Property Generation by a New Combinatorial Approach</b>	<b>72</b>
J. Hulliger, M.A. Awan, B. Trusch , T. A. Samtleben, <i>Z. Anorg. Allg. Chem.</i> <b>2005</b> , 631, 1255 - 1260.	
5.1. Abstract	72
5.2. Introduction	73
5.3. Basics of the Single Sample Concept (SSC)	78
5.4. Magnetic Chromatography for Extracting Magnetic Phases	81
5.5. Search for Fe-based Ferromagnetic Oxides	82
5.6. Conclusions	84
5.7. Acknowledgements	84
5.8. References	85
<b>6. Magnetic Chromatography and Ceramic Synthesis : A new Combinatorial Approach for Finding Ferri-/Ferromagnetic Materials</b>	<b>86</b>
J. Hulliger, M. A. Awan, B. Trusch, <i>Z. Anorg. Allg. Chem.</i> <b>2004</b> , 630, 1689.	
6.1. References	88
<b>7. An Itinerary Report to the Synthesis of New Mg-Co and Zn-Co-oxide Ferromagnetic Materials</b>	<b>89</b>
7.1. Introduction	89
7.2. Combinatorial Synthesis for New Ferromagnetic Cobalt Oxides	89
7.3. Ferromagnetism in the System of Zn/Co Oxides	92

7.4. Ferromagnetism in the System of Mg/Co Oxides	95
7.5. References	99
<b>8. A First Attempt to Obtain Superconductivity by the SSC</b>	<b>100</b>
8.1. Introduction	100
8.2. Diamagnetism of Ceramic Materials	101
8.3. Superconducting Critical Behavior	102
8.3.1. Critical Parameters for Superconductivity	103
8.4. Four-Probe Technique for Electrical Resistance Measurements	105
8.5. Cryostat (Leybold : RGS 20) : Instrumentation	106
8.6. Combinatorial Synthesis for Oxide Superconductive Materials	110
8.7. Results and Discussion	111
8.7.1. Four-probe Electrical Resistance and SQUID Measurements	111
8.7.2. EPR Measurements through Low Field Microwave Absorption	118
8.8. Conclusions	123
8.9. References	124
<b>9. Resume</b>	<b>125</b>



## Summary

Combinatorial approaches have been applied (from biochemistry to organic, organometallic, inorganic and polymer chemistry) in order to facilitate the discovery and optimization of compounds with novel or enhanced materials properties. Recently, these approaches have applied to solid-state synthesis, i.e. the task for preparing and testing libraries of products. Parallel 2D combinatorial approaches have been established for more than 25'000 pixels representing starting compositions. However, these resulting libraries are still small as compared to chemical diversity of compositions resulting from elements of the periodic table.

This work describes a new combinatorial approach as a *single sample concept* (SSC). It provides chemical diversity by starting of with about  $10^{12}$  of grains of a size  $\sim 1 \mu\text{m}$  in a sample of  $1 \text{ cm}^3$ , using up to  $N \leq 61$  components of metal oxides ( $M_xO_y$ ). Theoretical calculations showed that within a single sample, the number of local configurations is reasonably exceeding the number of possible phase formations. The SSC is particularly of interest for property-oriented syntheses of ferri-/ferromagnetic or superconducting compounds.

Magnetic chromatography separation (MCS) is introduced in materials chemistry by the development of vertical column and horizontal magnetic separators. Magnetic separators are useful to isolate ferromagnetic oxides from a suspension.

The present application of the SSC bears evidence for ferromagnetic materials in the system of Fe-La, Fe-La-W-Zr, Co-Mg, Co-Zn oxides, and also for new superconducting materials with an onset  $T_c \sim 100 \text{ K}$  and nominal starting compositions of about  $0.12\text{Y}_2\text{O}_3$ ,  $0.33\text{B}_2\text{O}_3$ ,  $0.10\text{PbCO}_3$ ,  $0.50\text{Tl}_2\text{O}_3$ ,  $2\text{BaO}_2$ ,  $1.36\text{CaCO}_3$ ,  $4\text{CuO}$  and  $0.125\text{Y}_2\text{O}_3$ ,  $\text{BaO}_2$ ,  $0.25\text{PbCO}_3$ ,  $1.81\text{SrCO}_3$ ,  $1.36\text{CaCO}_3$ ,  $0.125\text{Tl}_2\text{O}_3$ ,  $0.175\text{La}_2\text{O}_3$ ,  $\text{Bi}_2\text{O}_3$ ,  $5\text{CuO}$  (other compositions also yielding superconductivity). The electron spin resonance spectroscopy, four-probe electrical resistance measurements and the SQUID technique were used for demonstrating the existence of superconductivity.

# 1. Combinatorial Chemistry

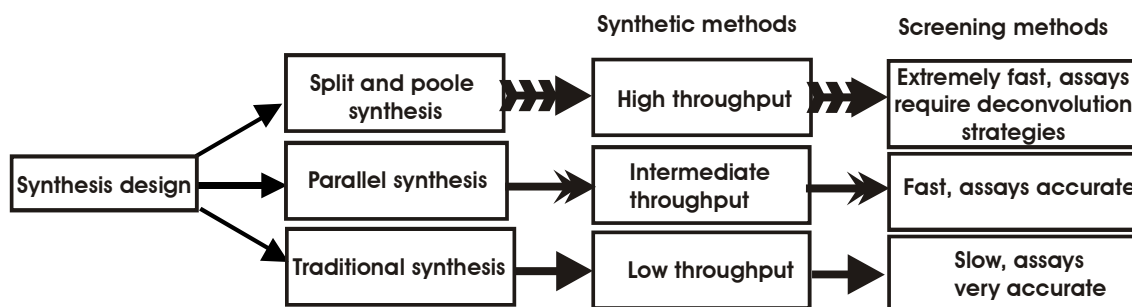
## 1.1. Introduction

Combinatorial chemistry plays an integral role in today's chemical endeavor, as chemistry has become increasingly interdisciplinary. Fundamental scientific problems focus on the chemical nature of matter. The term “combinatorial” refers to a large-scale trial and error technique. Combinatorial concepts took hold by which a collection of molecules is targeted, simultaneously producing a library of compounds instead of a single product. May be *nature* has been utilizing the same principles since the beginning while molecular biologists, biochemists, and materials chemists have recently, learned how to harness combinatorial power for a number of different uses. By increasing the demand of new materials i.e. ferromagnetic/ferroelectric, catalysts, luminescent, high temperature superconductors, we are challenged to most efficient syntheses. <sup>[1]</sup> Conventional syntheses provide a slow throughput in considering “one-at-a-time” or serial manner to synthesize and characterize new materials. The “combinatorial chemistry” or “high throughput screening” (HTS), <sup>[1 - 3]</sup> opening a new research technology, has found wide spread applications from last few years and having an ongoing growth.

Commonly three different combinatorial approaches (i.e. traditional/conventional, parallel, and poole syntheses) are applied to the task for preparing and testing libraries of products by considering biochemistry and organic chemistry. A simple way to represent combinatorial strategies <sup>[4]</sup> is shown in scheme 1. Combinatorial methods are involved mainly in “*split and poole*” synthesis of compounds but often show lack of control over the purity level, while parallel synthesis represent an intermediate inbetween traditional/conventional and poole synthesis in a spatially addressable format with usually one compound per region, coupled to automated screens.

By applying combinatorial approaches, the *possibility* can be enhanced to synthesize a large number of compounds having a specific physical or chemical property. Combinatorial synthesis (considering biochemistry and organic chemistry) can be performed either in solution phase <sup>[5]</sup> or on solid supports. <sup>[5]</sup> Solid-state combinatorial

methods have been recently applied to inorganic, organometallic and polymer chemistry as described in section 1.4.



**Scheme 1.** Conventional, parallel and pooled combinatorial approaches to synthesized and screening of materials <sup>[5]</sup>.

## 1.2. Solution Phase Combinatorial Synthesis

Because of a main problem, to bring reactions to completion, more than one equivalent of reagent is frequently necessary. However, the use of excess reagent is only feasible if it can be removed at the end of a reaction. In normal solution phase chemistry devastating occurs by purification steps. Difunctional compounds, such as diamines, diacids react selectively in a monofunctional manner with only one or two groups resulting in a highly effective desummerization. The spatial separation of functional groups also renders the macrocyclization reaction a comparatively effective process. Solution phase chemistry often affords statistical mixtures of products under these conditions. <sup>[5]</sup>

In solution phase synthesis purification and isolation procedures were improved within the last few years. Nowadays, overcoming main problems in solution phase reactions such as removal of reagents may be possible by using scavenger resins, fluoruous-tags, polymer-support reagents, etc. (for further details, see Ref. [6]). In the beginning, solution phase reactions were not considered to be suitable for the preparation of large-scale libraries but presently, this approach showed to be a useful method, especially in biochemistry and organic chemistry. To synthesize multiple compounds: “Libraries” <sup>[7 - 9]</sup> of 1000 to 1’000’000 distinct components are routinely created and tested for biological activity.

### 1.3. Solid Phase Combinatorial Synthesis

Solid phase combinatorial chemistry relies on the fact that the molecule under construction is attached to a linker<sup>[10]</sup> making part of a polymeric carrier (bead). Linkers and their associated synthesis strategies play a pivotal role in the successful implementation of solid phase organic synthesis and its application to combinatorial chemistry.<sup>[11]</sup> The attachment of molecules to a particular resin<sup>[12]</sup> is strongly dependent on the nature of the linker. A starting material is attached reversibly to the linker, that makes direct bonding or through a spacer<sup>[13]</sup> (e.g. polyethylene glycol chain) with a resin.<sup>[14]</sup> Long chain spacers are more feasible for a clear distinction between linker and spacer, particularly for characterization after cleavage. The linker is the minimal part of the resin required for the functional cleavage. Thus, a spacer is the part between the linker and the resin. The group attached to the solid support is generally unchanged upon cleavage; the anchoring bond (e.g. *MeO*-polyethylene glycol) to the compound is sensitive to certain conditions, which then lead to bond cleavage and a release of a final compound. Normally, linkers were designed to release one functional group and act more or less bulky protecting groups. In some cases, a simple and rapid mixing of reagents is sufficient to derive the attachment to completion while in other cases tedious monitoring is necessary. Also, in some cases, the attachment proceeds under similar conditions as the detachment e.g. in the formation of ketals excess reagents used for completion the reaction. The polymer carrier (bead) and linker should be stable under the reaction conditions.<sup>[5]</sup> The reaction should be carried out in an excess reagent, which can simply removed by filtration. Due to its simplicity, this process can easily be automated and run in parallel for libraries of size about 1000 compounds.

The *split and combine* combinatorial technique has been commonly used for solid phase synthesis where polymer compounds split into separate vessels and each is treated with a different reagent and then recombined into a common pool.<sup>[5, 15]</sup> Repetition of this process yields a mixture of  $M^R$  compounds, where  $M$  is the number of separate vessel at each step and  $R$  is the number of steps. This has also been used in catalytic research where catalyst was a single organic species instead of an enzyme.<sup>[16]</sup>

## 1.4. Combinatorial Approaches to Synthesize Solid-State Materials

J. J. Hanak has introduced the “*Multiple-Sample Concept*” (MSC) <sup>[17]</sup> (1970) in material research to synthesize multi-component systems by single steps. Implementation of this concept <sup>[17]</sup> has been possible through the development of one-cathode multiple targets, radio frequency co-sputtering synthesis and a method of compositional analysis of co-sputtered film, based on film thickness measurement. The precursor compositions have been optimized by continuously varying its stoichiometry. Hanak uncovered a variety of new classes of compounds including superconductors, luminescences, magnetic recording, amorphous silicon semiconductors and catalyst materials etc. Although, using this route, he was able to find new materials much faster than by using a conventional route. For the search of high temperature superconductors, unlike Hanak approach, <sup>[17]</sup> the precursors are deposited on the substrate subsequently rather than simultaneously. Each section of substrate is exposed for different combinations of precursors by depositing each layer through a different mask. <sup>[18]</sup> The first library of 128-members (i.e. derived from BaCO<sub>3</sub>, Y<sub>2</sub>O<sub>3</sub>, Bi<sub>2</sub>O<sub>3</sub>, CaO, SrCO<sub>3</sub>, PbO, CuO) was generated <sup>[18]</sup> to determine the compatibility of different families of copper oxide superconductors with a common processing condition. With the application of specific reaction conditions BiSrCaCuO<sub>x</sub> and YBa<sub>2</sub>Cu<sub>3</sub>O<sub>x</sub> etc. were identified among examples of known superconductors.

Ideally, one can identify a property screened in the library format, which may allow interesting material identification related to known standards. Materials of proper compositions are then synthesized by applying classical routes to characterize their structural and physical properties. Important information obtained from this process should enhance knowledge for subsequent experiments.

How are libraries designed and processed by considering solid-state materials? Here, I would like to emphasize a specific example of 2D combinatorial approach (i.e. physical masking scheme) to find blue photo-luminescent materials.

J. Wang et al. <sup>[19]</sup> have applied a 2D combinatorial method in combination with photolithography to generate compositionally diverse thin-films of a phosphor library

containing 1024 different compositions. Optimized compositions were identified with the use of gradient libraries, in which the stoichiometry of a material was varied continuously.

A parallel imaging system and scanning spectrophotometer was used to identify compounds of the class  $\text{Gd}_3\text{Ga}_5\text{O}_{12}/\text{SiO}_2$  featuring an interesting luminescence behavior. This process led to the identification of efficient blue photo-luminescent (PL) composite materials. The libraries consisted of pixel of  $650\ \mu\text{m}$  by  $650\ \mu\text{m}$ , spaced by  $100\ \mu\text{m}$ . The silicium oxide and bulk sample was thermally oxidized and deposited on a substrate ( $\text{LaAlO}_3$ ). Radio frequency (RF) sputtering and pulsed-laser deposition (PLD) were used for thin-film preparation. The quaternary *masking scheme* deposition was carried out by using a series of  $n$  different masks that successively subdivide the substrate into a series of nested quadrant patterns, as shown in Figure 1. Each mask was used up to four depositions and each time the mask was rotated by  $90^\circ$ . With  $n$  different masks, this process allowed to generate up to  $4n$  different compositions in just  $4n$  deposition steps. The  $r$ th ( $1 \leq r \leq n$ ) mask contained  $4^{r-1}$  window, where each window exposes one quarter of the area deposited using the proceeding ( $r - 1$ ) mask. Each window represents an array of  $4^{r-1}$  opening, which can provide or create an underlying contact mask directly on the substrate by a photolithography technique. Each section of the substrate was thus exposed to a different combination of precursors by depositing each layer through a different mask.

Thin film deposition methods are synthetically quite versatile and they have progressed to enable atomic layer epitaxy and offer the ability to construct artificial lattices and patterned films of a variety of materials. Dopants are usually sandwiched between layers of the host material to avoid evaporation and to assure proper inter-diffusion. Subsequently, thermal processing provides a library of materials, showing the physical properties, which can be screened either by a contact or non-contact probe. The number of compounds that can be simultaneously synthesized by this technique is limited by the spatial resolution of the masks and detectors and by the degree to which synthesis can be carried out on a micro-scale.

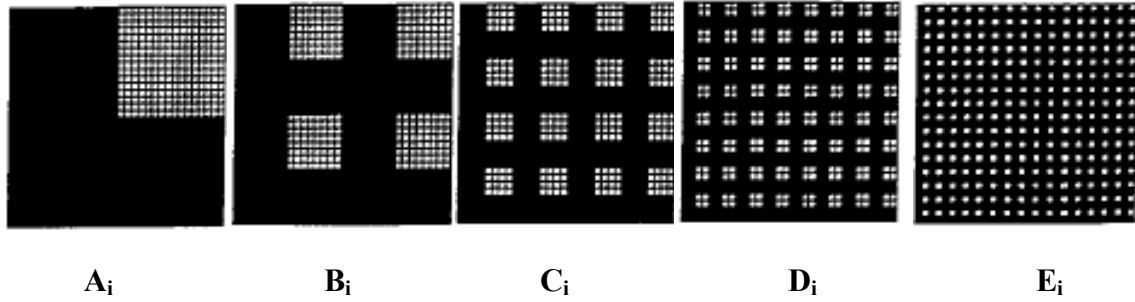


**Figure 1.** Quaternary library generates through masks, represents a deposition step with mask X rotated counter clockwise by  $(i - 1) \times 90^\circ$  [19].

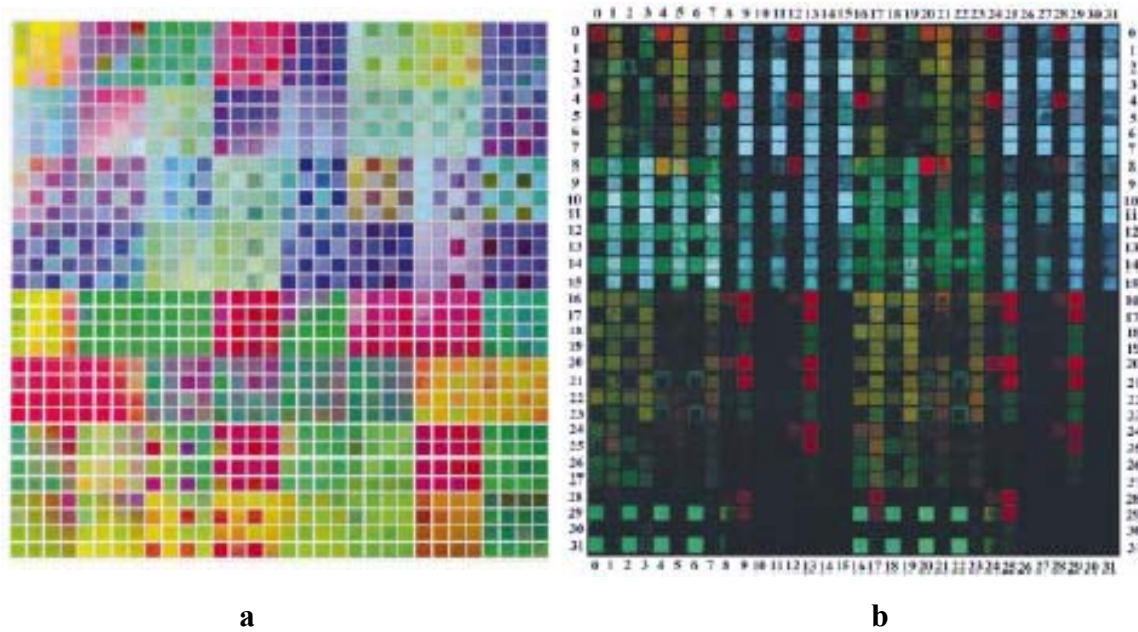


**Figure 2.** a) Photograph deposits as quaternary library under ambient light. The diversity of colors in the different pixels results from variations in film the thicknesses and the optical indices of refraction; b) Luminescent photograph of process quaternary library under irradiation [19].

$Zn_2MnSiO_4$  was included into the library as a reference material because it has silicon compatibility and efficient luminescent thin-films can be made quite reproducibly. A photograph of the library under ambient light is shown in Figure 2. The PL photograph of the library was taken under irradiation from the emission of an UV lamp ( $\sim 254\text{ nm}$ ).

For a quantitative analysis of the libraries, a scanning spectrometer was used to measure the excitation and emission spectra for individual luminescent pixels in the library. The emission and excitation spectra of about 100 selected bright blue, green and red photoluminescent pixels were collected. By incorporating a standard phosphor ( $\text{Zn}_2\text{MnSiO}_4$ ) in the library, one was able to obtain approximate relative photon outputs of each pixel. The high throughput 2D parallel screening technique was applied to the identification of other unusual luminescent materials such as  $\text{Sr}_2\text{CeO}_4$ ; <sup>[21]</sup>  $(\text{Gd}_{1.54}\text{Zn}_{0.46})\text{O}_{3-x} : \text{Eu}^{3+}_{0.06}$ ,  $\text{Gd}(\text{La}, \text{Sr})\text{AlO}_3$ . <sup>[21, 22]</sup>

Recently, <sup>[23]</sup> more than 25'000 compositions on libraries were prepared by applying of physical masking scheme and physical vapor deposition (PVD). For the generation of libraries, some problems are facing the effect of thermal processing conditions and deposition conditions. This involves the ability to simultaneously or serially generate identical libraries and process them under a variety conditions. Thermally induced gradient ovens are being used to workout processing conditions for libraries of metal oxides.

Combinatorial methods are likely to have a significant impact on catalysis, which play an increasingly important role in the chemical production and oil industries etc. Maier et al. <sup>[24 - 26]</sup> have described the discovery of new catalysts compositions such as  $\text{Mo}_{10}\text{V}_{10}\text{Sb}_{80}\text{O}_x$ ,  $\text{Hf}_3\text{Y}_3\text{Ti}_{94}\text{O}_x$ ,  $\text{Mn}_{6.7}\text{Co}_{93.3}$ ,  $\text{AlMn}_{6.7}\text{Co}_{92.3}$ , etc. by considering combinatorial methods.

In the light of above, one can conclude that combinatorial chemistry has demonstrated to be a fast route to the discovery of many new materials. However, the present methods are still far away to provide chemical diversity of the periodic table of elements as described in chapter 2.



## 1.5. References

- [1] W. F. Maier, *Angew. Chem. Int. Ed.* **1999**, *38*, 1216 - 1218.
- [2] W. F. Maier, G. Kirsten, M. Orschel, P.-A. Weiss, A. Holzwarth, J. Klein, *Comb. Chem. Mater. Polym. Catal. ACS. Symp. Ser.* **2002**, *814*, 1 - 21.
- [3] B. Jandeleit, D. J. Schaefer, T. S. Powers, H. W. Turner, W. H. Weinberg, *Angew. Chem. Int. Ed.* **1999**, *38*, 2494 - 2532.
- [4] B. Archibald, O. Brümmer, M. Devenney, D. M. Giaquinta, B. Jandeleit, W. H. Weinberg, T. Weskamp in *Handb. Combinatorial Chemistry*, (Eds. : K. Nicolaou, R. Handko, W. Hartwig), Wiley-VCH, Weinheim, **2002**, *II*, pp. 1018 - 1019.
- [5] a) S. Brase, S. Dahmen in *Handb. Combinatorial Chemistry*, (Eds. : K. Nicolaou, R. Handko, W. Hartwig), Wiley-VCH, Weinheim, **2002**, *I*, pp. 10 - 15; b) D. L. Coffen, J. E. A. Luithle in *Handb. Combinatorial Chemistry*, (Eds. : K.C. Nicolaou, R. Handko, W. Hartwig), Wiley-VCH, Weinheim, **2002**, *I*, pp. 60 - 61.
- [6] J. N. Cawse, *Acc. Chem. Res.* **2001**, *34*, 213 - 329.
- [7] B. A. Bunin, M. J. Plunkett, J. A. Ellman, *Proc. Natl. Acad. Sci. USA*, **1994**, *91*, 4708 - 4712.
- [8] L. A. Thompson, J. A. Ellman, *Chem. Rev.* **1996**, *96*, 550 - 600.
- [9] A. Nisonoff, J. E. Hopper, S. B. Spring, *The Antibody molecule*, Academic Press, New York, **1975**.
- [10] I. W. James, *Tetrahedron* **1999**, *55*, 4855 - 4946.
- [11] B. Carboni, F. Carreaux, J. F. Pilard, *Actual. Chimique* **2000**, 9 - 13.
- [12] P. H. H. Hermkens, H. C. J. Ottenheijm, D. Rees, *Tetrahedron* **1996**, *52*, 4527 - 4554.
- [13] C. T. Bui, F. A. Rasoul, F. Ercole, Y. Pam, N. J. Maeli, *Tetraheron Lett.* **1998**, *39*, 9279 - 9282
- [14] W. Rapp, in *Combinatorial Peptide and Nonpeptide Libraries*, Handb. Jung, G. (ed.), VCH, Weinheim, **1996**, 425 - 464.
- [15] A. Furka, F. Sebestyen, M. Asgedom, G. Dibo, *Proceeding of the 14th International Congress of Biochemistry*, Prague, Czechoslovakia, VSP, Utrecht, Netherlands, **1988**, *13*, 47.

- [16] R. H. Crabtree, *Chem. Commun.* **1999**, *17*, 1611 - 1616.
- [17] J. J. Hanak, *J. Mater. Sci.* **1970**, *5*, 964 - 971.
- [18] X. -D. Xiang, X. Sun, G. Briceno, Y. Lou, K. -A. Wang, H. Chang, W. G. W. - Freedman, S. -W. Chen, P. G. Schultz, *Science*, **1995**, *268*, 1738 - 1740.
- [19] J. Wang, Y. Yoo, C. Gao, I. Takeuchi, X. Sun, Wang, H. Chang, X. -D. Xiang, P. G. Schultz, *Science*, **1998**, *279*, 1712 - 1714.
- [20] E. Danielson, M. Derenney, D. M. Giaquinta, J. H. Golden, R. C. Hanshalter, E. W. McFarland, D. M. Poojary, C. M. Reaves, W. H. Weinberg, X. D. Wu. *Science* **1998**, *279*, 837 - 839.
- [21] X. -D. Sun, X.-D. Xiang, *Appl. Phys. Lett.* **1998**, *72*, 525 - 527.
- [22] E. D. Isaacs, M. Marcus, G. Aeppli, X. -D. Xiang, X. -D. Sun, P. Schultz, H. -K. Kao, G. S. Cargill III, R. Haushalter, *Appl. Phys. Lett.* **1998**, *73*, 1820 - 1822.
- [23] E. Danielson, J.H. Golden, E. W. McFarland, C. M. Reaves, W. H. Weinberg, X. D. Wu, *Nature*, **1997**, *9*, 1046 - 1049.
- [24] J. S. Paul, P. A. Jacobs, P.-A. Weiss, W. F. Maier, *Appl. Catal. A : General*, **2004**, *265*, 185 - 193.
- [25] J. Urschey, A. Kühnle, W. F. Maier, *Appl. Catal. A : General*, **2003**, *252*, 91 - 106.
- [26] J. W. Saalfrank, W. F. Maier, *Angew. Chem. Int. Ed.* **2004**, *43*, 2028 - 2031.

## 2. Challenges and the “Single-Sample Concept” (SSC) : A New Combinatorial Approach to Synthesize Solid- State Materials

### 2.1. Introduction

Our understanding of structure-property relations for solid-state materials has been developed during the last decades, including the ability to predict solid-states material properties. Although, there are cases for which predication is successful, current material science still works by using trial and error methods, especially for functional materials featuring complex properties such as superconductivity.

For elemental combinations, let us consider elements of the periodic table, which show that there are astronomical chemical combinations for varying the chemical stoichiometries between these elements. Bohacek et al. have estimated that there are  $10^{63}$  stable structures only for C, O, N, S and H. <sup>[1]</sup> Among this large number of molecular compounds there are about 1 % which form extended solid structures. <sup>[2]</sup>

Similarly, there are numerous stoichiometric combinations for finding inorganic *binary*, *ternary*, *quaternary*, *quinary* structural compounds. In *binary* systems there are more than 90 %  $M_mX_y$  compounds showing stoichiometries such as MX,  $MX_2$ ,  $MX_3$ , and  $M_3X_5$ . Additionally, there are varieties of structural types especially for intermetallic compounds such as  $Ni_5Zr$ ,  $Ni_7Zr_2$ ,  $Ni_3Zr$ ,  $Ni_{21}Zr_8$ ,  $Ni_{11}Zr_9$ ,  $Ni_{11}Zr_7$ ,  $NiZr_2$ . <sup>[3]</sup> Notably, for ternary, quaternary or for higher order systems, the structural variety is more likely as compared to binary compounds. Mathematically, one can calculate the number of elemental combinations by using Equation 1. see the data in Table 1.

$$\binom{N}{n} = \frac{N!}{n!(N-n)!} \quad (1)$$

Here,  $N$  is the total number of elements in the system and  $n$  is the number of elements used for formation of compounds of the type  $E_{x1}(1) E_{x2}(2) \dots E_{xn}(n)$ . From a formal point of view, stoichiometric coefficients may be continuously varied in compounds giving thus nearly an infinite fold of compositions.

**Table 1.** Combinations for a number of elements  $n$  selected out of e.g. 61 non-radioactive elements.

Selection of $n$ number of elements	Elemental combinations
2	1830
3	$3.5 \times 10^4$
4	$5.2 \times 10^5$
5	$5.9 \times 10^6$
6	$5.5 \times 10^7$

From Table 1, it is clear that the number of elemental combinations increases exponentially within a system. In order to form and characterize these phases, an extremely high number of compounds are to be considered, which seems to be impossible. It is a fundamental issue as well as an open question, whether chemistry would allow crystal structures built up by so many elements. On the bases of the literature data of oxide compounds we can say that the number of compounds decreases by increasing the number of elements in a single compound.

Let us take a specific example of a three metal oxide components (c) in a system such as the high temperature superconductor  $\text{YBa}_2\text{Cu}_3\text{O}_{7-x}$ , and investigate how many samples are required to be synthesized and tested to definitely include this compound in the output of a high-throughput method. Now, let us design a system which has a feasibility of experimental conditions for *ten* reaction pathways, *ten* variable pressures, *ten* variable temperatures, and including *ten* machines available for high throughput exploration, the

number of compositions for  $c$  components is  $I^c$  ( $I$  is obtained by assumption : every element  $A$  in a system contributes  $i_A$  ( $i_A = 1, \dots, I$ ) atoms to a formula unit.), i.e.  $10^3$  (where 10 is the number of reaction pathways and 3 being the number of components under consideration). Consequently, it is required to prepare  $3.6 \times 10^{11}$  samples (calculated by using Equation 2).<sup>[4]</sup>

$$\sum_{c=0}^{N=61} \binom{61}{c} I^c = (I+1)^{61} \cdot c_R \cdot c_T \cdot c_P \cdot c_M \quad (2)$$

Here,  $c$  is the number of components taking into experimental consideration,  $N$  is the total number of elements for selecting compositions, i.e. 61,  $I$  is described as above,  $c_R$  is the number of reaction pathways,  $c_P$  is the number of variable pressures  $P$ ,  $c_T$  is the number of variable temperatures  $T$ ,  $c_M$  is the number of machines available for high throughput exploration.<sup>[4]</sup>

From above mathematical estimations and possible elemental combinations within a *three* components system, if one would be able to prepare  $10^5$  compounds per day by using combinatorial high-throughput methods then, one might need 9863 years to provide chemical diversity for about  $10^{11}$  samples.<sup>[4]</sup>

There are a few methods<sup>[5]</sup> for syntheses which have been developed in inorganic chemistry, e.g. solid-state oxidations/reductions, catalytic polymerizations, mixing/milling, heating of defined solid-state mixtures and combinatorial methods of sequential deposition for thin films, etc. In solid-state syntheses, reactions are principally based upon the solid-state diffusion of the reactant and the nucleation of the product. By considering most recent knowledge about solid-state methods and combinatorial approaches for solid-state syntheses, it implies that these solid-state methods and syntheses are not sufficient to investigate the chemical diversity among the large number of elemental combinations. There is also not a viable concept in the combinatorial synthesis that is able to generate  $10^{11}$  number of new solid-state materials.

Let us consider solid-state mineralogical materials and chemical databases of oxides<sup>[6 a]</sup> which rely on the fact that the number of known oxide compounds strongly decreases

with respect to the number of elements per compound, i.e.  $q > 4$ , where  $q$  is the number of constitutional metallic/semi-metallic elements in oxide compounds to be formed. Today's science takes advantage for property generation such as ferromagnetism, ferroelectricity, diamagnetism, luminescence, semi-conductivity and superconductivity that could be possible for  $q$ , i.e. 1 – 4. In respect to the generation of these properties we may assume that progress should be possible by exploring the phase space limited to  $q \leq 6$ . These oxide compounds (ferromagnetic, ferroelectric, diamagnetic, luminescent, silicate/non-silicate mineral) can be estimated from the literature data to exist for only  $q$ -number up to *six*, i.e.  $q \leq 6$ .

The absence of high- $q$  compounds are most likely not stable against decomposition into structures representing for  $q < 6$ . Therefore, this allows us to conclude that properties generating compounds are those showing *six* or *less* metal oxides in a single compound, i.e.  $q \leq 6$ . It may be possible that high- $q$  compounds occur as transient products, and at our present knowledge we may not be able to identify them within a system.

Moreover, on the bases of the literature data search for oxide compounds, one can observe that the number of phases ( $\eta$ ) per diagram decreases by increasing  $q$ , e.g. for  $q = 2$ ,  $\eta = 3$  and for  $q = 3$ ,  $\eta = 2$ , respectively.<sup>[6 b]</sup> This allows us to conclude that the upper limit of oxide compounds for  $q \leq 6$  is certainly lower than  $\eta = 10$ .

In the light of the above discussion, it is essential to explore possible means of improving the discovery rate for exploring the chemical diversity for solid-state materials. Let us consider now non-radioactive elements up to a number of  $N \leq 61$  for forming metal oxides/carbonates ( $M_xO_y$ ).

By taking into consideration realistic upper limitations, i.e.  $q = 6$ ,  $\eta_{max.} < 10$  and  $N \leq 61$  for oxides, we should provide chemical diversity to access  $N_{oxides} \approx 10^8$ , calculated by using Equation 3<sup>[6 c]</sup>

$$N_{oxides} \cong \sum_{q=2} \eta_q N_q^{PD} \quad (3)$$

Here,  $N_q^{PD}$  is the number of phase diagrams calculated from Equation (4) and  $q$  for *binary* system = 2, for *ternary* = 3, for *quaternary* = 4, etc.

$$N_q^{PD} = \frac{N!}{q!(N-q)!} \quad (4)$$

To provide chemical diversity for  $N_{oxides} \approx 10^8$ , i.e. oxide phases, let us consider a new combinatorial approach where random mixing of components can be performed by the selection of  $q$  oxides out of total  $N$  metal oxides. Here, one can generate a combinatorial variety of local compositions (called local configurations C, its number being  $N_n^C$ ), which establish elemental and stoichiometric variation.

Let us consider the Figure 1, where randomly packed non-equal spheres are represented by different colors, which indicate local arrangements of oxide components in a close proximity (called a local configuration).

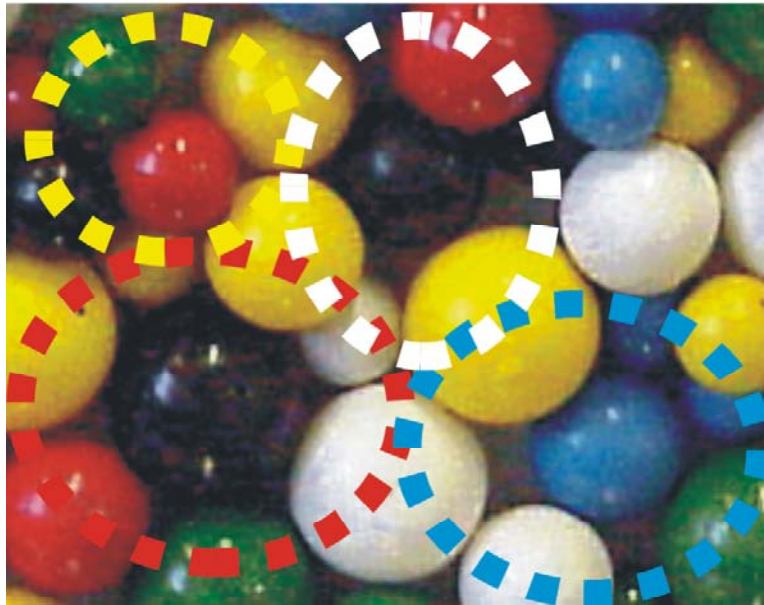


**Figure 1.** A mechanical model for randomly packed grains: randomly packing of non-equal spheres, e.g. six oxide components, represented by different colors. It is assumed that *locally* products are formed upon configurations of components. These components may belong to different configurations by sharing their masses through reactions. Broken lines indicate configurations sharing spheres.

In such a close proximity, a local configuration (i.e. local coordination between oxide components) can be achieved by pressing grains into a *single ceramic pellet*. The single

ceramic pellet may have a volume of about  $1 \text{ cm}^3$  in which there is assumed to be a number of about  $10^{12}$  grains.<sup>[6 c]</sup> The size of the grains is in a range of about  $1 \mu\text{m}$ .

Now let us consider the number of spheres around a selected one (i.e. coordination number) being in close contact to each other for the components in a bulk sample. An estimation of a coordination number for a real sample may be obtained by considering models, which were developed in the case of randomly packed of equal (size) spheres.<sup>[7]</sup>

For randomly packed of equal spheres, the mean voidages (porosity) vary in the range of  $0.36 - 0.44$ . However, the grains in a single ceramic pellets are pressed into dense form and therefore, in this case we can assume voidages range smaller than  $0.36 - 0.44$ . Consequently, we assume an average coordination number of above a value of 8.<sup>[6 c]</sup> However, there is yet no satisfactory analysis capable of explaining the value of voidages of random packing for *irregular bodies*.

To provide chemical diversity for metal oxides  $\text{M}_x\text{O}_y$ , the number of  $N_n^C$  local configuration should be larger than that for phase formations ( $N_q^{PD}$ ). Mathematical estimations imply that by increasing the number of oxides in a system, the number of local configuration also increases.<sup>[6 c]</sup>

However, if the metal oxides are about 61, then there are about  $7.4 \times 10^9$  local configurations in view of about  $5.6 \times 10^7$  phases (by considering realistic estimations, i.e. 6 elements per compound and 8 for locally reacting grains).

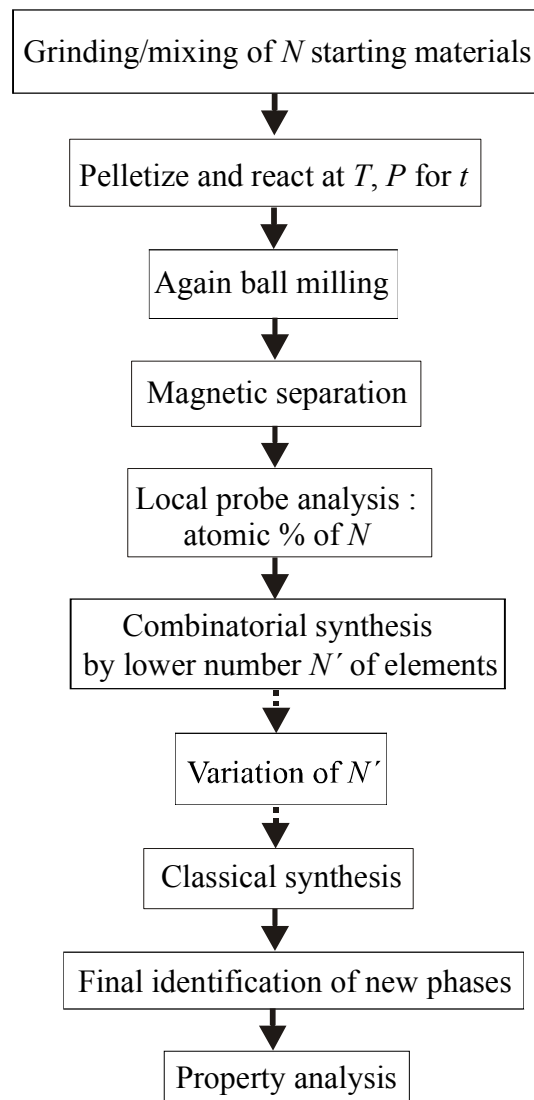
In a single ceramic pellet, there are about  $10^{12}$  grains (in case of  $1 \mu\text{m}$  size) a number higher than  $10^9$  oxide compounds. Therefore, a single ceramic pellet provides a possibility for local configuration ( $N_n^C > N_q^{PD}$ ), populating these many times. In this approach, metal oxides have a large possibility to react *locally*. The present combinatorial approach a “*single sample concept*”<sup>[6 c]</sup> seems therefore to provide an access to chemical diversity for a selected class of compounds.



## 2.2. Combinatorial Synthesis for Ferromagnetic Oxides

A number of metal oxides/carbonates are mixed with the preference of a *lead* ( $L$ ) element. The basic idea of the choice of a *lead* element is that for giving ferromagnetic ability by e.g. V, Mn, Fe, Co, Ni. For preparing local configurations within a system, we may take into consideration wt., mass or vol. percentage.

The SSC combinatorial procedure is represented systematically in scheme 1, which provides an overview of properties search for new ferromagnetic oxide phases.



**Scheme 1.** A schematic way for a property oriented search of magnetic materials.

Experimentally, oxides were ball-milled in excess (70 – 90 vol. %) isooctane to improve homogenization. The ball-mill was rotated at speed  $\sim 400$  rpm for 1 – 1.30 h, in which achat spherical balls of about 5 – 10 (diameter  $\sim 1 - 3$  mm) were used. Thereafter, ball-milled mixtures were filtered, dried and then pressed into single pellets. Ceramic pellets were made at about 7 – 9 t pressure for about 1 – 2 min. by using hydrostatic pressure machine (Perkin : 2445).

Ceramic pellets were placed in an aluminum ( $\text{Al}_2\text{O}_3$ ) crucible and heat-treated within a quartz glass tube (diameter  $\sim 3$  cm) which kept horizontally into a furnace (Heraeus : Ro 4/25). A temperature controller (Tecon : 232) was used for heating and cooling cycles (see Figure 2). Combinatorial reactions were performed by applying a maximum temperature ( $T$ ) of about 850 – 1000  $^\circ\text{C}$  (depends upon the melting points of the selected oxides) for a period of about 2 – 6 h. A heating rate  $\sim 150$   $^\circ\text{C h}^{-1}$  and cooling rate  $\sim 100$   $^\circ\text{C h}^{-1}$  was used. Oxygen gas ( $1 - 2$   $\text{L h}^{-1}$ ) during the annealing process was continuously flowed at  $P(\text{O}_2)$  of about 1 atm. After reaction, ceramic pellets were ball-milled again in excess isooctane slurry  $\sim 0.40 - 1$  h for down sizing of intergrown grains into the micrometer size range.

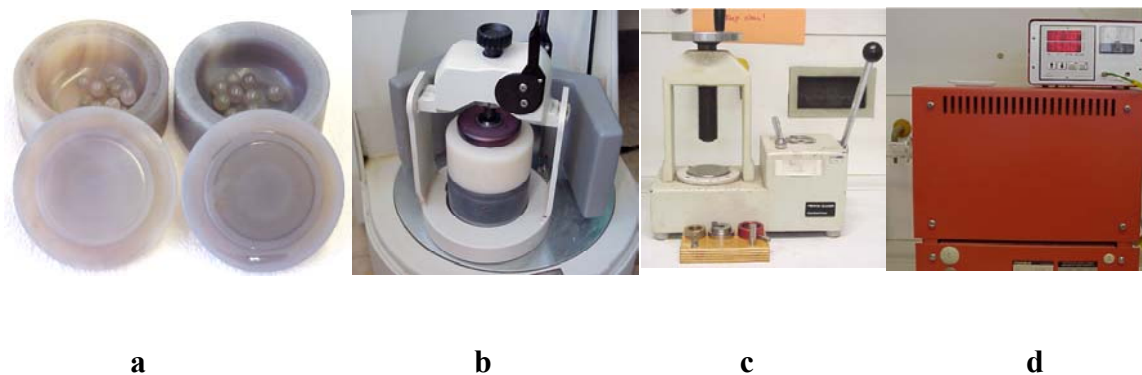


**Figure 2.** Different tools used for combinatorial syntheses, here a) is achat ball-mill boxes, b) a ball-mill motor, c) a pellet pressing machine and d) is a furnace with temperature controller.

### 2.3. Magnetic Isolation of Product Phases

Magnetic isolation of grains can be achieved by the action of magnetic field gradients, leading to attract ferri-, ferro-, para- or super-paramagnetic or deflect diamagnetic particles.<sup>[8, 9]</sup> Magnetic chromatography (MC)<sup>[10, 11]</sup> offers a new technique for isolating grains according to their size and magnetic strength.

The mechanical action is required along the magnetic field gradients, which depends upon the size of the magnetic grain. The magnetic forces<sup>[12]</sup>  $F$  applied to extract magnetic grains can be calculated by using Equation (5) :

$$F_z = \frac{\chi}{\mu_o} V B \frac{\partial B_z}{\partial z} \quad (5)$$

Here,  $B$  is the magnetic induction,  $z$  the direction of the gradient,  $V$  the particle volume,  $\chi$  the magnetic susceptibility (here assumed isotropic), and  $\mu_o$  is the vacuum permeability.

The magnitude of the magnetic force is proportional to the product of the field strength and its gradient. Magnetic field gradients can be produced by using e.g. magnetic sieves within a magnetic column.

In a case for which the magnetic column is filled with horizontal sieves, we may define a probability  $P_{i,i+1}$ , to describe the translocation of a grain from sieve  $i$  to  $i + 1$ . As a grain has to pass through all  $s$  sieves in order to exit the column, the probability  $P_s$  of passing through the entire column can be calculated by Equation 6:

$$P_s = (P_{i,i+1})^s \quad (6)$$

We have demonstrated that one can also use spherical iron balls of different sizes within the magnetic column to create magnetic field gradients. For instance, *fifty to hundred* iron balls within a magnetic column (~ 15 cm length) may be sufficient to provide magnetic field gradients for the extraction of either weak or strong magnetic grains.

Magnetic grains may have a different magnetic susceptibility due to different elemental combinations. It is possible that grains could aggregate and therefore, it is necessary to separate them before passing them through a magnetic column. The following issues are addressed :

- a) The SSC synthesis can yield multiphase particles (e.g. intergrown ferri-/ferromagnetic and diamagnetic phases), which may not disaggregate through ball-milling.
- b) Single or multiphase particles suspension in a fluid could aggregate due to interactions on surfaces.
- c) Aggregation can occur due to ferri- or ferromagnetic interaction.

Based on experimental observations the following suggestions may be appropriate to perform a magnetic isolation process to segregate magnetic and nonmagnetic grains:

- a) To find a suitable steric stabilizer or dispersion aid that could be able to stabilize dispersion during grinding or aging of the size particles, which are first formed.
- b) To wash grains with water free from iron particles within the magnetic column to facilitate the removal of contaminants, which adhered to magnetic particles.

### **2.3.1. Magnetic Column Separator**

A number of pre-rinsed magnetic wool or sieves ( $\sim 500$ , a mesh diameter  $\sim 75 \mu\text{m}$ ) were packed into a glass column (diameter  $\sim 1 \text{ cm}$ , length  $\sim 15 \text{ cm}$ ). Permanent magnets of NdFeB (Maurer Magnetic, N 35 : M 658.8) were placed vertically around the glass column. Nonmagnetic blocks (polyvinyl chloride (PVC)) were placed in a series between two permanent magnets as shown in Figure 3. These nonmagnetic blocks have the same size as the permanent magnets. These were used to provide space between the permanent magnets and helpful to adjust the permanent magnets around the column. However, such magnetic column separators were used to obtain magnetic grains separations from a *suspension*.

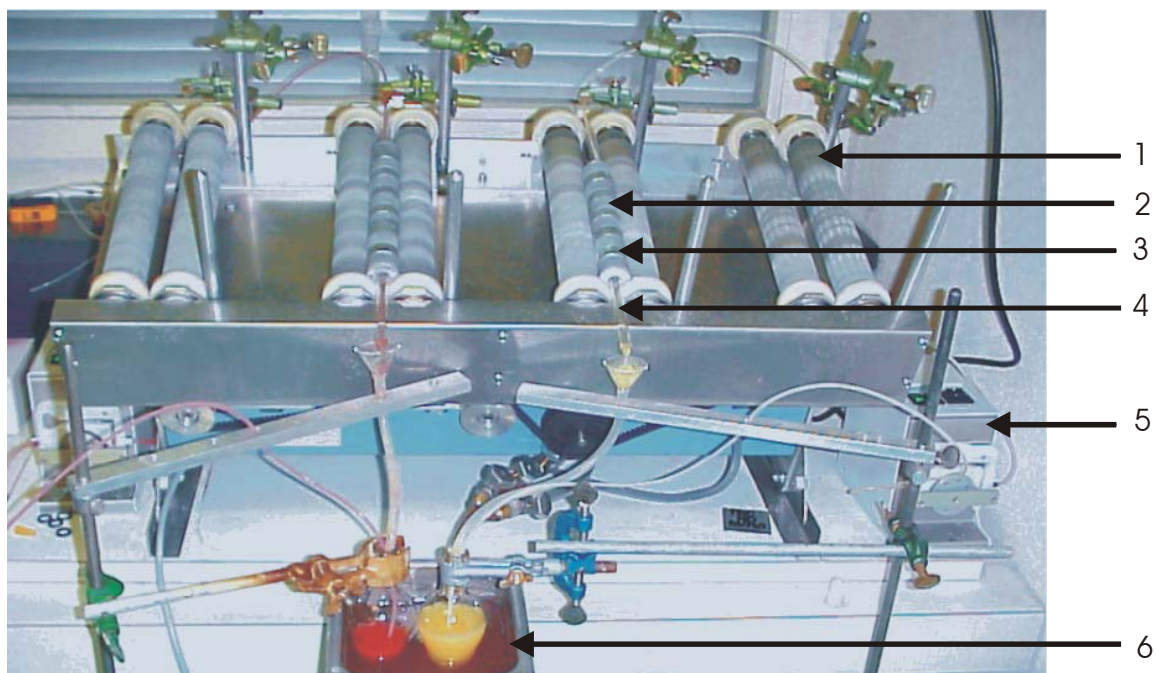


**Figure 3.** Magnetic column separator for the extraction of magnetic grains in a suspension, here 1) is a rotating roller, 2) a nonmagnetic block, 3) a permanent magnet, 4) a glass column, 5) a pump and 6) is an ultrasound bath.

A suspension was prepared by dispersing a reacted SSC sample of about 0.05 g into 250 ml of distilled water. To prevent the aggregation of the SCC sample about 50  $\mu$ l Decon 90 surfactant was added with  $\text{NH}_4\text{OH}(\text{aq})$  0.1M solution to adjust pH. Both a basic pH and surfactant addition facilitated and enabled to obtain a stable dispersion. To further facilitate and enhance the dispersion suspension was shaken and sonicated via ultrasonic-bath (Ismatic : ISM 829). The sonication was carried out for a period  $\sim 0.5 - 1.0$  h. From eyeballing, it was appeared that all these steps facilitated and assisted the formation of a stable dispersion and de agglomeration of the suspension.

Magnetic columns were placed at an angle  $\sim 33^\circ - 44^\circ$  and rotated at  $\sim 60$  rpm during the magnetic separation. The dispersion was passed through the magnetic column by using pump (Sonorex : RK 52) with continuous ultrasonication. The flow rate of the dispersion was adjusted by trial and error. The pumping of the dispersion at a rate close to  $\sim 100$  ml per hour, notable causing some magnetic grains to pass through the magnetic column,

also at a flow rate  $\sim 10$  ml per hour was not favorable because nonmagnetic impurities were observed within the extraction of the magnetic grains. However, pumping rate  $\sim 50$  ml/h successfully enabled to optimize both an optimum throughput and also enabled to maintain non-magnet impurities at the lowest level. Therefore, for further experiments, the pumping of the dispersion was kept at  $\sim 50$  ml per hour.

Additionally, from this experience it was noted that when sieves were used for the column packing, it introduced micro-size iron impurities. In order to find a remedy of this issue, spherical iron balls (diameter  $\sim 0.5 - 2$  mm) were proposed and tested experimentally. It was observed that the replacement of the spherical iron balls were not only easy to handle, it also offered the opportunity to achieve better magnetic separation from these impurities.

### **2.3.2. Magnetic Horizontal Separator**

In a horizontal magnetic separator, permanent magnets of NdFeB (Maurer Magnetic, N 35 : M 658.8) were used and placed horizontally around the grooves (width  $\sim 0.5$  cm, depth  $\sim 0.2$  cm). It should be noted that the level of the horizontal separator is at balanced position to avoid touching of the permanent magnets within a suspension or a groove. The overall horizontal magnetic separator is shown in Figure 4.

For making a suspension, a sample of about  $0.01 - 0.05$  mg was taken into distilled water  $\sim 10$  mL. Then, a few drops (i.e.  $\sim 10$   $\mu$ L) of a surfactant Decon 90 and  $0.1M$   $NH_4OH(aq.)$  were added and activated  $0.10 - 0.30$  min. in an ultrasonic bath (Ismatic : ISM 829). The suspension  $\sim 5$  mL was placed into a groove and the remaining part of the groove was filled with distilled water containing a surfactant. Magnetic separation was performed (at room temperature) for a few days to a week by applying horizontal magnetic rotation at a speed  $\sim 2 - 5$  rpm.

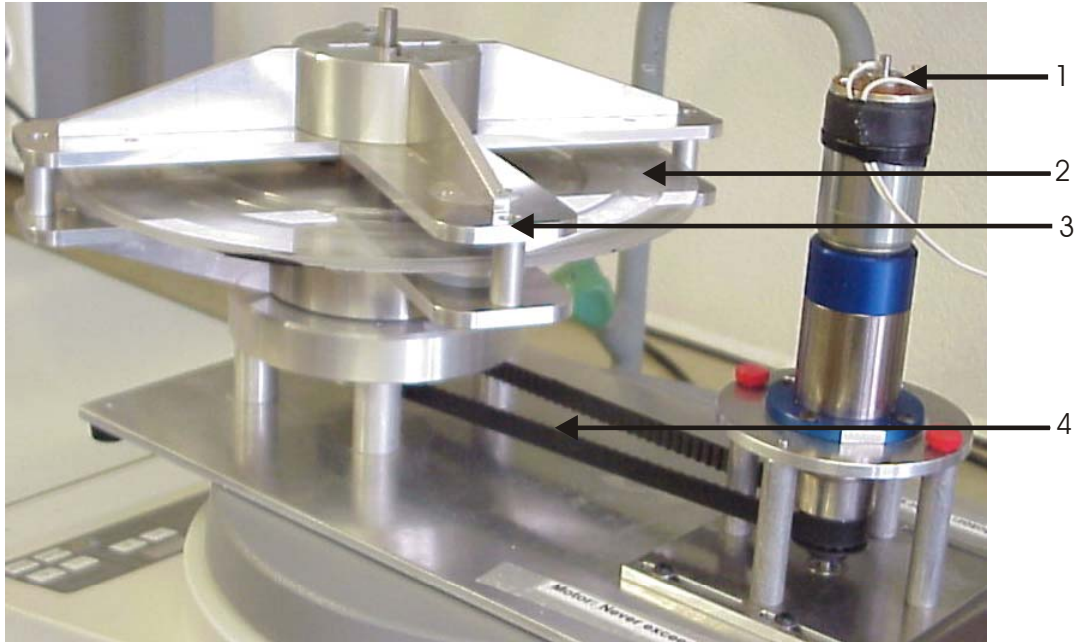


**Figure 4.** A horizontal magnetic separator, here 1) is an electrical motor, 2) a groove, 3) rotating arms with permanent magnets and 4) is a rotation ballet.

The magnetic grains having strong magnetic strength were moved in the direction of the permanent magnets movement and deposited at the end of a groove, while less magnetized grains were left behind.

## **2.4. Property Search through EDX Analysis**

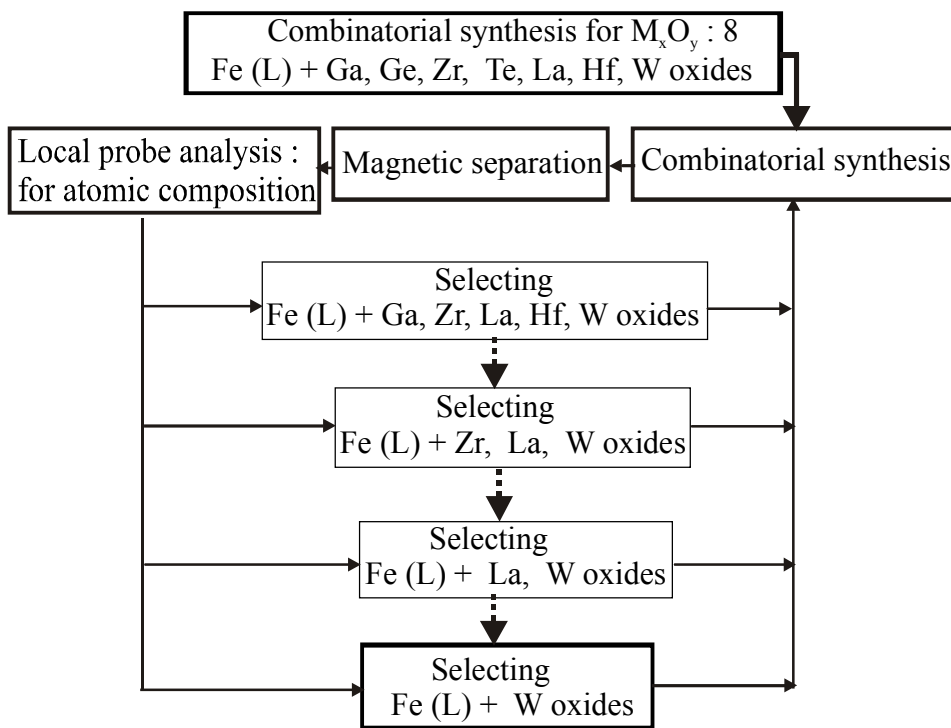
Energy dispersive X-ray (EDX) analysis is a micro-analytical technique used for identifying the elemental composition of a specimen (an area of interest) by analyzing the energy content of X-rays emitted by the specimen. In EDX, the specimen emits the characteristic spectrum of X-rays after excitation by high-energy electrons to obtain information about the elemental composition.

Chemical analysis of solids can be routinely carried out via the use of spectrometers attached to electron microscopes. The ranges of elements detectable by EDX are from Boron to Uranium. A spatial resolution is determined by the probe size, beam broadening within the specimen and the effect of backscattered electrons on the specimen around the point of analysis.

EDX spectrometer (Hitachi : S-3000 N) was selected to identify elements in different grains obtained by SSC. Essentially, we were looking for the most prominent elements in single grains of the magnetically separated material. These elements can indicate possible compound formation. In case some of the elements used do not appear in separated grains, we conclude that such elements may not be forming ferromagnetic compounds under the applied conditions of reaction.

A selection of several, i.e. 5 – 10 grains might be sufficient for getting an overview on their chemical compositions. The grains size (i.e.  $\sim 180$  nm to  $1 \mu\text{m}$ ) was observed through the scanning electron microscopic technique (Jeol : JSM 840). For X-ray powder diffraction, a X-ray powder diffractometer (Stoe Powder : PW 2273-20 Phillips) with  $\text{CuK}_{\alpha 1}$  radiation (wavelength ( $\lambda$ ) :  $1.540598 \text{ \AA}$ ) was used.

An example of reduction of elements from the SSC samples for finding new ferromagnetic Fe-oxides is shown in scheme 2.



**Scheme 2.** A systematic reduction of elements to find new ferromagnetic Fe-oxides.



- i) In a first SSC experiment we selected  $\text{Fe}_2\text{O}_3$  (lead) and oxides of Ga, Ge, Zr, Te, La, Hf, W. As there were many oxide elements present in the system after reaction, one might expect that the X-ray powder diffraction shows many lines related to these elements.  
By applying an EDX analysis, we could show that Ge, Re and Te were almost not present in product grains, consequently we ignored them for a next SSC experiment.
- ii) A second experiment was performed by selecting  $\text{Fe}_2\text{O}_3$  (lead) and oxides of Ga, Zr, La, Hf, W.
- iii) In the same way, a third experiment was performed by selecting  $\text{Fe}_2\text{O}_3$  (lead) and oxides of Zr, La, W. Here, Ga, Hf were neglected. A further reduction ended with Fe, La and W.
- iv) Finally, only oxides of W, Fe were used for a classical synthesis.

X-rays powder diffraction for the SSC sample i) (i.e. oxides of Fe, Ga, Ge, Zr, Te, La, Hf, W) prior to reaction, after reaction and magnetically separated showed deviation with respect to many lines (see Figure 5). For comparison of the d-values for these samples and those of a few known compounds (used for SSC) see Table 2. From this analysis we can conclude that the starting materials (after reaction) were consumed.

It was observed that there is agreement for many intense lines for reacted and magnetically separated samples (see Table 2).

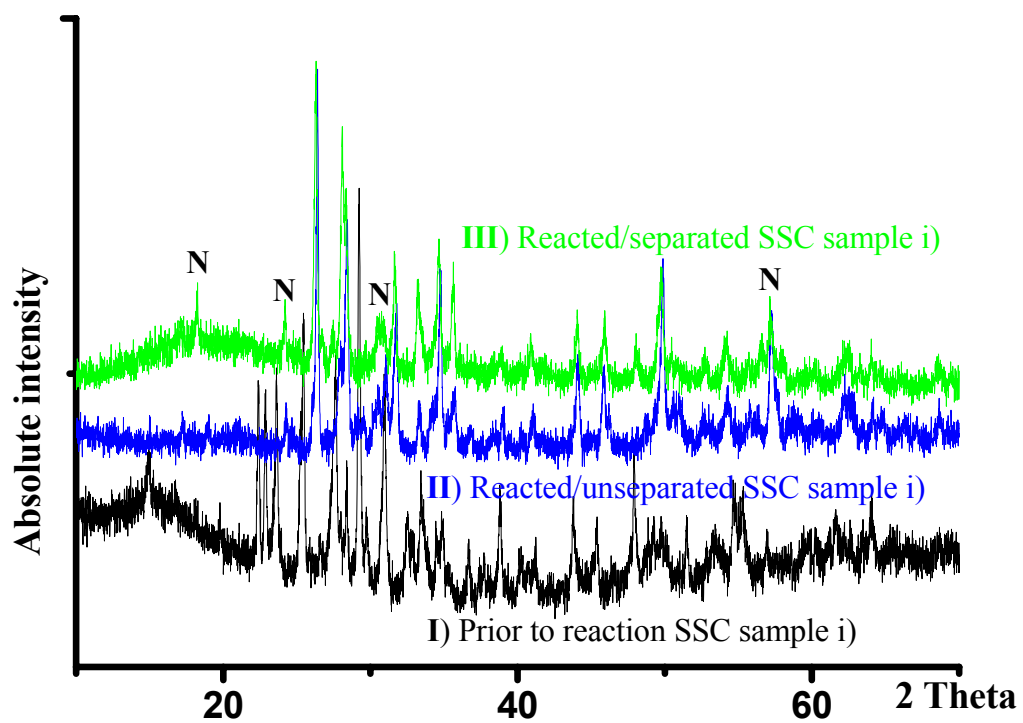


**Figure 5.** Comparison X-ray powder diffraction patterns for SSC samples i) oxides of Fe, Ga, Ge, Zr, Te, La, Hf, W I) prior to reaction, II) after reaction and III) magnetically separated. N : New lines.

**Table 2.** The d-values of X-ray powder diffraction data of Figure 5, for the SSC sample i) oxides of Fe, Ga, Ge, Zr, Te, La, Hf, W I) prior to reaction, II) after reaction, III) magnetically separated and for the SSC sample and for the known compounds \* Fe<sub>2</sub>O<sub>3</sub> (alpha phase, X-ray powder diffraction PDF file No. 84 – 308], \*\* ZrO<sub>2</sub> (X-ray powder diffraction PDF file No. 83 – 810]

d-values for the SSC sample i) prior to reaction I)	d-values for $\alpha$ -Fe <sub>2</sub> O <sub>3</sub> *	d-values for ZrO <sub>2</sub> **	d-values for the SSC sample i) after reaction II)	d-values for the SSC sample i) magnetically separated III)
3.764*			3.674	3.674
3.498 *				
<b>3.366</b>	<b>3.365*</b>		<b>3.380</b>	<b>3.379</b>
			<b>3.373*</b>	<b>3.370</b>
3.226*			<b>3.139*</b>	<b>3.131*</b>
3.053		3.170	2.877	
<b>2.885*</b>		<b>2.889*</b>	<b>2.814*</b>	<b>2.820*</b>
<b>2.682</b>	<b>2.686*</b>	2.733 *	2.696*	
2.602			<b>2.581*</b>	<b>2.586*</b>
<b>2.571</b>	2.507*	<b>2.555*</b>	<b>2.516</b>	<b>2.515</b>
<b>2.448</b>			2.310	
<b>2.190*</b>	<b>2.196*</b>		2.210	2.208
<b>2.066</b>		<b>2.071, 2.095</b>	2.052	2.054
<b>1.996</b>		<b>1.986*</b>	1.978	1.974
<b>1.830</b>	<b>1.832</b>			
1.773		<b>1.776</b>	<b>1.820*</b> , 1.793	<b>1.819*</b>
<b>1.681</b>	<b>1.686*</b>	1.672	<b>1.695</b>	<b>1.694</b>
1.617			<b>1.607*</b>	<b>1.610</b>

\* Represents intense lines. Bold numbers represent d-values matching.

After the reduction of elements through EDX analysis we performed XPD for the SSC samples ii) oxides of Fe, Ga, Zr, La, Hf, W; sample iii) oxides of Fe, Zr, La, W, and sample iv) oxides of Fe, W. A comparison of XPD for these magnetically separated SSC samples (ii, iii, iv) with the unreacted SSC sample i) showed differences in view of many lines (see Figure 6).

The d-values obtained for the reacted and magnetically separated samples as shown in Table 3. In this case many new lines were found for the separated powder.

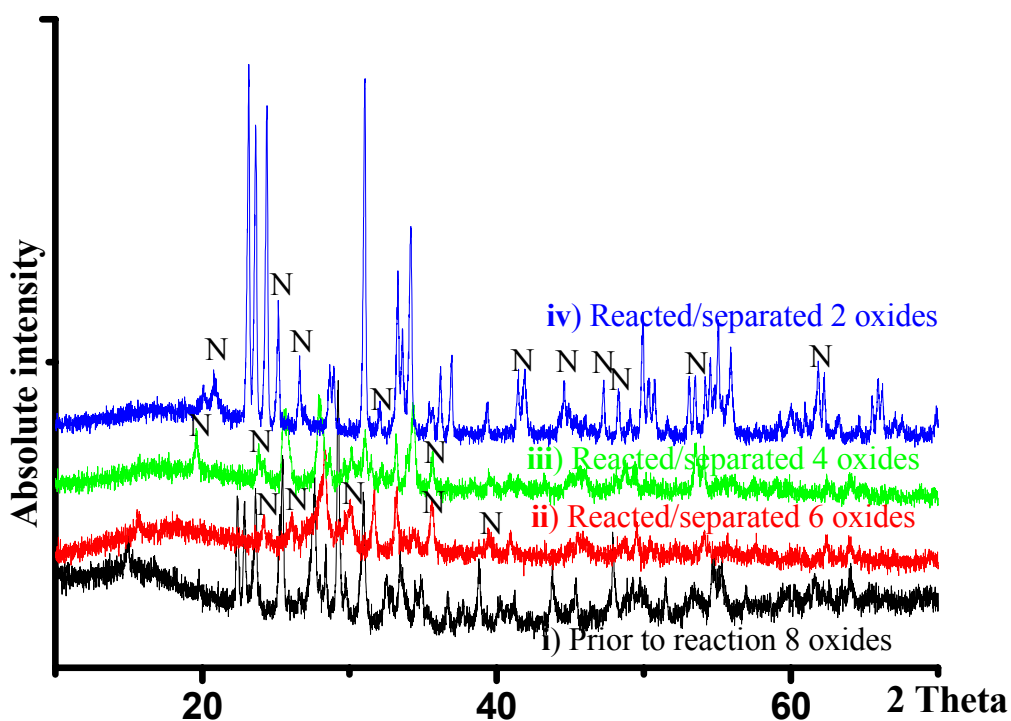


**Figure 6.** Comparison of X-ray powder diffraction patterns for the SSC samples i) oxides of Fe, Ga, Ge, Zr, Te, La, Hf, W prior to reaction with reacted and magnetically separated SSC samples ii) oxides of Fe, Ga, Zr, La, Hf, W; for the SSC sample iii) oxides of Fe, Zr, La, W and for the sample iv) oxides of Fe, W. N : New lines.

**Table 3.** The d-values of X-ray powder diffraction of Figure 6, for the reacted and magnetically separated the SSC sample i) oxides of Fe, Ga, Ge, Zr, Te, La, Hf, W; for the SSC sample ii) oxides of Fe, Ga, Zr, La, Hf, W; for the SSC sample iii) oxides of Fe, Zr, La, W and for the SSC sample iv) oxides of Fe, W.

<b>d-values for the SSC sample i) magnetically separated</b>	<b>d-values for the SSC sample ii) magnetically separated</b>	<b>d-values for the SSC sample iii) magnetically separated</b>	<b>d-values for the SSC sample iv) magnetically separated</b>
<b>3.674</b>	<b>3.679</b>	3.729	4.268
3.379	3.416	3.484*	3.838*
	3.173*	3.194*	3.648*
3.131*	3.150*	2.964	3.536
<b>2.820*</b>	<b>2.821*</b>		3.347
	<b>2.698</b>	<b>2.698</b>	3.084
			2.879*
2.586*	<b>2.629</b>	2.612	<b>2.622*</b>
<b>2.515</b>	<b>2.520*</b>	<b>2.524</b>	2.480
	<b>2.274</b>	<b>2.274</b>	2.287
<b>2.208</b>	<b>2.202</b>	2.187	2.152
2.054		2.092	2.150
1.974	<b>1.991</b>	<b>1.990</b>	1.921
<b>1.891</b>			<b>1.900</b>
<b>1.819*</b>			<b>1.824</b>
	1.839	1.866	
<b>1.694</b>	<b>1.693</b>	1.710	1.790
1.610*	1.600	1.637	
<b>1.493</b>	<b>1.486</b>	1.452	

\* Represents intense lines. Bold numbers represent d-values matching.

In the light of the above observations, the XPD comparison showed that in case of sample i) after reaction and magnetic separation, most intense lines agreed and changes were observed if compared to the unreacted state. However, the X-ray powder diffraction diagrams revealed an important fact that the starting materials were consumed. By following up the above systematic way, one might be able to workout for new ferromagnetic oxides phases, which are present in SSC samples.

## 2.5. References

- [1] R. S. Bohacek, C. McMartin, G. Colin, C. Wayne, *Med. Res. Rev.* **1996**, 16, 3 - 50.
- [2] F. J. DiSalva, *Pure Appl. Chem.* **2000**, 72, 1799 - 1807.
- [3] E. M. Levin, H. F. Mcurdie in *Phase Diagrams for Ceramists*, ACS. Ohio, Vol. III, **1975**, p. 88
- [4] M. Jansen, *Angew. Chem. Int. Ed.* **2002**, 41, 3746 - 3766.
- [5] W. F. Maier, *Angew. Chem. Int. Ed.* **1999**, 38, 1216 - 1218.
- [6] a) See Chapter 5; b) See Chapter 3 of reference 11; c) See Chapter 3.
- [7] a) Dullien, F. A. L. Structural Properties of Packing Particles, in *Handbook of Powder Science & Technology*, 2nd ed.; Fayed, E. M.; Otten, L., Eds.; Chapman & Hall : New York, **1997**, pp. 53 - 95; b) Bernal, J. D.; Mason, J. *Nature* **1960**, 188, 908 - 911; c) Wade, W. H. *J. Phys. Chem.* **1965**, 69, 322 - 326; d) Ridgway, K.; Tarbuck, K. J. *Brit. Chem. Eng.* **1996**, 12, 384 - 388.
- [8] J. Boehm in *Ind. IEEE. Transform. Appl. Supercond.* **2000**, 10, 710 - 715.
- [9] J. Svoboda in *The Physical Principles of Magnetic Separation in Magnetic Methods for the Treatment of Minerals*, Elsevier, Amsterdam, **1987**, 1 - 76.
- [10] T. Ohara, S. Mori, Y. Oda, Y. Wada, O. Tsukamoto, *Trans. IEE*, **1996**, 166-B, 979 - 986.
- [11] T. Nomizu, K. Yamamoto Tsukamoto, M. Watanabe, *Ana. Sci.* **2001**, 17, i177 - i180.
- [12] J. H. P. Wastson, *J. Appl. Phys.* **1973**, 44, 4209 - 4213.

### 3. A 'Single Sample Concept' (SSC) :

#### New Approach to Combinatorial Chemistry of Inorganic Materials

J. Hulliger, M. A. Awan, *Chem. Eur. J.* 2004, 10, 4694 - 4702.

#### 3.1. Abstract

Combinatorial estimations show that within a single un-reacted ceramic sample made up by mixing  $N$  different starting materials  $M_xO_y$  with average particle size  $\sim 1 \mu\text{m}$ , there are about  $10^{12}$  grains per cubic centimeter, being sufficient for local reaction to occur that may produce a larger number of product oxides than presently accessible by 2D plate techniques. A *single sample concept* (SSC) is proposed to perform property directed syntheses for the preparation of ferri-/ferromagnetic or superconducting compounds. Because of magnetic properties of products, libraries of product grains can be sorted using magnetic separation techniques. For materials with a large magnetization, the separation efficiency is as high that traces of products can be isolated. The SSC concept was tested experimentally to prepare Fe-based oxides ( $N = 17, 24, 30$ ). The large yields ( $< 75 \text{ wt } \%$ ,  $N = 17$ ) of products grains agree with literature data, which indicate that 3d metal magnetic oxide phases ( $T_c > 300 \text{ K}$ ) are most probably Fe oxides. In combination with magnetic separation techniques the SSC seems particularly adapted for exploring the solid-state chemistry of metallic lead elements that form ferri-/ferromagnetic or superconducting oxide phases difficult to detect systematically within the large phase space of theoretically existing compounds.

**Key Words** : Ceramic synthesis, chromatography, combinatorial chemistry, ferromagnetic properties, magnetic separations, superconductors.



## 3.2. Introduction

<< ... all chemical compounds capable of existence ...  
are already present on the energy landscape  
and are just waiting to be discovered. >> [1]

Joseph J. Hanak's idea of the “*multiple sample concept*” (MSC) [2] has within the last ten years found widespread extension through 2D plate approaches where pixel-wise elemental compositions for *parallel syntheses* have been prepared by mixing starting materials via the vapor or liquid phase. Many analytical techniques have been developed to perform phase and property analyses also in parallel. [3 – 8] As the number of initial elemental starting compositions on one reaction plate has reached more than 25'000, combinatorial synthesis may be considered “ ... the first rational concept to tap the potential wealth of chemical diversity in a more systematic way. [5] » Combinatorial chemistry now makes the exploration of the diversity of certain compound classes a realistic endeavor.

However, *realistic restrictions* are required to limit both the number of starting components ( $N$ ) and the number of elements ( $q$ ) per compound formed, otherwise combinatorial functions will by far exceed the feasibility of any practical synthesis. Given these general constraints, we may, nevertheless, try to find a solution to the impossible [9] by asking : What is the minimum number ( $q$ ) of e.g. metallic elements in a crystal structure or amorphous phase that can provide sufficient *chemical diversity* to be able to determine the conductive, magnetic, luminescent or catalytic properties of the material?

High-temperature superconductivity [10] is possible for  $q = 3 - 4$  metallic elements. Other important properties such as ferri-/ferromagnetism, luminescence and catalysis have been determined for only  $q = 2 - 3$ . In recognition of many properties, it is likely to assume that novel properties or an advanced performance of known compounds might be accessible for a rather low number of constitutional metals in oxides, halogenides, sulfides, and so forth.

Therefore, present estimations concerning the “existing”<sup>[1]</sup> phases to be prepared by a new combinatorial synthesis with  $N$  components as starting materials are limited to  $q \leq 6$  (the number of constitutional metals in e.g. oxide compounds). Given  $N$  building blocks, these components are grouped to constitute binary ( $q = 2$ ), ternary ( $q = 3$ ), etc.  $(T, x)$ –phase diagrams ( $P(O_2)$  defined by experimental conditions) for which we can attribute an average number  $\eta_q$  ( $q = 2 - 6$ ) of solid phases present in each diagram. The average maximum number of  $N_{oxides}$  phases to be synthesized is thus given by

$$N_{oxides} \cong \sum_{q=2} \eta_q N_q^{PD}, \quad (1)$$

in which  $N_q^{PD}$  is the number of generally unknown phase diagrams, calculated from Equation (2) ( $N$  is the number of building blocks :  $q = 2$  (binary),  $q = 3$  (ternary), etc.

$$N_q^{PD} = \frac{N!}{q!(N-q)!} \quad (2)$$

What is a realistic estimate for  $\eta_q$ ? Although available phase diagrams for oxides<sup>[11]</sup> are by no means complete, they are considered representative to gain an estimate for the diversity of solid phases ( $\eta$ ) :

In the case of  $q = 2$ , the average number of binary metallic oxides is just about 3 (100 representative diagrams selected from volumes I – VIII of reference [11]), whereas the percentage of purely eutectic binary diagrams is  $\sim 10\%$  (for a sample of 470 diagrams<sup>[11]</sup>). For ternary systems a rough estimate of  $\eta_3$  yielded only 2 (86 suitable diagrams;<sup>[11]</sup> Here, because of incomplete compositional scans,  $\eta$  may be higher). This allows us to conclude that the upper limit of  $\eta_6$  is certainly lower than, say 100 (number of  $E_i E_j E_k E_l E_m E_n O_y$  phases of a certain stoichiometry).

This means that the number of oxide phases a combinatorial procedure will have to provide access to is less than  $N_{oxides} \approx 100 \cdot N_6^{PD}$ . The number of phase diagrams for increasing  $N$  is shown in Figure 1 : By varying of  $N$  (10 to 61; the maximum number of non-radioactive metallic elements) components, we can conclude that a realistic upper

limit for  $N_{oxides}$  is about  $6 \times 10^9$  ( $N = 61$ ,  $q = 6$ ,  $\eta_{max} \approx 100$ ). Consequently, a corresponding number of experiments are required to explore this diversity. Present combinatorial techniques are still far off this upper limit, however, they have led to the discovery of new phases by varying  $N$  from about 10 to 30.

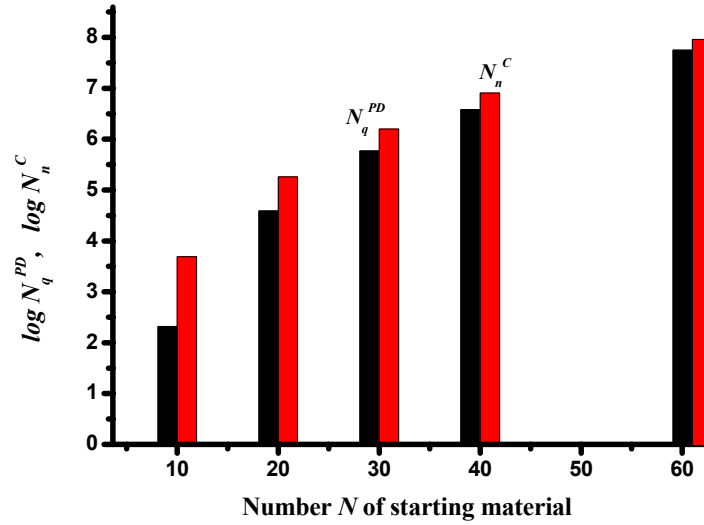


**Figure 1.** Calculated number of possible phase diagrams  $N_q^{PD}$  and local configurations  $N_n^C$  for  $N$  starting components and  $n = 6$  elements in product grains.

We present here a new method for performing combinatorial syntheses using a *single sample concept* (SSC) : Mixing together  $N$  micrometer sized starting oxides to prepare a ceramic sample (see Figure 2) yielding a randomly packed state of particles representing different components and sizes. A combinatorial variety of local compositions (called configurations,  $N_n^C$ ) is generated which establishes 1) elemental and 2) stoichiometric variation. The elemental variation constitutes phase diagrams of the order  $q$ , along with some stoichiometrical variation ( $n$ ), whereas the particle size distribution populates the compositional axes of phase diagrams.

A combinatorial estimation of the number  $N_n^C$  shows that it can be larger than the number  $N_q^{PD}$  of phase diagrams [see Figure 1 and Equation (3)] :

$$N_n^c < \binom{N + n - 1}{n} \quad (3)$$

(excluding those configurations consisting of the same elements;  $n$  is the number of grains in a configuration, with  $n \geq q$ ).



**Figure 2.** Mechanical model of spheres of different colors and size to visualize *local configurations*, i.e. grain contacts by  $n$  starting materials to obtain a diversity of product grains distributed within a bulk sample.

The SSC therefore provides access to the manifold of phase diagrams. As  $N_n^c$  is of the same order than  $N_q^{PD}$  (see Figure 1;  $n \approx q$ ), the particle size distribution is effectively needed to provide a dense population of the compositional axes of phase diagrams. Finally, we have to make sure, that a typical sample of about  $1 \text{ cm}^3$  contains sufficient grains for both the elemental and the size distribution : In case of an average grains size of  $1 \mu\text{m}$ , there are about  $10^{12}$  grains per cubic centimeter. Assuming a reasonable number  $N$  of components (10 - 40), the number of grains is orders of magnitudes larger than the estimated number of oxide phases. The number  $N_p$  of micrometer sized product grains

per phase is in the order  $10^6$  to  $10^3$  ( $N$  : 10 to 40), which, if given in ppm, is a small density, generally below a few ppm ( $N > 10$ ).

The SSC thus provides access to a library that may unravel a defined ( $N, q, \eta$ ) chemical diversity for a selected class of compounds. Once such a library is obtained, we face the task of how reading it.

Today's, analytical techniques have reached a resolution down to the nanometer size both for compositional and structural analysis. [12] Nevertheless, property characterization is much more difficult using the present concept than when applying 2D plate techniques. However, if we focus on specific properties such as those of ferri-/ferromagnetic or superconducting materials, highly efficient *particle separation techniques* can be applied. Consequently, we have introduced *magnetic separation* into materials chemistry that allows particle extractions for  $\mu\text{m}$  sized product phases.

The SSC may be applied in different ways :

- 1) A mixture of similar amounts (mass, volume or moles) of  $N$  metal oxides is reacted to form  $q$ - type oxides. In this case oxygen is the *lead* ( $L$ ) element without a preference for any one metal in setting up the starting composition.
- 2) A *lead oxide* is added in larger quantity than the others constituents in order to preferably form  $E_i E_j E_L \dots O_y$  instead of  $E_i E_j E_k \dots O_y$ ; ( $i, j, k, \dots, \neq L$ ) compounds.

In the present study we concentrate on second application by using Fe to produce a diversity of iron oxides with a selected number  $N$  (17, 24, 30) of nonmagnetic elements. Lead element Fe was selected to demonstrate the feasibility of the SSC in combination with magnetic separation. In further studies the SSC will be applied to search for i) new ferri-/ferromagnetic 3d transition metal oxides and ii) superconductors.

### 3.3. Results and Discussion

#### 3.3.1. Isolation of Product Phases by Magnetic Separation

A single sample combinatorial synthesis may produce a *small number*  $N_p$  of product grains representing the material of interest. In most cases bulk analysis would not be successful thus making separation techniques necessary. In case of either strongly ferri-/ferromagnetic or diamagnetic materials, magnetic separation can be applied.

Magnetic separation of mixtures of small particles featuring different magnetic properties is achieved by the action of an inhomogeneous magnetic field which leads to a attraction (ferri-, ferro-, para- or superparamagnetic) or deflection (diamagnetic) of particles dispersed in a gas or fluid passing through a separator column. [13, 14] As samples show separate distributions for the particle size and the magnetization strength, *magnetic chromatography* [15-17] offers a new technique to separate particles according to their size and magnetization. In industry large-scale magnetic separation using conventional or superconducting magnets, so called *High Gradient Magnetic Separation* (HGMS), [18] is applied in the purification of minerals (kaolin, talc) and is used in mining to recover ores (hematite, siderite, elite). [19]

In material science, magnetic separation was mainly applied to separate, purify and characterize ceramic copper oxide superconductors. Simple equipment allowed deflecting of grains of superconducting phases at liquid nitrogen temperature [20-27]. However, solid states chemistry has not yet made systematic use of this technique to extract phases from for example a combinatorial synthesis.

The magnetic force  $F$  exerted on a particle is given by Equation (4) [28]

$$F_z = \frac{\chi}{\mu_0} V B \frac{\partial B_z}{\partial z}, \quad (4)$$

in which  $B$  is the magnetic induction,  $z$  the direction of the gradient,  $V$  the particle volume,  $\chi$  magnetic susceptibility (here assumed to be isotropic) and  $\mu_0$  the permeability of the vacuum.

The magnitude of the force is thus proportional to the product of the field strength and its gradient. The mechanical action is along the field gradient. In a practical set up generation of the strongest field inhomogeneity is given by ferromagnetic wires (wool or sieve). The maximum force has been estimated for a wire diameter of 2 - 3 times the particle size. [20, 29] Given today's ultra high field magnets (pulsed), there are many perspectives for magnetic particle separation in materials science. In the case of superconductors, however,  $B$  must be less than  $B_c$ , the critical field above which diamagnetism decreases. Here, the gradient has to be maximized. Furthermore, superconductive particles must be sufficiently large because of the London penetration depth. [30]

An important issue in particle separation is aggregation, i.e. cake formation [31]. In our case there are three origins of aggregation :

- 1) Synthesis can yield multiphase particles (e.g. intergrown ferri-/ferromagnetic and diamagnetic phases) that are not separated through ball milling.
- 2) Single or multiphase particles suspended in a fluid can aggregate owing to of interactions between surfaces. Practical separation in industry therefore uses surfactants.
- 3) Aggregation can occur due to ferri- or ferromagnetic interaction.

Our laboratory set ups for continuous extraction of e.g. ferri- or ferro-, paramagnetic, or super-paramagnetic ( $T = 300$  K) particles from a suspension is shown in Figure 3 : Particles pass through a column through a column surrounded by permanent magnets, and stick to the wall of the column (3a), or a vertical tube is filled with magnetic sieves (mesh size:  $\sim 75$   $\mu\text{m}$ ) surrounded by a number of permanent magnets (Figure 3b). A low-density suspension (activated by ultrasound) is continuously pumped through the column. After a first step of separation step, only fluid is passed through the column to wash out retained nonmagnetic particles. The magnets are then removed to release the magnetic particles from the walls (Figure 3a) or sieves (Figure 3b). In all systems  $\text{B}_8\text{Fe}_{17}$   $\text{Nd}_{15}$  magnets were used in all systems.

In the case in which the column is filled with horizontal sieves (Figure 3b), we may define a probability  $P_{i,i+1}$ , to describe the translocation of a grain from sieve  $i$  to  $i + 1$  (Figure 4). As a grain has to pass through all  $s$  sieves in order to exit the column, the probability  $P_s$  of passing through the entire column is given by Equation (5)

$$P_s = (P_{i,i+1})^s \quad (5)$$

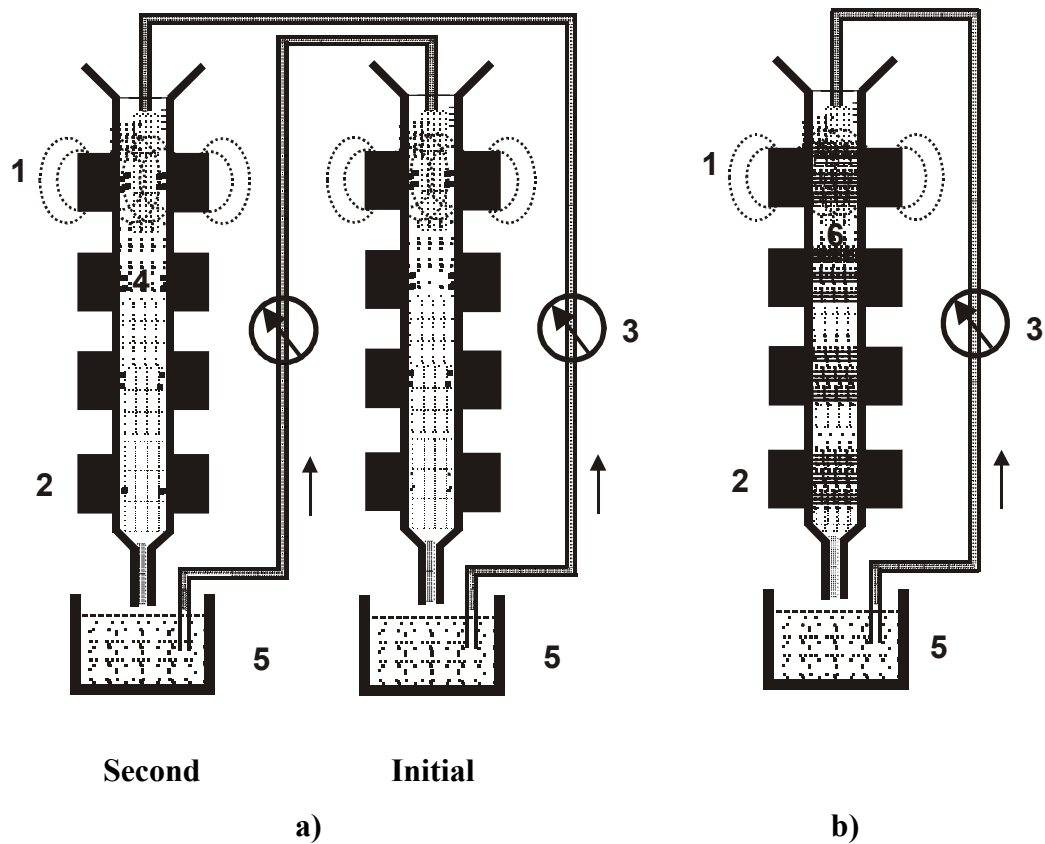


**Figure 3.** Two types of constructed magnetic separators used to extract magnetic particles from a SSC reaction mixture : Vertical column exposed to the effect of a magnetic field (1) by permanent magnets (2). A liquid carrying product grains is pumped (3) through the column. Magnetic particles stick (4) at locations of strong magnetic gradients. For disaggregation of particles the liquid is continuously passing an ultrasound bath (5). Similar to a), using 75  $\mu\text{m}$  wide horizontal magnetic sieves (6) to retain magnetic particles by the effect of a strongly inhomogeneous field on the sieves.



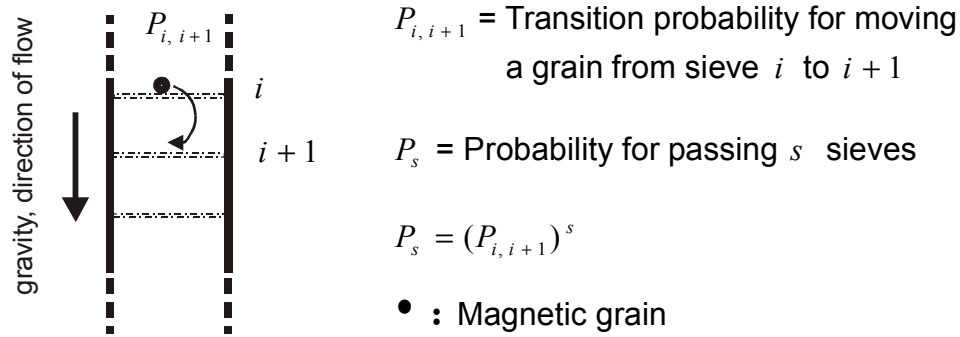


**Figure 4.** Estimation of the probability for passing grains through a magnetic column (see also Table 1).

Table 1 gives realistic data for  $P_s$  that cover low to high  $P_{i,i+1}$  values. For the present separators (Figure 3b),  $s$  is approximately ten. New separators providing  $s = 1000 - 3000$  are under development.

Strongly ferromagnetic particles can safely overcome the effect of gravity and forces imposed by the flow of liquid. For strong forces,  $P_{i,i+1}$  for these materials is almost zero. Consequently, the retention efficiency for strongly magnetic materials is nearly 100

**Table 1.** Probability  $P_s$  for passing particles over a series of  $s$  sieves.

$P_{i,i+1}$	$P_s$	$P_s$	$P_s$
	$s = 10$	$s = 100$	$s = 1000$
0.01	0	0	0
0.10	$10^{-10}$	0	0
0.50	$9.8 \times 10^{-4}$	0	0
0.90	0.35	$2.7 \times 10^{-5}$	0
0.99	0.90	0.37	$4.3 \times 10^{-5}$
0.999	0.99	0.90	0.37

%. Although superconducting materials show a different behavior in an inhomogeneous magnetic field, it is nevertheless unlikely to pass grains efficiently through a column of large  $s$ . Therefore, separators shown in Figure 3b show great potential to extract small fractions of superconducting materials contained in SSC syntheses. The separation efficiency was tested by passing through a mixture of ( $\text{Al}_2\text{O}_3$ ,  $\text{La}_2\text{O}_3$ ,  $\text{TiO}_2$ ,  $\text{ZnO}$ ,  $\text{ZrO}_2$ ) and  $\text{BaFe}_{12}\text{O}_{19}$  (10 and 20 wt %) particles in water, containing a surfactant<sup>[32]</sup> (Decon 90 +  $\text{NH}_4\text{OH}(\text{aq.})$ ) : through the column (see Figure 3a). The separation ( $\text{BaFe}_{12}\text{O}_{19}$ ) yield was 10 and 20 wt %, respectively. For trace analysis, about 1 ppm (wt) of  $\text{BaFe}_{12}\text{O}_{19}$  grains in a mixture with non-magnetic oxide powder was passed through the column. Using magnetic sieves, some ferromagnetic particles were recovered, showing, that in principle, a pin could be found in a haystack !

### 3.3.2. Results for Magnetic Oxides

Preparation of configurations [Equation (3)] requires a dense population of grains that locally undergo local reactions. Mixing  $N$  starting oxides  $M_xO_y$ , ball milling (adding a liquid to improve of homogenization) and pressing into a pellet is known as the classical ceramic preparation. Long terms ball milling may achieve elemental homogenization and reduce the particle size. Scanning electron microscopy (SEM) mapping of the elements confirmed this. Major difficulties in bringing such a sample to reaction as proposed may involve 1) liquid formation (eutectic compositions and low-melting compounds) and 2) spreading of elements over the sample because of high vapor pressure components.

In experiments with  $N = 10 - 30 M_xO_y$ , reaction temperatures in the range of 1000 – 1100 K, reaction times of minutes to hours, 1) visual inspection of pellets, 2) DSC, and 3) SEM showed no evidence for significant liquid phase formation. Transmission electron microscopy (qualitative elemental analysis) performed on 30 single particles in the range of 100 – 300 nm confirmed crystalline particles reflecting a broad distribution of elemental compositions. The average number of different elements in the grains was six to seven (for 12 starting  $M_xO_y$  materials used for a basic test). The starting materials (except for the lead element) were mostly consumed. Powder X-ray diffraction showed

no obvious background scattering this would be typical of amorphous phases. In view of the many compounds  $N_{oxides}$  a sample might contain, the number of intense diffraction lines was generally very small. For most phases the net amount per phase was probably too low or the number of grains per phase was not sufficient to produce a sharp powder pattern.

Configurations in bulk ceramic samples are interfering and sharing grains for reactions. Compared with powder samples, reaction of *isolated aggregates* of particles would match conditions set up by Equation (3) more reasonably. A surface providing support for configurations  $N_n^C$  would thus be of great use. Certainly, we are working with sodium chloride to disperse aggregated  $M_xO_y$  starting grains onto NaCl particles ( $\langle d \rangle_{NaCl} \gg \langle d \rangle_{oxides}$ ). By keeping the reaction temperature 976 – 1126 K below melting. The NaCl surface in the state of (eutectic systems) liquid formation may enhance reactivity and promote crystallization of single-phase grains. Reaction of NaCl with most oxides should not represent a serious problem (for example solid solution and oxychloride formation) as NaCl is commonly used in the flux growth of various oxide compounds. After the reaction, dissolution of the supporting material liberated particles, showing a smaller degree of intergrowth than those obtained from the powder sample. Both routes were explored to synthesize *ferri-/ferromagnetic* materials.

Selecting Fe as the *lead element*, databases provided a rather small number of about 53 ferri- or ferromagnetic Fe oxides ( $T_c > 300$  K, containing no other magnetically active element). In the case of V, Cr, Mn, Co and Ni the number of compounds characterized is even smaller (Figure 5). For Cu only one class of compounds ( $MgCu_2O_3$ ,  $Ca_2CuO_3$ ,  $BaCuO_3$ )<sup>[33, 34]</sup> was found, for which evidence of ferromagnetic coupling above 300 K is reported. However, these structures expectedly show 1D antiferromagnetic ordering. Excess oxygen is reported to induce spin flips and ferromagnetic interchain coupling<sup>[35]</sup>. Given present knowledge, Fe seems to be the leading 3d transition element for obtaining magnetic oxides ( $T_c > 300$  K).

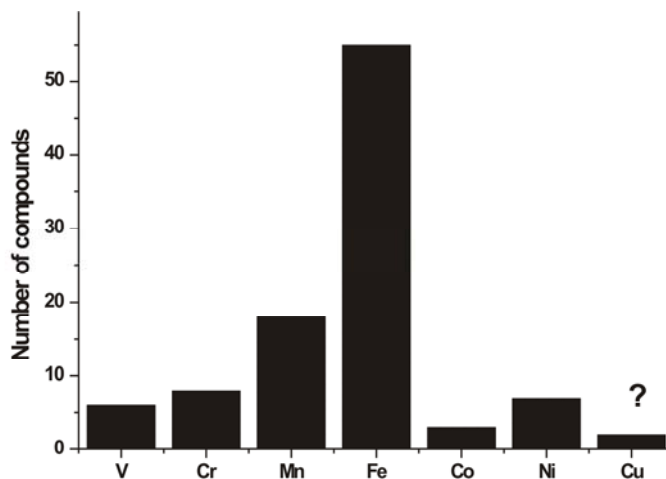


**Figure 5.** Results of literature search on ferri- or ferromagnetic M(3d) – oxides ( $T_c > 300$  K). The search clearly found more Fe oxides than other 3d metals.

For SSC syntheses, we started either from 17 (Li, Na, Mg, Si, K, Ca, Sr, Y, Nb, Mo, Sn, Te, Ba, La, W, Pb, Bi), 24 (Li, B, Na, Mg, Al, Si, K, Ca, Ti, Ga, Ge, Sr, Y, Zr, Nb, Mo, In, Sn, Te, Ba, La, W, Pb, Bi) and 30 (Li, B, Na, Mg, Al, Si, K, Ca, Ti, Zn, Ga, Ge, Rb, Sr, Y, Zr, Nb, Mo, Cd, In, Sn, Te, Cs, Ba, La, Ta, Hf, W, Pb, Bi) elements ( $M \neq \text{Fe}$ ; equal amounts in wt % for each oxide) to which was added a variable amount of  $\text{Fe}_2\text{O}_3$ , ranging from 5 to 25 wt %. Metals were added in the form of oxides, peroxides and carbonates. For mixing and downsizing, starting materials were ball milled (achat mortar and balls; added isooctane for the improvement of mixing) for 2 - 3 h. The average particle size after ball milling was in the same range than found after sintering, as seen by scanning electron microscopy (SEM).

We distinguish two different routes :

***Rout I - ceramic bulk sample preparation*** : The mixture of components was pressed into several pellets yielding a total volume of  $1 \text{ cm}^3$ . The pellets were filled in a ceramic ( $\text{Al}_2\text{O}_3$ ) boat that was placed in a horizontal furnace (quartz tube), heated at a rate of  $150 \text{ K h}^{-1}$ , held at 1126 K for 2 h and then the temperature was reduced at a rate of  $100 \text{ K h}^{-1}$ . An oxygen flow of  $\sim 600 - 800 \text{ mL h}^{-1}$  was passed through the furnace at 1 atm.

After heating period, pellets on average showed a weight loss  $\Delta g$  of  $\sim 10 - 15 \%$ , a shrinkage in diameter of  $10 - 15 \%$  and reduction in thickness of  $\sim 5 - 10 \%$ , and were not deformed. The color appeared to be homogeneous (yellowish - brown). SEM pictures (Figure 6) showed homogeneous polycrystalline samples with a particle size of  $\sim 100 - 900 \text{ nm}$ . Previous to magnetic separation, the reacted samples were ball milled (1.5 h, in isooctane), dried and dispersed (ultrasound) in water containing a surfactant (Decon 90 +  $\text{NH}_4\text{OH}_{(\text{aq.})}$ ). This may result in the loose of some compounds by reaction with water. However, dispersing the samples in water did not give rise to a significant change in pH. For separation, the suspension was first pumped (Figure 3) through an ultrasonic bath before entering the separator column (Figure 3a, 3b).

Surprisingly high yields of magnetically retained grains were obtained (Figure 7) : On

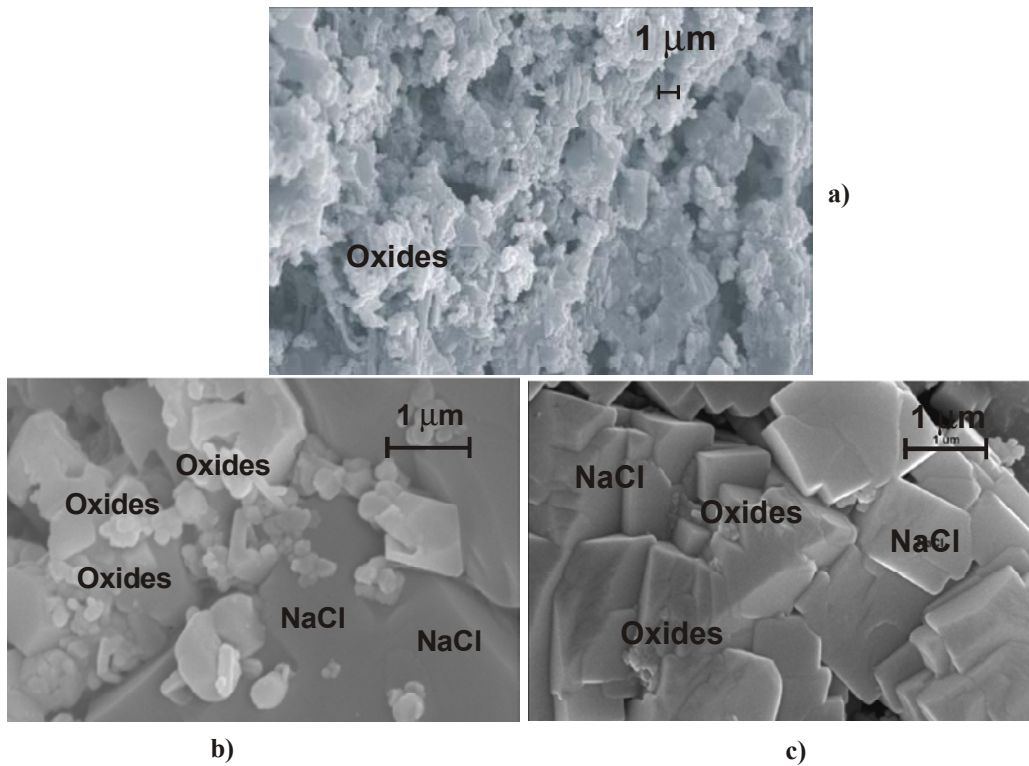


**Figure 6.** SEM micrographs showing the particle morphology for SSC attempts (inside of pellets) a) : 17 oxides including 15 wt % of  $\text{Fe}_2\text{O}_3$ , route I for reaction (see text). b) 17 oxides including 15 wt % of  $\text{Fe}_2\text{O}_3$ , route II (see text). c) Same as b) but prior to reaction : Unreacted oxides particles distributed over the surface of NaCl crystals.

varying the content of  $\text{Fe}_2\text{O}_3$  from 5 - 25 wt %, corresponding yields of 7.5 to 75 wt % were obtained. Passing the separated particles through the columns a second time did not improve present yields significantly. Although ball milling disaggregates intergrown particles, it is likely that diamagnetic material is adheres to ferri- or ferromagnetic crystallites to some extent. The effective yields are thus certainly smaller than shown in Figure 7.

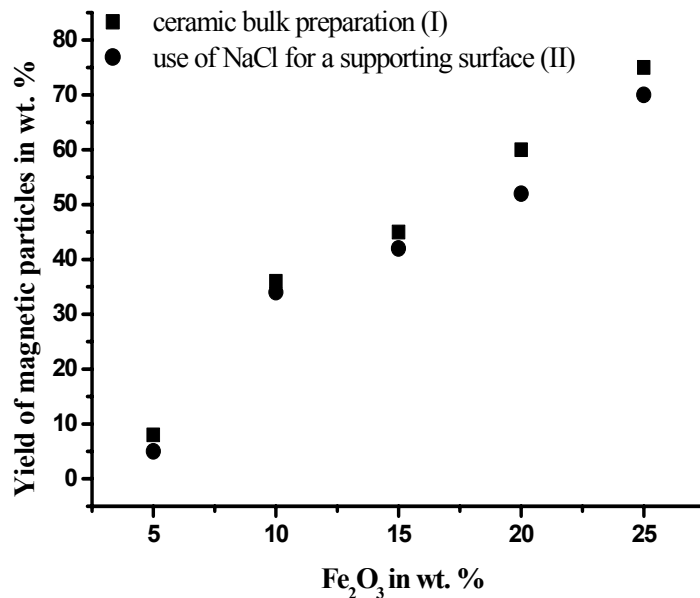


**Figure 7.** Yield of magnetic particles retained by a magnetic separation column shown in Figure 3a. Example of 17 oxides and a variable amount of  $\text{Fe}_2\text{O}_3$ . Results for route I and II (see text) products show very similar yields, although the particle morphologies are clearly different (see Figure 6).

In view of the many compounds which could form (see Figure 1), powder X-ray diagrams did not show as many lines as expected (see Figure 8) : A rather weak scattering intensity of a few of the lines may be indicative for compounds that were preferably formed under the present conditions. Using all data available in the X-ray powder diffraction PDF file, no significant matching with any known compound containing elements we used was possible. Powder diffraction is probably not very helpful in this case for analyzing SSC products as evident from comparing the X-ray diagrams of magnetically separated samples with that of as obtained and residual powder

: In all three cases, the most intense lines present in Figure 8 were present. Changes were only observed for weak lines. However, powder diffraction diagrams revealed an important fact : The starting materials were consumed.

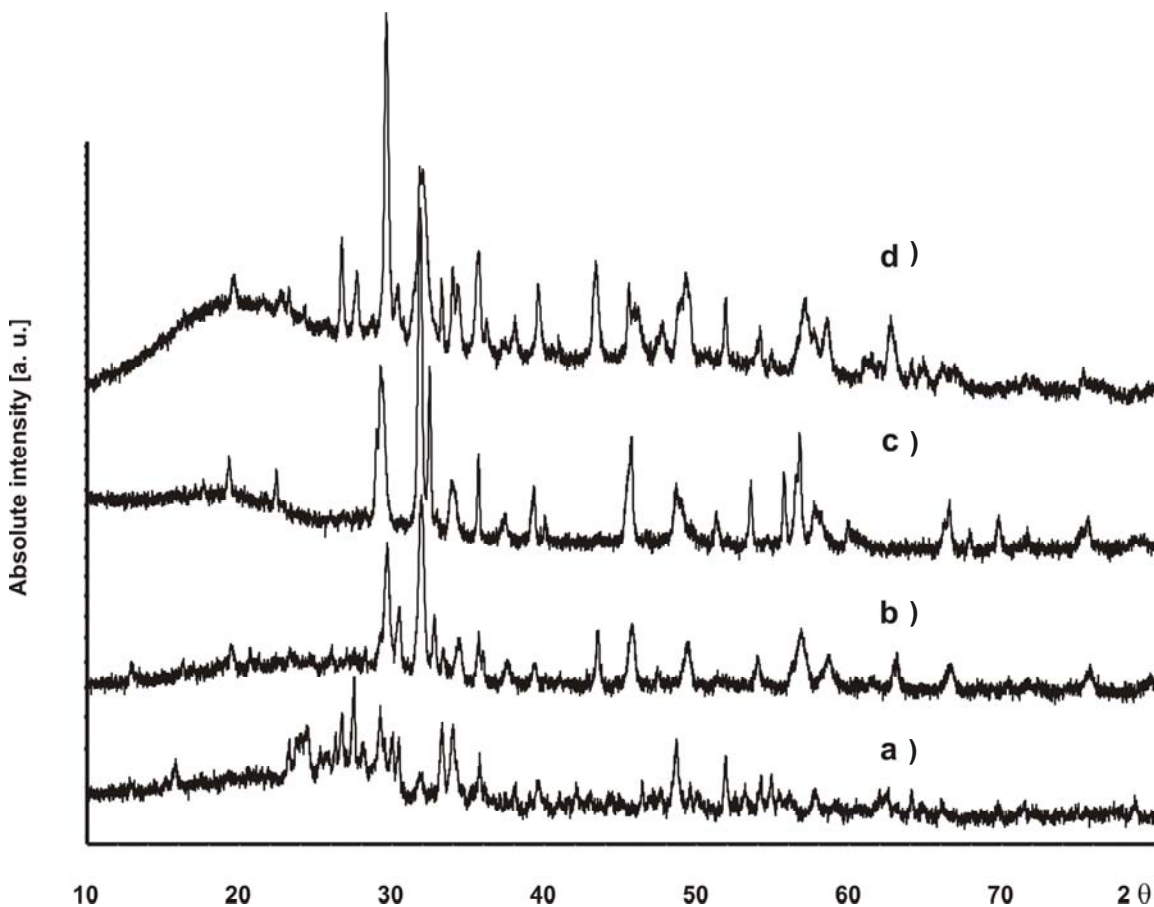


**Figure 8.** X-ray diffraction of SCC samples (17 elements plus 15 wt %  $\text{Fe}_2\text{O}_3$ ) : a) prior to reaction, b) after reaction, c) after magnetic separation, d) reaction performed on NaCl (s).

**Rout II - Use of NaCl for as a supporting surface** : In this case we proceeded in the same way except that an additional ball milling step (2 - 3 h, in isooctane) was applied load the NaCl particles with premixed (ball milled) oxide particles (10 wt % oxides, 90 wt % NaCl; see Figure 6, right). The reaction was performed at a maximum temperature of 1026 K. After heating, the pellets appeared homogeneously colored (dark brown) and showed no significant deformation. We take this for as an indication that also in this case liquid phase formation was not a dominant process. Figure 6 shows the inner surfaces of

typical pellets. Although the reaction temperature was 100 K lower than for route I, the yield of magnetic particles in the case of Fe was nearly the same for both routes. From this we can conclude that local reaction mixtures form various kinds of solid materials. It is likely that on the surface of the NaCl particles a liquid film, which dissolves the oxides, is involved in the reactions and the crystallization of new phases. Figure 6 shows small crystallites ( $\sim 100 - 900 \text{ nm}$ ) on top of much larger NaCl particles. Most of which show crystal faces. The degree of intergrowth can be seen to be much less than found for route I (Figure 6, left). Powder X-ray diagrams of materials obtained from route II are very similar to those obtained by route I, although a difference with respect to weak lines can be seen in Figure 8.

Although higher reaction temperatures can be used when applying a non-reactive support, there are not many salts available. For this purpose  $\text{BaCl}_2$  (melting point : 1236 K) may provide an extension of about 100 K over NaCl. Improvement along to route II would include a reduction in the degree of loading of NaCl particles by oxides in order to obtain

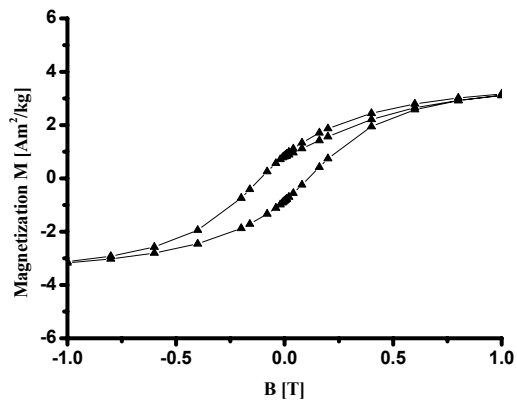
**Table 2.** SQUID measurements for SSC products.

$\text{Fe}_2\text{O}_3$ [wt. %] <sup>[a]</sup>	$m$ [emu] <sup>[b]</sup> /sample weight [mg]	$M_s$ (300 K, $B = 5 \text{ T}$ ) [ $\text{Am}^2\text{kg}^{-1}$ ] <sup>[c]</sup>
10 (I)	0.044/11.1	4.0
15 (I)	0.040/14.9	2.7
15 (II)	0.092/13.5	6.8
20 (I)	0.060/13.7	4.4
25 (I)	0.027/15.1	1.8
$\text{BaFe}_{12}\text{O}_{19}$ <sup>[38]</sup>	0.330/6.12	54 <sup>[d]</sup>

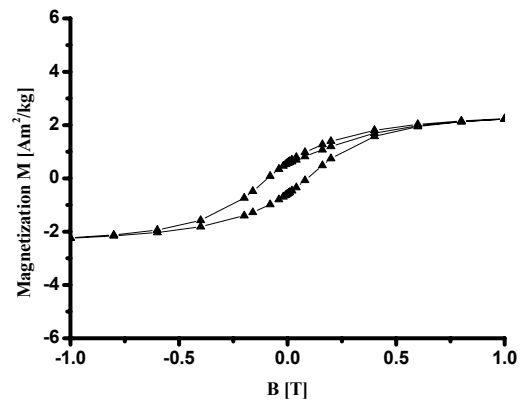
[a] Reaction conditions : 17 nonmagnetic elements and various wt % of  $\text{Fe}_2\text{O}_3$  : Route I and II : See text for method of sample preparation. [b] Measured on Quantum Design SQUID magnetometer (XL 5S) at 300 K.  $m$  = magnetic moment. [c]  $M_s$  = saturation magnetization; for simple Fe oxides :  $M_s \leq 100$  (300 K).<sup>[36]</sup> [d] 76 gauss  $\text{cm}^2 \text{g}^{-1}$ ,  $B = 0.6 \text{ T}$ , extrapolated to zero Kelvin.<sup>[39]</sup>



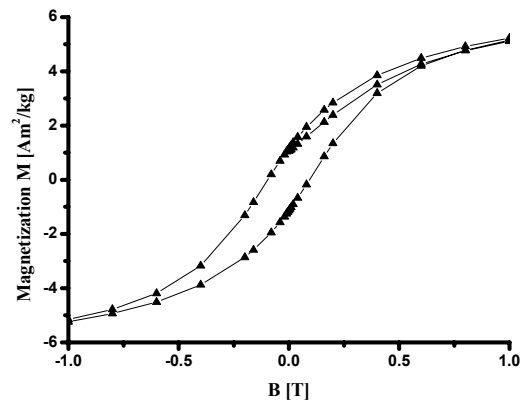
a lower degree of aggregation of product particles, preferably many single particles. A low degree of aggregation will be needed to be able to use *single-particle analyses* (compositional and structural). Confirmation for the existence of ferri- or ferromagnetic materials was obtained from susceptibility measurements (7.5, 10, 15, 20 wt % Fe<sub>2</sub>O<sub>3</sub>; 17 M<sub>x</sub>O<sub>y</sub>, route I, and 15 wt % Fe<sub>2</sub>O<sub>3</sub> route II) : Hysteresis loops were recorded (Figure 9). Table 2 summarizes the data obtained for the SSC attempts for a different amount of Fe<sub>2</sub>O<sub>3</sub>. Because superparamagnetic behavior is expected for iron oxides with a particle size smaller than about 10 nm, <sup>[36]</sup> we assume that the present particles (on average 10 - 90 times larger), are in the ferro- or ferrimagnetic state. When we have many hysteresis loops characterizing the individual compounds of a mixture, there are upper and lower limits for  $M_s$ , (saturation magnetization),  $M_{rem}$  (remanent magnetization) and  $H_c$  (coercive field). The superposition of all data can result in a rather narrow hysteresis curve, as shows in Figure 10 : For a mathematical demonstration we have taken a tangens hyperbolic to approximate a hysteresis loop :  $M \approx \alpha \tanh (\beta \cdot H + \gamma)$ , where values for  $\alpha$ ,  $\beta$ ,  $\gamma$  were selected randomly from fixed intervals to generate a large number of curves which were summated. The present samples have a saturation magnetization, which is about 5 – 10 % of a strongly magnetic reference material (BaFe<sub>12</sub>O<sub>19</sub>). This may be interpreted in two ways : 1) SSC syntheses produce mostly weak ferri- or ferromagnetic materials, or 2), there are large individual  $M_s$  components, but adherent nonmagnetic particles reduce the  $M_s$  value. Interestingly, samples of 15 wt % Fe<sub>2</sub>O<sub>3</sub> (route I and II) feature almost the same particles yield (see Figure 7), but the synthesis with NaCl has produced a materials with a much higher  $M_s$ .



a)



b)



c)

**Figure 9.** Hysteresis loops for typical SSC products. All measurements started at  $B = 0$  T ( $T = 300$  K). Loops were recorded after magnetic separation by the separator, as shown in Figure 3a. a) 10 wt %  $\text{Fe}_2\text{O}_3$  plus 17 elements, ceramic route I; b) 15 wt %  $\text{Fe}_2\text{O}_3$  plus 17 elements, ceramic route I; c) 15 wt %  $\text{Fe}_2\text{O}_3$  plus 17 elements on NaCl, route II.

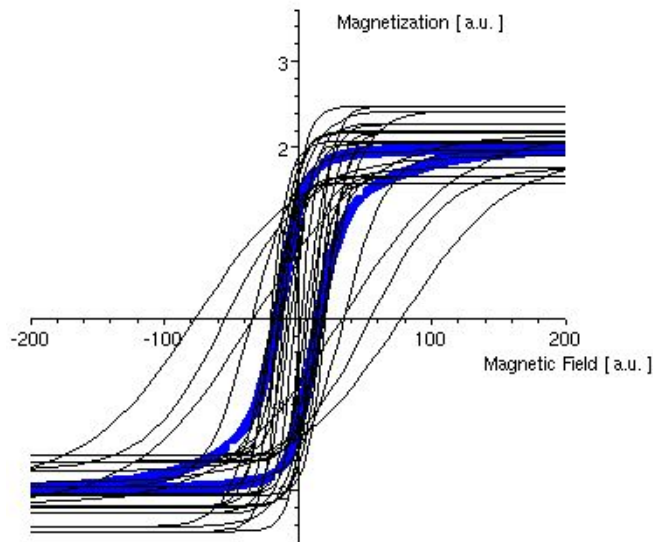


**Figure 10.** Numerical example showing how a large number of individual hysteresis loops can summed to form observable curve (see Figure 9) for samples containing many different particles in the magnetic state. Compared to possibly occurring  $H_c$  fields, the average field  $\langle H_c \rangle$  may be much smaller than the individual  $H_c$  fields. Number of summed curves 15 (tanh function assumed).

To gain inside into the elemental distribution of the particles, we performed qualitative elemental analyses using scanning electron microscopy (see Table 3). As some elemental emission lines overlap, we extracted those of the most elements present.

**Table 3.** Results of qualitative analysis of the particles using scanning electron microscopy.<sup>[a]</sup>

Grains	Main elements detected <sup>[b]</sup>	Compounds from literature <sup>[c]</sup>
1	Fe > Mg, Ca > Sr, Si > Pb	MgFe <sub>2</sub> O <sub>4</sub> , CaFe <sub>15</sub> O <sub>25</sub> , MoFe <sub>2</sub> O <sub>4</sub> ,
2	Fe > Ca, Mg, Sn > Sr, Ba, Bi	SrFe <sub>12</sub> O <sub>19</sub> , Ca <sub>2</sub> MoFeO <sub>6</sub> , Li <sub>5</sub> Fe <sub>2.5</sub> O <sub>4</sub> ,
3	Fe > Ca, Mg > Sn, Pb	Y <sub>3</sub> Fe <sub>5</sub> O <sub>12</sub> , PbFe <sub>12</sub> O <sub>19</sub> , Sr <sub>2</sub> MoFeO <sub>6</sub> ,
4	Fe, Mg, Ca > Sr, Nb	Ba <sub>1.6</sub> Sr <sub>0.4</sub> MoFeO <sub>6</sub> ,
5	Fe, Ca > Pb	Ba <sub>1.28</sub> Sr <sub>0.32</sub> La <sub>0.4</sub> MoFeO <sub>6</sub> , Nb <sub>0.5</sub> PbFe <sub>0.5</sub> O <sub>3</sub> ,
6	Ca > Fe > Sr, Mg	...
7	Fe, Ca, Mg > Y, W	
8	Ca > Fe, Mg > La, Mo, Si	

[a] Elements used for SSC : SSC: Fe, Li, Na, Mg, Si, K, Ca, Sr, Y, Nb, Mo, Sn, Te, Ba, La, W, Pb, Bi. [b] Elements are listed in order to abundance; an energy dispersive spectrometer (Noran IX NSS 200) was used. [c] Main compounds found in the literature with  $T_c > 300$  K ( $q \geq 2$ ) containing elements used in this study.

Clearly, these randomly selected grains mostly reflect Fe-oxides formed by Ca, Mg, and Sr, as well as Sn, Pb and other elements. Known compounds ( $T_c > 300$  K, Table 3) contain mostly Ca, Mg, Sr, Ba, Mo, Pb, and Y, and also Sn, La and Nb. Of the 17 elements we have used, only K, Te, and Li (not detectable) were not found. From the small number of grains we examined at we at least can conclude that the SSC produced typical Fe-oxides.

### 3.4. Conclusions

As “ all chemical compounds capable of existence (with a certain lifetime) are already present on the energy landscape, and are just waiting to be discovered ”<sup>[1]</sup>, all we have to do is effective and property-directed procedures for preparing and isolating compounds of interest. In view of large phase space (compositions,  $T$ ,  $P$ , and also time) given by a combinatorial function determining the number of phase diagrams ( $N_q^{PD}$ ), and an unknown number ( $\eta_q$ : which may be accessible by using theoretical methods<sup>[37]</sup>) of thermodynamically stable/metastable compounds appearing in the phase diagrams, it is logical that only a combinatorial approach based on combinatorial functions of the same power may provide access to a principally existing chemical diversity. We have demonstrated that the number  $N_n^C$  of local configurations can be larger than the number  $N_q^{PD}$  of local phase diagrams, and that the number of grains (including their size distribution) can even exceed the number of  $\eta_q \approx 100$  times  $N_q^{PD}$ .

A second innovation with respect to materials chemistry concerns the application of magnetic separation columns, which can attain extremely high separation efficiency for strongly magnetic materials. The combination of SSC synthesis and magnetic separation is thus considered a new approach for detecting *traces* of magnetic and probably also superconducting materials.

So far, we have focused on thermodynamically stable compounds. The present concept however, is also suited as well to obtain transient products, merely by the application of short-term reaction techniques from the field of ceramic materials. Summarizing experimental results, we have shown that we can obtain high yields of magnetic particles in the case of Fe-based oxides. This is reflected by comparison of our results with those in the literature.

With the aim of finally knowing the chemical composition of SSC products, we are working on lead elements  $E_L$  which may provide *a very low yield* of product grains. This brings the analysis of individual grains within practical feasibility. There are two

evident goals of interest : A  $T_c > 300$  K for i) ferri- or ferromagnetic oxides involving Cu, and ii) oxide superconductors.

### **3.5. Acknowledgements**

J. H. would like to thank the MPI for Solid-state Research, Stuttgart (group of Professor A. Simon), for the opportunity of a sabbatical in 2000, where the SSC work was started and first presented (18. July. 2000). We thank Dr. L. Kienle and B. Frey for the microscopy analysis, Professor S. Decourtins for the use of susceptibility equipment, Dr. W. Marx and T. Samtleben for data literature search, C. Belandinelli for calculating the hysteresis loop and B. Trusch for technical assistance.

### 3.6. References

- [1] M. Jansen, *Angew. Chem.* **2002**, *114*, 3896 – 3917; *Angew. Chem. Int. Ed.* **2002**, *41*, 3746 - 3766.
- [2] J. J. Hanak, *J. Mater. Sci.* **1970**, *5*, 964 - 971.
- [3] B. Jandeleit, D. J. Schaefer, T. S. Powers, H. W. Turner, W. H. Weinberg, *Angew. Chem. Int. Ed.* **1999**, *38*, 2494 - 2532.
- [4] W. F. Maier, G. Kirsten, M. Orschel, P.-A. Weiss, A. Holzwarth, J. Klein, *Comb. Chem. Mater. Polym. Catal. ACS. Symp. Ser.* **2002**, *814*, 1 - 21.
- [5] E. Dainelson, X. D. Wu, *Science*, **1998**, *279*, 837 - 839.
- [6] E. J. Amis, X-D. Xiang, J-C. Zhao, *MRS. Bull.* **2002**, *27*, 295 - 297(issue on combinatorial material science).
- [7] S. H. DeWitt in *Combinatorial Chemistry: Synthesis and Application*, (Eds. : S. R. Wilson, W. Czarnik), Wiley-Interscience, New York, **1997**, pp. 25 - 38.
- [8] C. L. Chen, P.S. Strop, M. Lebl, K. S. Lam in *Combinatorial Chemistry*, (Eds. : J. N. Abelson, M. I. Simon Academic Press, *2nd ed.* New York, **2003**, pp. 211 - 219.
- [9] F. J. DiSalvo, *Pure Appl. Chem.* **2000**, *72*, pp. 1799 - 1807.
- [10] C. P. Poole, Jr, A. P. Ramirez, P. C. Canfield in *Superconductivity*, (Ed. : C. P. Poole, Jr.), Academic Press, New York, **2000**, pp. 71 - 108.
- [11] a) B. O. Mysen in *Phase Diagrams for Ceramists, VIII*, ACS, Ohio, 1990; b) L. P. Cook, H. F. McMurdie, H. M. Ondik, K. M. Kessell, M. J. Rodtely in *Phase Diagrams for Ceramists, VII*, ACS, Ohio, **1998**; c) R. S. Roth, J. R. Diennis, H. F. Mc Murdie in *Phase Diagrams for Ceramists, VI*, ACS, Ohio, **1987**; d) R. T. Negas, L. P. Cook in *Phase Diagrams for Ceramists, V*, ACS, Ohio, **1983**; e) L. P. Cook, R. Lowrance in *Phase Diagrams for Ceramists, IV*, ACS, Ohio, **1981**; f) E. M. Levin, H. F. Mc Murdie in *Phase Diagrams for Ceramists, III*, ACS, Ohio, **1975**; g) E. M. Levin, C. R. Robbins, H. F. Mc Murdie in *Phase Diagrams for Ceramists, II*, ACS, Ohio, **1969**; h) E. M. Levin, C. R. Robbins, H. F. Mc Murdie in *Phase Diagrams for Ceramists*, ACS, Ohio, 1964, *II*.
- [12] A. Carlsson, T. Oku, J. -O. Bovin, R. Wallenberg, J.-O. Malm, G. Schmid, T.

- Kubicki, *Angew. Chem.* 1998, 110,1275 – 1278; *Angew. Chem. Int. Ed.* **1998**, 37,1217 - 1220.
- [13] “The Physical Principles of Magnetic Separation” J. Svoboda in *Magnetic Methods for the Treatment of Minerals*, Elsevier, Amsterdam, **1987**, pp. 1 - 76.
- [14] J. Boehm in *Ind. IEEE. Transform. Appl. Supercond.* **2000**, 10, 710 - 715.
- [15] T. Ohara, S. Mori, Y. Oda, Y. Wada, O. Tsukamoto, *Trans. IEE*, **1996**, 166-B, 979 - 986.
- [16] T. Nomizu, K. Yamamoto Tsukamoto, M. Watanabe, *Ana. Sci.* **2001**, 17, i177 - i180.
- [17] K. C. Karli, E. R. Whitby, S. V. Patankar, C. Winstead, T. Ohara, X. Wang, *Appl. Math. Model.* **2001**, 25, 355 - 373.
- [18] G. Gillet, F. Diot, *Miner. Metall. Process.* **1999**, 16,1 - 7.
- [19] V. D. Sidorenko, I. A. Gerasimenko, A. M. Kutin, V. B. Yupherov, Ye. I. Skibenko, V. V. Gladky, *IEEE Trans. Magn.* **1996**, 32, 2691 - 2694.
- [20] L. M. Besley, *Ceram. Dev. Mater. Sci. Forum*, **1988**, 34/36, 941 - 945.
- [21] S. Vieira, A. Aguiló, M. Hortal and M. Pazos, *J. Phys. E: Sci. Instrum.* **1987**, 20, 292 - 293.
- [22] M. Barsoum and D. Patten, S. Tyagi, *Appl. Phys. Lett.* **1987**, 51, 1954 - 956.
- [23] K. Hayashi, Y. Yokota, S. Morita, N. Hanada, S. Hayashi, *Jpn. J. Appl. Phys.* **1988**, 27, 856 - 861.
- [24] E. Oba, H. Miyajima, Y. Ishikawa, S. Haseyama, S. Yoshizawa, *Physica C.* **1991**, 185/189, 489 - 490.
- [25] S. Labroo, Y. Ebrahimi, J. Y. Park, W. J. Jeh, *IEEE Trans. Magn.* **1992**, 28, 1895 - 898.
- [26] A. C. Pierre, K. MA, *Eur. J. Solid State Inorg. Chem.* **1993**, 30, 1083 - 1094.
- [27] S. Labroo, J. Y. Park, R. J. Kearney, W. J. Jeh, *Cryogenic*, **1993**, 33, 1063 - 1065.
- [28] J. H. P. Watson, *J. Appl. Phys.* **1973**, 44, 4209 - 4213.



- [29] L. Bolt, J. H. P. Watson, *Supercond. Sci. Technol.* **1998**, *11*, 154 - 161.
- [30] M. Marinelli, G. Morpurgo, G. L. Olcese, *Physica C*, **1989**, *157*, 149 - 158.
- [31] E. J. Griffith, *Cake Formation in Particulate Systems*, VCH. New York, **1991**.
- [32] J. S. Reed in *Principle of ceramic processing*, New York, *2nd. Ed.* **1995**, pp. 135 - 1995.
- [33] M. A. Abdelgadir, L. Chow, *Hyperfine Interact.* **1999**, *121*, 507-512.
- [34] M. A. Abdelgadir, R. S. Burrows, *J. Mater. Res.* **1996**, *11*, 1804 - 1809.
- [35] R. S. Burrows, D. H. McDaniel, M. Abdelgadir, *J. Magn. Magn. Mater.* **1993**, *125*, 269 - 271.
- [36] R. M. Cornell, H. C. U. Schwertmann in *The Iron Oxides*, Wiley-VCH, Weinheim, *2nd. Ed.* **2003**, pp. 121 - 123.
- [37] N. Saunders, A. P. Miodownik in *CALPHAD-Calculation of Phase Diagrams a Comprehensive Guide*, Elsevier, Oxford, 1998, *1*.
- [38] P. Kersch, R. Grössinger, C. Kussbach, R. Sato-Turtelli, K. H. Müller, L. Schultz, *J. Magn. Magn. Mater.* **2002**, *242 - 245*, 1468 - 1470.
- [39] H. P. J. Wijn in *Landolt-Börnstein*, (Ed. : K. H. Hellwege), Springer, New York, **1970**, *4*, pp. 572 - 576.

## 4. “Single Sample Concept”: Theoretical Model for a Combinatorial Approach to Solid-State Inorganic Materials

J. Hulliger, M. A. Awan, *J. Comb. Chem.* 2005, 7, 73 - 77.

### 4.1. Abstract

A theoretical model for a “single sample concept” (SSC) applied to the combinatorial chemistry of solid-state inorganic compounds is presented. The SSC is performed by reacting  $N$  starting materials (randomly mixed) in a single sample of  $\sim 1 \text{ cm}^3$ . Combinatorial calculations demonstrate that the number of reasonably estimated phases to be found in the space of  $N$  components grouped into compounds (e.g. oxides, sulfides or halogenides) containing up to  $q \leq 6$  metallic elements is smaller than combinations set up by starting conditions for local reactions within the bulk of a single ceramic sample. Recently, the SSC proved to work in the case of synthesizing libraries of 3d metal oxides, from which magnetic particulate matter was extracted by a magnetic separation technique. The SSC may be applied in a first screening cycle followed by 2D approaches of combinatorial chemistry.

### 4.2. Introduction

Following up just combinatorial arguments to combine elements for reactions into solid-state compounds, properties of combinatorial functions make it impossible to set up all compositions in real experiments.<sup>1-4</sup> In view of a limited amount of chemicals available we may conclude to have therefore no access to the manifold of possibly existing compounds generated by combinatorial functions. However, present knowledge bears no evidence for a realization of most combinatorial compositions by thermodynamically stable compounds<sup>5</sup>: The number of compounds appearing in binary, ternary, etc. phase

diagrams is by far not as high as combinatorial variations of elements and stoichiometry would allow.

There are further issues related to the dimension of the phase space we have to enface by synthesis: (i) As reflected by minerals and entries for synthetic compounds in databases, there is no evidence for particularly numerous compounds made of *many* constitutional ( $q$ ) (for a list of symbols, see Appendix) elements.<sup>2,6</sup> (ii) With respect to physical properties, all known effects (magnetism, ferroelectricity, superconductivity and many others) were obtained for a *low* number  $q$  of constitutional metallic elements ( $q \leq 4$ , e.g. for metals in oxide materials).<sup>5,6</sup> This let us anticipate that for finding new materials featuring interesting physical properties, we most likely will not need compounds made of, say  $q$  larger than 6 or even more metallic elements.

By reasonable arguments we may thus set an upper limit for the number  $q$  of constitutional elements in compounds to be found by combinatorial chemistry. Redefined as such, combinatorial searches for new inorganic solid-state materials become a feasible endeavor, provided combinatorial functions representing the experimental method reach the same order of combinations as those describing a realistic number of existing compounds. In the following chapters we introduce a theoretical model demonstrating that local reactions taking place within a single ceramic sample (made by mixing up  $N$  components) can provide access to existing compounds in a high dimensional phase space.

Present combinatorial techniques rely on 2D plate techniques,<sup>6,7</sup> in which the number of experiments performed in parallel is limited by the number of spots on a plate.

Recently, a single sample concept (SSC) operating on the basis of using a random mixture of  $N$  starting materials making up a single sample of  $\sim 1 \text{ cm}^3$  was presented.<sup>5</sup> Experimental implementation has demonstrated the syntheses of libraries for ferri- or ferromagnetic oxides: Mixtures made of 17 (Li, Na, Mg, Si, K, Ca, Sr, Y, Nb, Mo, Sn, Te, Ba, La, W, Pb, Bi), 24 (Li, B, Na, Mg, Al, Si, K, Ca, Ti, Ga, Ge, Sr, Y, Zr, Nb, Mo, In, Sn, Te, Ba, La, W, Pb, Bi) and 30 (Li, B, Na, Mg, Al, Si, K, Ca, Ti, Zn, Ga, Ge, Rb, Sr, Y, Zr, Nb, Mo, Cd, In, Sn, Te, Cs, Ba, La, Ta, Hf, W, Pb, Bi) nonmagnetic oxides containing 5 - 25 wt % of  $\text{Fe}_2\text{O}_3$  (all had the others same amount in wt. %) were pressed

into pellets and reacted at  $T = 850 \text{ }^\circ\text{C}$  (for 4 h,  $p(\text{O}_2) = 1 \text{ atm}$ ), to effect local reactions inbetween all kinds of combinations of grains represented by  $N + 1$  different elements. After the reactions, ball milling was used to liberate the manifold possible compounds to prepare a suspension to pass through a magnetic separation column. Through the effect of a magnetic field gradient ferri- or ferromagnetic particles were extracted up to 75 wt % for 25 wt % of  $\text{Fe}_2\text{O}_3$ , and  $N = 17$ . Single-grain analyses performed by scanning electron microscopy revealed a library consisting of individual grains representing magnetic Fe oxides. Bulk susceptibility measurements confirmed hysteresis loops. To improve the formation of single grains, reactions were also performed using NaCl (90 wt %) particles loaded by oxides (10 wt %). In the case of cuprates, single sample reactions as described

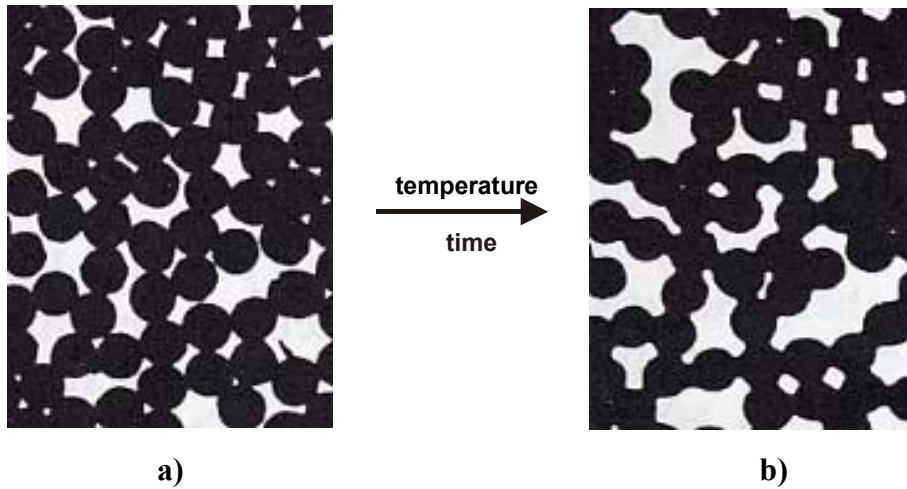


**Figure 1.** Displacement and states of densification of spherical copper particles of the same size. (a) 1 min at  $T = 1273 \text{ K}$ , (b) 12 hours at  $T = 1273 \text{ K}$ . Original diameter:  $30 \text{ }\mu\text{m}$ . (a) Binary contacts present at the beginning, on time more and transform into a clustered state (b). After ref. 9 a.

above ( $N$ : Ca, Sr, Y, Ba, La, Tl, Pb, Bi, Cu) have produced superconductivity up to 100 K (confirmed by measuring the resistance and a Meissner effect).<sup>8</sup> For more details on the preparation and analysis of magnetic libraries, see ref. 5.

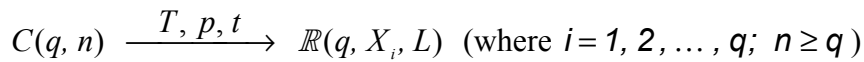
### 4.3. The SSC : Assumptions and Basic Ideas

The present concept uses ceramic samples, that is an assembly of densely packed grains of many ( $N$ ) starting materials, which are brought to reaction by thermal activation (calcination). As known from studies on the densification of assemblies of grains<sup>9</sup> (Figure 1), we can assume local reactions inbetween grains in spatial proximity.

In traditional ceramic synthesis just a small number  $N$  of components ( $N \sim 2 - 4$ ) are brought to reaction.<sup>9</sup> Consequently, local densification can produce a stable product nearly at any place within a sample, at least after a long time of reaction. By SSC a large number  $N$  of starting materials are randomly mixed in order to effect local reactions which may produce a high variety of products across just one sample of a volume of  $\sim 1 \text{ cm}^3$ . This because of a randomly constituted neighborhood of grains (called a *local configuration: C*) representing different elements and corresponding masses. In Figure 2, we show randomly mixed spheres in 2D to illustrate local configurations : in particulate matter (panel a :  $N = 2$ , panel b :  $N = 6$ ).

A local configuration is thus made up of  $n$  grains of  $q$  different elements which can locally react to a compound  $\mathbb{R}(q, X_i, L) \equiv E_{x_1}(1)E_{x_2}(2)E_{x_3}(3) \cdots E_{x_q}(q)E_{x_L}(L)$  ( $E_L$  : lead element, e.g. oxygen, sulfur or halogens).

Local reactions



produce a library, obtained at conditions of  $T$ ;  $p$ ; and reaction time  $t$ .

Breaking crystallites apart by milling reacted ceramic samples liberates single phase and intergrown crystallites, which can be characterized by local probe techniques (electron microscopy) providing a lateral resolution of a few hundred nanometers.

The SSC is particularly of interest for searching materials featuring magnetic properties (ferri- or ferromagnetic or superconducting) because of the application of magnetic separation techniques<sup>10-12</sup> to extract minor quantities of grains retained by magnetic separation columns.<sup>5</sup>

Conceptually, SSC may be performed in two ways: (i)  $N$  starting materials are mixed in equal portions with no preference for a metallic lead element ( $E_L$ ). (ii) Adding a larger

quantity of a metallic  $E_L$  statistically enhances formation of products containing element  $E_L$ . Presently we apply path (ii) for searching ferri- /ferromagnetic or superconducting metal oxides of  $E_L$  (Fe, Co, ... etc; Cu, respectively) formed by compounds involving other nonmagnetic elements. For a brief summary on first results, see the Introduction. Summarizing, the SSC is performed by following up a scheme as shown in Figure 3. In the search for new magnetic or superconducting materials SSC<sup>5</sup> may thus be applied as a primary screening followed by a 2D secondary screening, mode. However, as indicated by arrows, SSC bears the possibility of a convergent procedure, reducing the number of starting materials ( $N$ ) per cycle.

#### 4.4. Combinatorial Model

Given  $N$  chemically different components (starting materials), the number  $N_q^{PD}$  of phase diagrams constituted by  $q$  components ( $q \in N$ ) is equal to the number of combinations made up by  $q$  elements selected out of  $N$  (multiple selections of a single element being not allowed).<sup>13</sup>

$$N_q^{PD} = \frac{N!}{q!(N-q)!} . \quad (1)$$

Each of these phase diagrams contains a number  $\eta_q$  of phases involving  $q$  elements. On average, phase diagrams of the order  $q$  contain  $\langle \eta_q \rangle$  phases, representing basic structural types of compound classes to be found. The total number of phases  $N^P$  ( $q \geq 2$ ) in SSC samples attempted to produce is given by:

$$N^P = \sum_{i=2}^q \langle \eta_i \rangle N_i^{PD} . \quad (2)$$

The number of experiments set up by whatever combinatorial procedure has thus to provide combinations for starting materials that are at least as numerous as  $N^P$ , including a broad variation in the number of locally available components (stoichiometry).

The basic requirement is met by the number  $N_n^C$  of local configurations  $C$ , which reads as :

$$N_n^C = \binom{N + n - 1}{n} - N \quad (3)$$

(combinations including multiple selections of the same element).

Here,  $n$  is the number of grains associated with a particular  $C(q, n)$  ( $n \geq q$ ). The second term in eq (3) accounts for those configurations that contain a single element; these do not yield products.

Variable  $n$  is a characteristic quantity representing the local degree of close packing of grains in an unreacted ceramic sample. The occurrence of  $C(q, n)$ s follows a distribution for which we define an average number  $\langle n \rangle$  of grains in  $C(q, n)$ s.

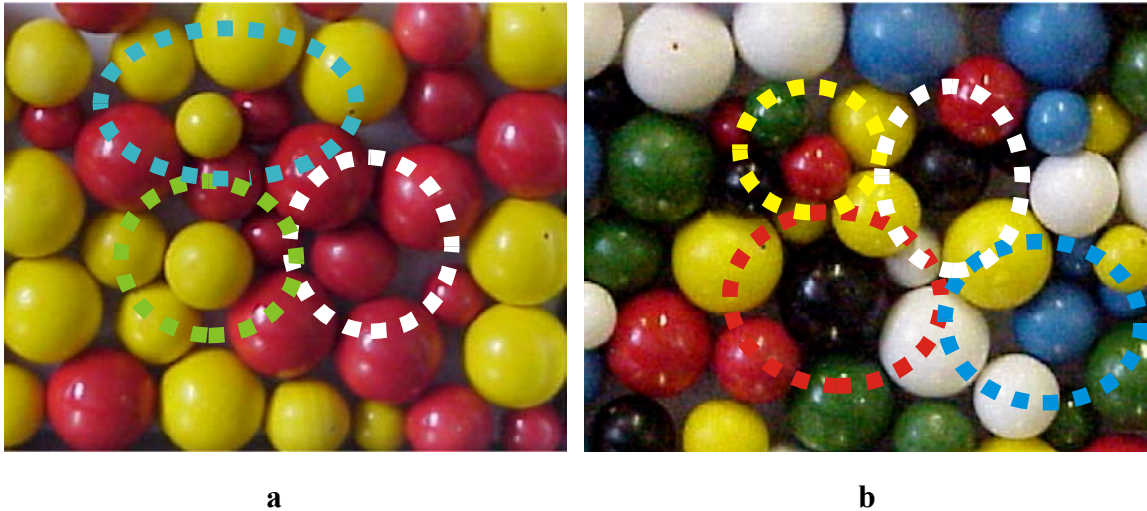


**Figure 2.** 2D random packing of spheres of different colors and sizes: a) Two components, b) six components. Indicated are local arrangements of spheres in close proximity (called a local configuration  $C$ ). It is assumed that *locally* products are formed upon configurations of particles. Note that particles may belong to different configurations (sharing mass through reactions).

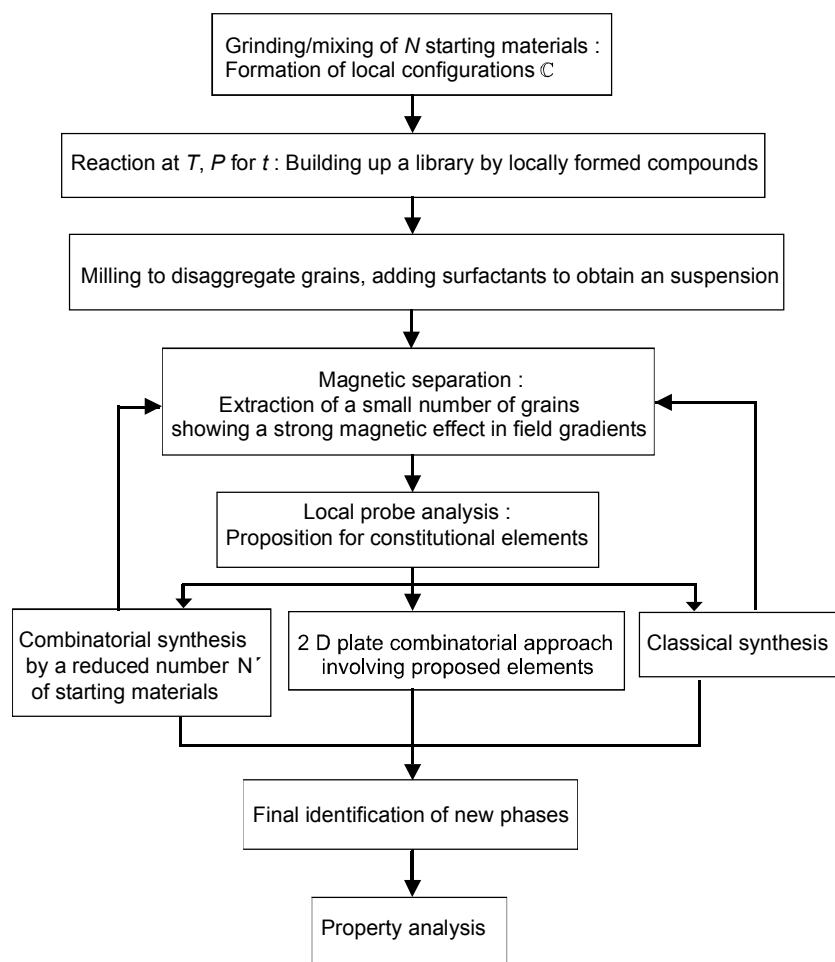


**Figure 3.** Schematic summary of how to process the *single sample concept* in the case of a property oriented search for *magnetic* materials.

An estimation of  $\langle n \rangle$  for a real sample may be obtained by models developed in the case of randomly packed spheres of equal size.<sup>14 - 16</sup> Figure 4 was generated from literature data<sup>14</sup> showing a correlation between the mean voidage  $\langle \varepsilon \rangle$  (porosity) and the average coordination number  $\langle \tilde{n} \rangle$  (number of spheres around a selected one being in close contact with neighbors). For various types of random packs of equal spheres  $\langle \varepsilon \rangle$  vary in the range of 0.36 to 0.44.<sup>14</sup> However, grains in SSC samples are pressed into dense pellets. In this case we can assume a smaller  $\langle \varepsilon \rangle$  than found in studies of the packing of spheres. Consequently, we assume a  $\langle n \rangle = \langle \tilde{n} \rangle + 1$  above a value of 8 (see Figure 4).



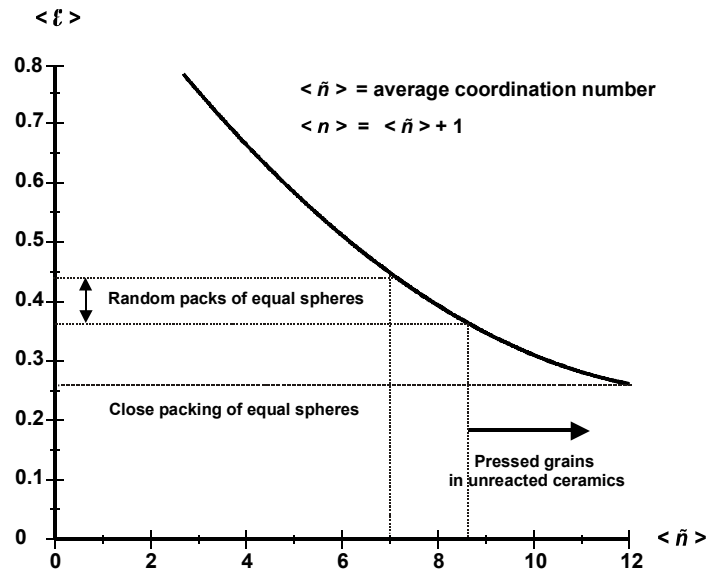


**Figure 4.** Correlation between the voidage (porosity)  $\langle \epsilon \rangle$  and the coordination number  $\langle \tilde{n} \rangle$  for randomly packed spheres of equal size.<sup>17</sup> For pressed unreacted ceramic samples we can assume a  $\langle \tilde{n} \rangle$  larger than found for studies on spheres no pressure was applied.

For providing a large reservoir of grains from which configurations randomly form during grinding/mixing of components, a grain size in the range of 10 down to 1  $\mu\text{m}$  is suitable because in one  $\text{cm}^3$  there are  $\sim 10^9$  to  $10^{12}$  grains,<sup>17</sup> respectively. A high number of starting grains allow one to set up possible configurations many times. The realization of configurations by a distribution for the grain size provides stoichiometric variation. This is considered very important, because stoichiometric variation is needed to explore corresponding phase diagrams defined by  $q$  elements within a configuration. Exploration of phase diagrams of the order  $q$  becomes effective also through  $C(q, n)$ 's ( $n > q$ ), even for  $\langle \eta_q \rangle$  values that are fairly high.

Because the SSC does not attempt to produce large quantities of single-phase products, minor quantities of new phases can be obtained by population of a limited number of trajectories in phase diagrams of the order  $q$ . This is because phases  $\mathcal{R}_i$  ( $i = 1, 2, \dots, \eta_q$ ) appear in compositional domains (fields, volumes and higher dimensional space) that are more likely to hit by a random choice of compositions than by finding lines or points. In Figure 5, we illustrate how randomly selected compositions

(through  $C(q,n)$ 's with  $n > q$  or the grain size distribution) may fall into existence fields of phases: For producing a minor quantity of phases  $\mathbb{R}_1$ ,  $\mathbb{R}_2$  and  $\mathbb{R}_3$ , in principle, just a small number of trials is necessary. Applied to higher order ( $q > 2$ ) diagrams, we can say that the number  $\eta_q$  of existing phases (given  $T$  and  $p$ ) can be explored by a number of compositional combinations that is in the same order as  $\eta_q$  ( $q = 2, 3, \dots$ ), however, preferably much larger in real experiments.

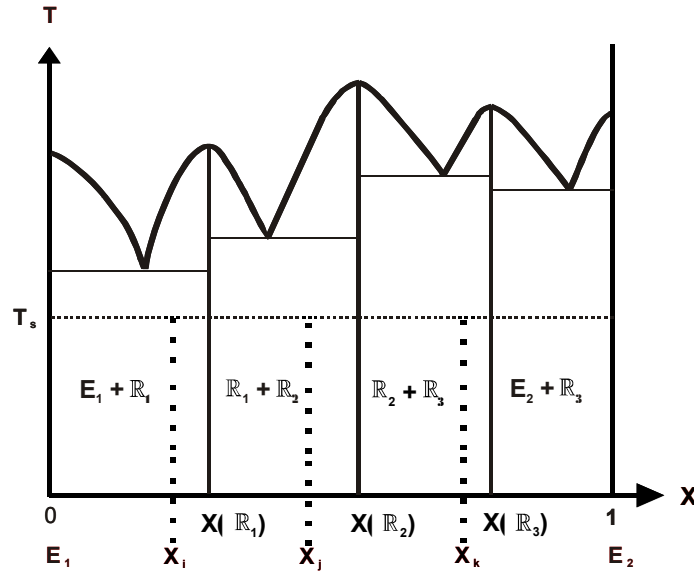


**Figure 5.** A schematic binary phase diagram of components  $E_1$  and  $E_2$  showing the existence fields of three phases ( $\mathbb{R}_1$ ,  $\mathbb{R}_2$  and  $\mathbb{R}_3$ ). Because of existence fields, two randomly selected compositions ( $X_i$  and  $X_k$  or  $X_j$  and  $X_k$ ) can produce minor quantities of  $\mathbb{R}_1$ ,  $\mathbb{R}_2$  and  $\mathbb{R}_3$ . This illustrates, that for finding phases we do not necessarily need to hit the stoichiometric composition ( $X(\mathbb{R}_1)$ ,  $X(\mathbb{R}_2)$ ,  $X(\mathbb{R}_3)$ ) on the X axis.  $T_s$  : Subsolidus temperature for reaction.

In case the number of grains  $N_E$  available for each element  $E$  is by orders of magnitude larger than necessary to populate each  $C(q,n)$ 's, *stoichiometric* variation is brought into the configurations by the distribution for the grain size. A large excess of grains is similarly in favor of a processable number of product grains that is grain to be isolated after passing a suspension through a separation column.

Table 1 provides calculated values for  $N_q^{PD}$  and  $N_n^C$ , ( $N \leq 40$ ): Using an average grain size  $\langle d \rangle$  in the range of 1  $\mu\text{m}$ ,  $C(q, n)$ s may be realized more than  $10^8$  ( $N = 10, n \geq 8$ ) to  $10^4$  ( $N = 40, n \geq 8$ ) times, depending on the number,  $N$ , of starting materials involved.

$N$	$q$	$N_q^{PD}$	$\langle n \rangle$	$N_n^C$
10	4	$2.1 \times 10^2$	6	$4.9 \times 10^3$
			8	$2.4 \times 10^4$
	6	$2.1 \times 10^2$	10	$9.2 \times 10^4$
20	4	$4.8 \times 10^3$	6	$1.8 \times 10^5$
			8	$2.2 \times 10^6$
	6	$3.9 \times 10^4$	10	$2.0 \times 10^7$
30	4	$2.7 \times 10^4$	6	$1.6 \times 10^6$
			8	$3.9 \times 10^7$
	6	$5.9 \times 10^5$	10	$6.4 \times 10^8$
40	4	$9.1 \times 10^4$	6	$8.1 \times 10^6$
			8	$3.1 \times 10^8$
	6	$3.8 \times 10^6$ calcd by eq 1	10	$8.2 \times 10^9$ calcd by eq 3

**Table 1.** Approximate Numerical Values for Combinatorial Functions Describing the Number of Phase Diagrams and Local Configurations ( $C$ ) Depending on the Total Number  $N$  of Components (Metallic Elements) That Is Oxides, Sulfides or Halogens.

We are about to conclude that because in unreacted ceramic samples  $\langle n \rangle$  may be above 8, consequently the number of configurations is larger than the number of phase diagrams ( $N_q^{PD}$ ), and  $N_n^C$  is of similar order or even larger than the number  $N^P$ , of possibly existing phases.

The SSC is as simple as this by taking advantage of a large number of local configurations described by a combinatorial function, which for a given number  $N$  of elements can surpass the theoretical number of phase diagrams and phases therein. The SSC model is thus able to account for (i) the number of phase diagrams set up by a random sample of  $N$  components; (ii) the stoichiometric variation to scan these phase diagrams; and (iii) an available number of starting grains in  $1 \text{ cm}^3$  to exceed realistic estimations for the number of phases present in the phase diagrams.

#### 4.5. Conclusions

The present analysis shows that the SSC can take advantage of combinatorial functions that realistically can exceed those similar functions that describe possibly existing solid-state inorganic compounds: In the case that the chemical systems in the solid state do not show a preference to form thermodynamically stable compounds for high  $q$  values, the number of combinatorially possible compounds does not reach those astronomical numbers, which are reported in general discussions on the principal limitations of experimental combinatorial chemistry. Consequently, the single sample combinatorial chemistry seems to merge into an endeavor in which we should be able to explore of what is “there”.

In this case we are right in claiming that important materials properties may be obtained by a limited number  $q$  of constitutional elements in solid-state compounds; there is no real need for attempting compounds exceeding  $q \approx 6$  significantly. For property-directed syntheses, application of magnetic separation techniques proved recently<sup>5</sup> to be very efficient in extracting magnetic phases from SSC samples. This is presently being applied to search for ferri- or ferromagnetic copper based oxides showing a  $T_c \geq 300 \text{ K}$ . Knowledge on such phases is of particular interest for the interpretation of experimental data showing similarity to superconductivity.<sup>18</sup> In summary, SSC may be used in a first screening step followed by a refined cycle using 2D procedures. Present calculations show that within a *single ceramic sample* the number of reactions performed in *parallel* can be by orders of magnitude higher than achieved by present 2D approaches.

## 4.6. Nomenclature

- $N$  : number of components e.g.  $M_xO_y$  to bring to reaction
- $N_E$  : number of starting grains per element
- $N_q^{PD}$  : number of phase diagram ( $PD$ ) constituted by selecting  $q$  elements out of  $N$
- $N^P$  : total number of phases to be estimated here
- $q$  : number of constitutional metallic/semimetallic elements in for example oxide compounds to be formed
- $\eta_q, \langle \eta_q \rangle$  : number (average) of phases per diagram of the order  $q$
- $C, C(q, n)$  : local configurations, i.e., assembly of  $n$  grains in a powder sample which undergoes a reaction; a configuration is characterized by  $q$  and  $n$
- $N_n^C$  : number of local configurations ( $C$ ) set up by  $N$  different elements
- $\langle n \rangle$  : average number of grains in a configuration
- $\langle \tilde{n} \rangle$  : average coordination number, that is, number of grains in  $C$  s around a central particle
- $\langle \varepsilon \rangle$  : mean free space in a random pack of spheres
- $\mathcal{R}, \mathcal{R}_I$  : compounds formed
- $\mathcal{R}(q, X_i, L)$  : compound  $\mathcal{R}$ , indicating elements ( $q$ ), stoichiometry ( $X_i$ ) and lead element  $E_L$

## 4.7. Acknowledgements

We thank Dr. R. Kremer (MPI for solid-state research, Stuttgart) for the susceptibility and resistance measurements.

## 4.8. References

- (1) (a) Kirsten, G.; Maier, W. F. *Appl. Surf. Sci.* **2004**, 223, 87 – 101. (b) Maier, W. F.; Kirsten, G.; Orschel, M.; Weiss, P.-A.; Holzwarth, A.; Klein, J. *Comb. Chem. (ACS Symposium Series)* **2002**, 814, 1 - 21. (C) Maier W. F. *Angew. Chem. Int. Ed.* **1999**, 38, 1216 - 1218.
- (2) DiSalvo, F. J. *Pure. Appl. Chem.*, **2000**, 72, 1799 - 1807.
- (3) Jansen, M. *Angew. Chem. Int. Ed.* **2002**, 41, 3746 - 3766.
- (4) Amis, E. J.; Xiang, X-D.; Zhao, J.-C. *MRS. Bull.* **2002**, 27, 295 - 297.
- (5) Hulliger, J.; Awan, M. A. *Chem. -Eur. J.* 2004, 10, 4694 - 4702.
- (6) Jandeleit, B.; Schaefer, D. J.; Powers, T. S.; Turner, H. W.; Weinberg, W. H. *Angew. Chem. Int. Ed.* **1999**, 38, 2494 - 2532.
- (7) Schultz, P. G.; Liu, D. R. *Angew. Chem., Int. Ed.* **1999**, 38, 36 - 54.
- (8) (a) Hulliger, J.; Awan, M. A.; Trusch B. Z. *Anorg. Allg. Chem.* **2004**, 630, 1689. (b) Hulliger, J.; Gaschen, A.; Awan, M. A. Presented at Third International Conference Inorganic Material; Konstanz, Germany, 7 - 10 Sept. **2002**, A abstract, pp O 40.
- (9) (a) Schatt E. H. W. in *Sintervorgänge*; VDI-Verlag: Düsseldorf, **1992**, pp 45 - 48. (b) Kingery, W. D.; Bown, H. K. Uhlmann D. R. *Introduction to Ceramics*; 2nd ed.; John Wily & Sons: New York, **1976**.
- (10) Ohara, T.; Mori, Sadao, M.; Oda, Y.; Wada, Y.; Tsukamoto, O. *Trans. IEE Jpn.* **1996**, 166-B, 979 - 986.
- (11) Nomizu, T.; Yamamoto, K.; Watanabe, M. *Ana. Sci.* **2001**, 17, i177 - i180.
- (12) Karki, K. C.; Whitby, E. R.; Patankar, S. V.; Winstead, C.; Ohara, T.; Wang, X. *Appl. Math. Model.* **2001**, 25, 355 - 373.
- (13) Levin, E. M.; Robbins, C. R.; Mc Murdie H. F. In *Phase Diagrams for Ceramists*, Reser, M. K., Ed.; American Chemical Society: Columbus. Ohio, **1964**, 1, p. 27.
- (14) Dullien, F. A. L. Structural Properties of Packing Particles, in *Handbook of Powder Science & Technology*, 2nd ed.; Fayed, E. M.; Otten, L., Eds.; Chapman & Hall: New York, **1997**, pp. 53 - 95.

- (15) Bernal, J. D.; Mason, J. *Nature* **1960**, *188*, 908 - 911. (b) Wade, W. H. *J. Phys. Chem.* **1965**, *69*, 322 - 326.
- (16) Ridgway, K.; Tarbuck, K. J. *Brit. Chem. Eng.* **1996**, *12*, 384 - 388.
- (17) Funk, J. E.; Dinger, D. R. *Predictive Process Control of Crowded Particulate Suspensions*; Kluwer Academic Publisher: Boston, **1994**; pp 161 - 164.
- (18) (a) Panagopoulos, C.; Majoros, M.; Petrovic, A. P. *Phys. Rev. B: Condens. Matter Mater. Phys.* **2004**, *69*, 144508. (b) Raveau, B.; Maignan, A. *Eurphys. News* **2003**, *34*, 1 - 6. (c) Singh, A.; Aswal, D. K.; Gupta, L. C.; Gupta, S. K.; Yakhmi, J. V.; Sahni, V. C. *Supercond. Sci. Technol.* **2004**, *17*, 342 - 346. (d) Chmaissem, O.; Jorgensen, J. D.; Shaked, H.; Dollar, P.; Tallon, J. L. *Phys. Rev. B: Condens. Matter Mater. Phys.* **2000**, *61*, 6401 - 6407.

## 5. Chemical Diversity

### in View of Property Generation by a New Combinatorial Approach

Jürg Hulliger, M. A. Awan, B. Trusch, T. A. Samtleben,  
*Z. Anorg. All. Chem.* **2005**, 631, 1255 - 1260.

#### 5.1. Abstract

Even the exploration of the phase space given by a large number  $N$  ( $N \leq 61$ ) of components but a limited number  $q$  ( $q \leq 6$ ) of elements  $E_i$  in e.g. metal oxides  $E_{x1}(1)E_{x2}(2)\dots E_{xq}(q)O_y$  is a demanding task and needs a combinatorial approach which, by setting up starting conditions for solid-state reactions, is taking favour of efficient combinatorial functions. Estimations showed that within a single sample prepared by mixing  $N$  starting components, the number of local reaction centres (configurations) is exceeding the number of phase systems. A huge amount of about  $10^{12}$  starting grains for a sample of one  $\text{cm}^3$  provides population of each configuration many times. The distribution for the grain size and the number of grains building up a configuration allows exploring compositional fields in phase diagrams of the order  $q$ . The *single sample concept* (SSC) is particularly of interest for *property-oriented* syntheses, where e.g. magnetic materials are produced in minor quantities. Magnetic chromatography is applied to extract ferromagnetic materials formed by the SSC. A horizontal separator is presented and applied to extract new ferromagnetic Fe-based oxides from SSC reaction mixtures.

**Keywords:** combinatorial chemistry, magnetic properties, ferromagnetism, materials science.



## 5.2. Introduction [1]

In front of a periodic table of the elements we might get the impression that chemical diversity generated by combining elements to form all kind of possible *solids* will nearly be infinite. Indeed, mathematically speaking the number  $N_c$  of combinations representing a selection of  $n$  elements  $E$  out of a total of e.g.  $N = 61$  non radioactive elements forming compounds  $E_{x_1}(1)E_{x_2}(2)\dots E_{x_n}(n)$  is described by a combinatorial function (Equation 1) which for an intermediate  $n$  will surpass the feasibility of present approaches for setting up syntheses of these compounds (Figure 1) :

$$N_c = \binom{N}{n} = \frac{N!}{n!(N-n)!} \quad (1)$$

However, to the *right* side of Figure 1, the number of combinations is of the same order as to the *left*, an area which is commonly investigated. It is a fundamental issue as well an

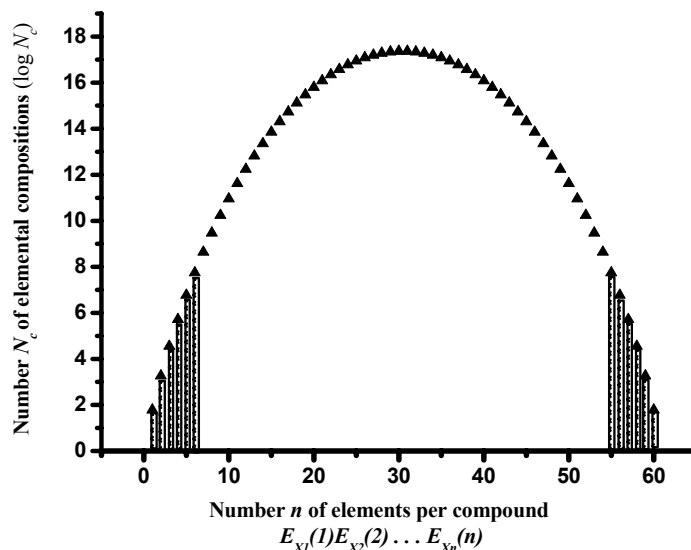


**Figure 1.** Number  $N_c$  of elemental combinations obtained by a set of e.g. 61 elements combined to compounds containing  $n$  different elements. Note, that  $N_c$  does not comprise stoichiometric variation. Shaded areas to the right and left are fields, which may be explored by SSC.

open question, whether chemistry would allow crystal structures built up by so many elements. Although  $N_c$  for itself can reach very high numbers (mid part of Figure 1), we have additionally to take into account stoichiometric variation. From a formal point of view, stoichiometric coefficients in compounds  $E_{x1}(1)E_{x2}(2)\dots E_{xn}(n)$  may be continuously varied. Consequently, mathematical reasoning would lead us to a rather pessimistic perspective to support whatever endeavour for exploring the chemical diversity of solid compounds. Fortunately, chemistry by its nature is *structuring*, which means, the manifold of combinations exceeds a dramatic reduction for a number of reasons:

**Expression of similarity of the elements:** To populate all combinations including stoichiometry, elements should provide pronounced individuality, a condition which is contradicted by the similarity of elements belonging to a group, including grouping across the periodic table according to the ionic size, oxidation number, polarizability and presence of lone pairs. Similarity is expressed by a limited number of existing structural types, including preferences for some of them [2,3].

Thermodynamically speaking, it is observed that the number  $\eta_q$  of (ordered) phases in phase diagrams is by far not as large than a continuous variation of stoichiometry would anticipate (except solid solutions which are an expression of similarity). Kinetically speaking, recent calculations [4] have demonstrated that a number of less stable structures can exist, even in the case of NaCl (s). A limited number a structural types and a rather low density of phases present in measured phase diagrams let us conclude that structural/compositional diversity is bound to certain limits. The diversity of minerals provides nice examples, because groups of them accept numerous substitutions [5]. Instead of increasing structural diversity, hosting of elements is taking place: About 37 % of known (purely) oxide minerals undergo substitutions (examples taken from Ref. [5]).

**Evidence for an upper limit for the number  $q$  of constitutional elements in compounds:** Mineralogical and chemical databases let us conclude (see Tab. 1) that the number of e.g. known oxides is strongly decreasing above  $q = 4$  ( $q$ : number of constitutional metallic/semimetallic elements in oxides;  $q_t$  : total number of metallic/semimetallic elements including substations, while  $q_t > q$ ). Data on  $6 \leq q_t \leq 30$

were found, however, minerals/compounds showed only  $q$ -values up to  $q \leq 6$ . In the case of minerals, random sampling from the geochemical system allows to say: Predominantly oxide minerals (no  $\text{OH}^-$ ,  $\text{CO}^{2-}$ ,  $\text{PO}_4^{3-}$  etc; no  $\text{Si}^{+4}$ ) up to  $q = 4$  were found. For silicates same examples up to  $q = 6$  are known (see Table 2). For chemistry, a search has found just a few examples of oxides containing metals/semimetals for  $q$  up to 6. Among examples representing  $q = 5$  to 6 examples, most compounds are cuprates. The absence of a representative expression of high- $q$  compounds let us anticipate that such structures most likely are not stable against decomposition into structures representing  $q < 6$ . High- $q$  compounds may, however, occur as transient products or are difficult to access by nucleation.

**Table 1** : Literature review on the existence of metal oxides containing an increasing number of metallic elements.

$q_t$ <sup>a)</sup> (number of metals in oxides)	$N(q_t)$ <sup>b)</sup>	Number of oxides classified as minerals	Number of oxides classified as chemical compounds	
1	1465	79	1386	
2	7136	555	6581	
3	7271	126	7145	
4	1477	8	for examples, see Tab. 2	
5	463	21		1469
6	44	19		442
			125	

$q_t$  : total number of different metals/semimetals in a compound. Not all of these are constitutional. Inorganic Crystal Structure Database (ICSD). Compounds with a total number of elements of  $q_t + 1$ , containing oxygen, but excluding : H, B, C, N, F, Si, P, S, Cl, Se, Br, I. Peroxides and superoxides were counted as oxides.  $N(q_t)$  : total number of entries, i.e. sum of numbers to the right side.

**Table 2** : Representative examples of high- $q$  compounds found in mineralogy and chemistry. The present search did not reveal an expression of significant examples for  $q > 6$ .

$q$	Non-silicate oxide minerals	Name
	$(\text{Ca,Na})_4(\text{Mg,Fe,Zn})_5\text{Sn}_4\text{Al}_{16}\text{O}_{41}$	Mengxianminite
4	$(\text{La,Ce})(\text{Y,U})(\text{Fe,Zn})_2(\text{Ti,Fe})_{18}\text{O}_{38}$	Davidite
	$(\text{Mn}^{+2},\text{Mn}^{+3})_3\text{Nb}_2(\text{Nb,Ta})_3\text{W}_2\text{O}_{20}$	Koragoite
	$(\text{Ca,Fe,Y})_2\text{Fe}(\text{Ti,Nb})_3\text{Zr}_2\text{O}_{14}$	Zirconolite
$q$	Oxide silicate minerals	Name
	$\text{Na}_2\text{Fe}_3\text{TiSi}_6\text{O}_{20}$	Aenigmatite
4	$\text{Ce}_4\text{Fe}_3\text{Ti}_2(\text{SiO}_7)\text{O}_8$	Chevkinite
	$\text{Ca}_3\text{TiAs}_6\text{BeSi}_2\text{O}_{30}$	Asbecasite
5	$\text{KNa}_2\text{Al}_2\text{Li}_3\text{Si}_{12}\text{O}_{30}$	Sugilite
	$\text{KLiMn}_2\text{Na}_2\text{Ti}_2\text{Si}_8\text{O}_{24}$	Neptunite
6	$\text{Ca}_2\text{Mg}_4\text{FeSbBe}_2\text{Si}_4\text{O}_{20}$	Welshite
$q$	Chemical compounds	
	$\text{Na}_2\text{BiMg}_2\text{V}_3\text{O}_{12}$	
4	$\text{Bi}_8\text{PbTi}_4\text{W}_2\text{O}_{27}$	
	$\text{HgBiSr}_7\text{Cu}_2\text{SbO}_{15}$	
5	$(\text{Gd,Tb, Eu, Dy, Sm})_2\text{Ba}_2\text{CaCu}_2\text{Ti}_3\text{O}_{14}$	
	$\text{Nd}_2\text{BaCaCeTi}_2\text{Cu}_2\text{O}_{14}$	
6	$(\text{Sm}_{1.1}\text{Ce}_{0.9})\text{Ba}_2\text{Sm}_2\text{Cu}_2\text{Ti}_2\text{GaO}_{16}$	

**Does property generation need high- $q$  compounds?** In materials research strategies were developed for finding materials featuring a best possible performance of interesting properties. Here, we recognize that properties we can take advantage of today became possible already for  $q \leq 1 - 4$  (Table 3). In respect to property generation we may thus assume that progress should be possible by exploring the phase space limited to  $q \leq 6$ .

**Table 3** : Representative examples for important physical properties made possible by a limited number of known compounds. Important to notice that most properties could be obtained for  $q = 1$  to 4.

Property	Examples	Range of $q$
Ferromagnetism	$\text{Sm}_2\text{Co}_7$ , $\text{B}_8\text{Fe}_{77}\text{Nd}_{15}$ , $\text{BaFe}_{12}\text{O}_{19}$ , ...	1 – 3
Ferroelectricity	$\text{BaTiO}_3$ , $\text{LiNbO}_3$ , $\text{KNbO}_3$ , ...	2 – 3
Luminescence	$\text{Al}_2\text{O}_3:\text{Cr}^{3+}$ , $\text{Y}_3\text{Al}_5\text{O}_{12}:\text{Nd}^{3+}$ , $\text{Sr}_2\text{Si}_5\text{N}_8:\text{Eu}^{2+}$ , ...	1 – 3
Superconductivity	$\text{Nb}_3\text{Ge}$ , $(\text{Ba}_{1-x}\text{K}_x)\text{BiO}_3$ , $\text{Tl}_2\text{Ba}_2\text{Ca}_2\text{Cu}_3\text{O}_{10}$ , ...	1 – 4
Semiconductors	Si, GaAs, InP, GaN, ...	1 – 3

Accepting constraints we have introduced so far ( $N \leq 61$ ,  $q \leq 6$ ,  $\eta_q$  : small) we may look differently at the periodic table: Exploration of a most prominent and relevant compound class, the metal/semimetal *oxides* would have to enface an upper limit of about  $5 \cdot 10^7$  unknown phase diagrams, wherein we estimate to have a maximum number of ordered and stable structures (for given  $T$  and  $P_{O_2}$  where materials are formed) in the order of about  $5 \cdot 10^8$  ( $\eta_6 \leq 10$ ) [8]. A considerable number of metastable phases are expected as well. Evidently, non of the classical nor the established combinatorial synthetic procedures [6, 7] are able to handle this diversity. Recently, we have presented a *single sample concept* (SSC) [8, 9] for which combinatorial investigations showed, that in principle, the SSC can generate a number of about  $5 \cdot 10^8$ , or even more oxide phases within a *single ceramic sample* of just  $1 \text{ cm}^3$ .

### 5.3. Basics of the Single Sample Concept (SSC)

For reacting solids, starting materials of an average grain size  $\langle d \rangle$  in the range of a few hundred  $nm$  to a few  $\mu m$  are typically used. Within a powder sample of, say, one cubic centimetre a huge number of grains ( $\sim 10^{12}$  for  $\langle d \rangle \approx 1 \mu m$ ) can undergo local reactions through solid-to-solid contacts assisted by vapour transport. Dependent on the density of packing, i.e. local coordination of grains, reactions may occur inbetween *pairs* of adjacent grains or within *clusters* of grains (Figure 2). Given a diversity of interfaces, spontaneous nucleation may produce metastable and stable phases belonging to phase diagrams constituted by the number  $q$  of components participating in locally occurring phase formation.

In the case of a low number  $N$  starting materials ( $N = 2$  to  $4$ ) and for a long reaction time, an initially inhomogeneously distributed manifold of phases turns into most stable solids belonging to a certain  $(x_i, T, p)$ -field of existence. In the initial phase of transformation we may thus have kinetic control, whereas at long term, most likely, thermodynamic control is dominating. This may explain why in solid-state chemistry we generally obtain a relatively low number of phases produced within a powder sample. However, theoretical calculations have shown, that the number of potentially accessible phases in solid-state reaction systems is much larger, than usually found by standard routes of formation [4]. Because of the driving potential to form a few or just one particularly stable phases/phase within a system of  $q$  components, other phases featuring a higher free energy may disappear as inter-conversion of grains is advancing the homogenization of a bulk sample.

A rather different situation can arise if we allow for a large number  $N$  of starting materials: At first, local reaction conditions are similar as discussed above, however, further formation of compounds ( $q > 2$ ) encounters a situation where the availability of matter and the diversity of compounds in the nearest and next nearest neighbourhood is different from a case of low  $N$ . If the number  $N$  is surpassing the average coordination number  $\tilde{n}$  of grains, instantaneous mass exchange through solid to solid contacts can not occur for all  $N$  components (low partial pressure of components assumed here). Consequently, an assembly of grains constituted by  $N$  larger about 12 may thus produce a

larger number of phases than expected for a system approaching thermodynamic equilibrium. For long reaction times, most stable phases may nevertheless emerge, but as a result of a series of interconversions of previously formed product grains (reducing thus the overall kinetic). A combinatorial treatment [8, 9] has demonstrated that the number  $N_n^C$  of starting compositions set up by local configurations of grains (a local configuration being set up by totally  $n$  grains, where of  $q$  represent different starting

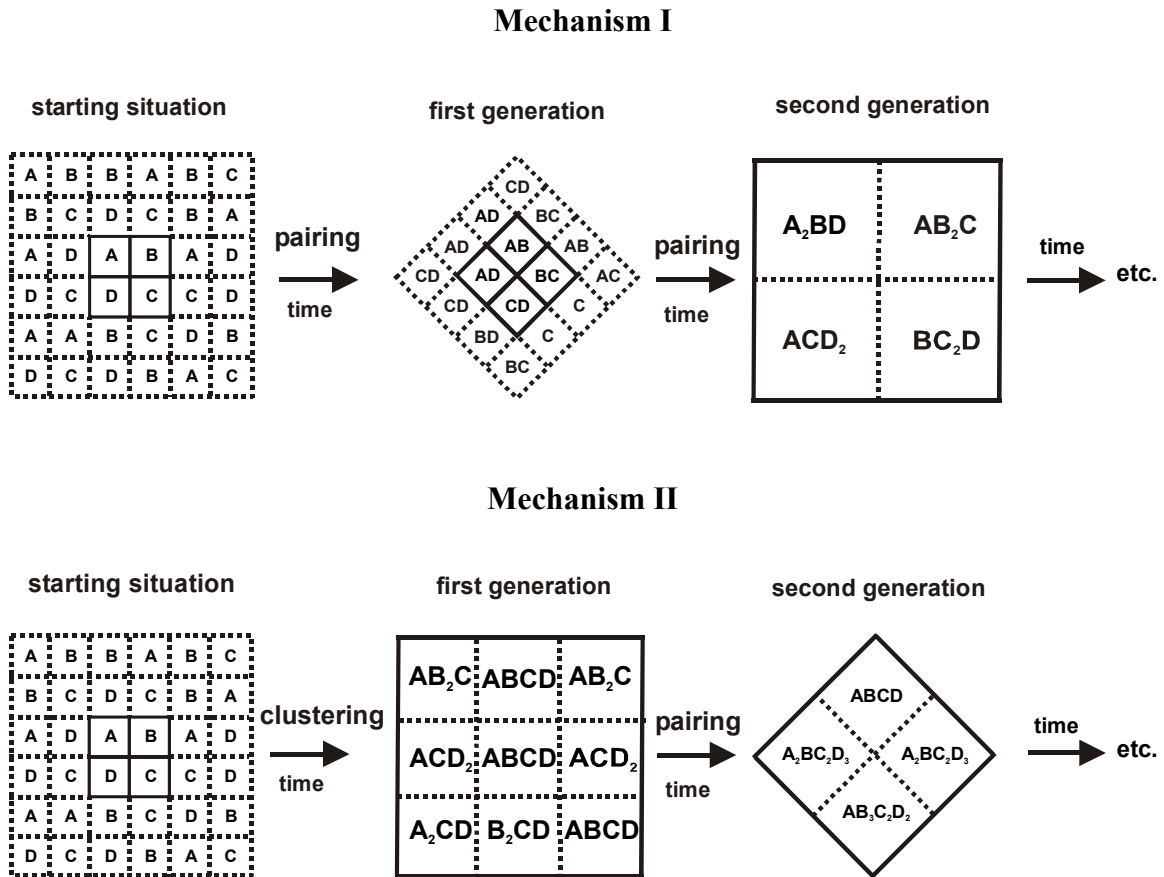


**Figure 2.** Schematic representation how in an assembly of randomly mixed grains of starting materials A, B, C, D product grains may form through (i) pair-wise reactions of grains (mechanism I) or (ii) cluster-wise reactions of grains followed by pair-wise reactions (mechanism II). As grains can belong to different local configurations (see text), the first and following generations of grains are represented here as a result of reactions with all nearest neighbours. (Rotation of squares is to indicate how product grains appear by sharing grains inbetween configurations.)

components) can be much larger than the number of phase systems (constituted by  $q$  components) times reasonably estimated number ( $\eta_q$ ) of phases therein.  $N_n^C$  is given by

$$N_n^C = \binom{N+n-1}{n} - N. \quad (2)$$

An important point for screening compositional ranges of phase systems of the order  $q$  is, that the production of minor amounts (few grains in the limit) of a certain phase needs to hit corresponding compositional fields instead of e.g. a line in phase diagrams. Therefore, the number of grid points to explore phase diagrams by the SSC is lower than one might expect at first. Combinatorial functions together with the distribution of the grain size are in principle sufficient to provide enough grid points for exploration.

Summarizing, the theoretical discussion demonstrates a synthetic ability of the SSC which should allow to explore a large phase space through locally occurring reactions producing product grains where of many of these can appear within a single sample (several pellets making up  $\sim 1 \text{ cm}^3$ ). Thereby, a very large number of starting grains in the order of  $10^{12}$  allow populating all these combinatorically predicted configurations.

Once such a library is obtained, what we may do for reading it out? Here, we encounter a situation, which is similar to that of mineralogists on their quest for finding new minerals: Like the earth's crust, ceramic samples are considered mines, which can be explored analytically, i.e. grain by grain. Electron microscopy enables to identify randomly selected crystallites, which may represent new phases to be made then by conventional methods. Obviously, this represents an analytical task, which exceeds the feasibility of the state of the art in today micro-phase analysis. Being aware of a chemical diversity impeding a case-by-case analysis, we apply the SSC in view of the formation of compounds featuring specific properties, which are not met by the majority of the product grains.

So far the SSC was applied by adding of a *lead* metallic element for giving rise to a variety of magnetic and non-magnetic oxide phases. The SSC turned out to be especially efficient in the case of *property-oriented syntheses*, where magnetic separation techniques allow extraction of *minor* quantities of new phases out of a large number of



others being not magnetic. In Chapter 3 we present a new method to perform magnetic chromatography applied to extract e.g. Fe-based oxides formed in SSC samples.

#### 5.4. Magnetic Chromatography for Extracting Magnetic Phases

Magnetic separation techniques, i.e. the extraction of minor quantities of wanted minerals out of rocks is well known in the mining industry [10, 11]. In materials chemistry we recently have introduced magnetic separation columns, which were used to extract magnetic grains in the case of SSC syntheses [8]. Here, we present a new horizontal separator which is acting on principles known in general chromatography (Figure 3) : A powder sample is deposited (spot) at the starting point of a circular trace (a groove on a brass plate, plated by polished chromium). 4 arms, equipped by one or two (optional)

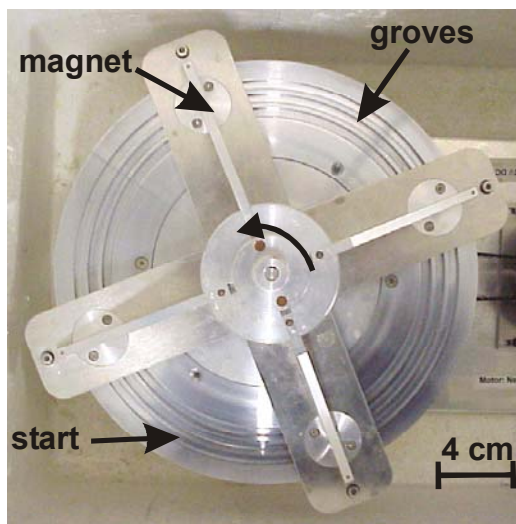


**Figure 3.** Horizontal magnetic separator (viewed from the top) for extracting ferromagnetic grains out of a mixture (suspension). A horizontal plate provides 3 grooves for transporting grains along a circular trace. 4 arms equipped with magnets move over (here upper and lower side of the plate) the grooves. Magnetic particles are transported along grooves up to an angle  $\omega < 2\pi$ , from where they can be recollected for analysis.

permanent magnets (e.g.  $B_8Fe_{77}Nd_{15}$ ) rotate along the circular trace at a constant speed  $\omega$ . Starting- and end-points of the trace are separated by a gap in the suspension of particles.

Because magnets provide a strong field gradient, grains exceed a force to move in the direction of rotation, when an arm is passing over the sample spot. Friction forces imposed by other grains, the groove materials and the viscosity of the liquid retain grains to follow the magnet. In the case of e.g. magnetoplumbite ( $\text{BaFe}_{12}\text{O}_{19}$ ) mixed up with diamagnetic oxides, immediate separation was seen, i.e. grains of magnetoplumbite were following the movement of magnetic arms. In case, reaction mixtures contain less and/or weakly ferromagnetic grains, separation may be achieved after a few hours up to several days. In favour of chemical analyses and property directed research, largest grains being strongly magnetic are those exceeding best separation. For a demonstration of the effect of separation, see Figure 4.

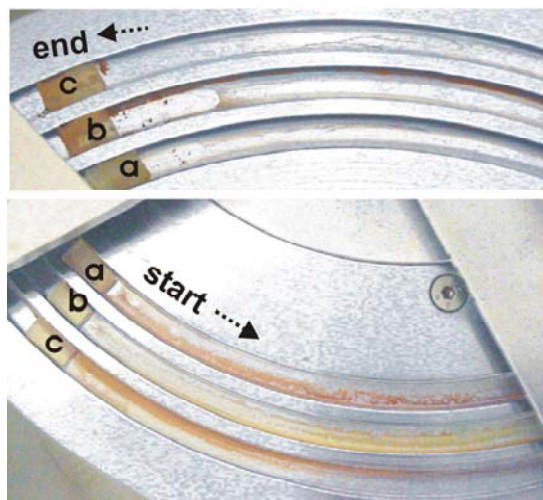


**Figure 4.** Demonstration of the effect of separation (apparatus see Figure 3) : a) Combinatorial mixture of Ga-, Ge-, Zr-, La-, W- oxides and 15 wt. % of  $\text{Fe}_2\text{O}_3$ , b) La : Fe (6 :1; mol. %), c) Ga-, Ge-, Te-, Zr-, La-, Hf-, W-, Re- oxides and 15 wt. % of  $\text{Fe}_2\text{O}_3$ . In all grooves some of the grains were transported to the end of the trace. These grains may belong to the most magnetic ones. Grains from here were used for elemental analysis by EDX.

## 5.5. Search for New Fe-based Ferromagnetic Oxides

In the course of our recent analysis [8], we were investigating up to  $N = 17$  to 30 non-magnetic elements using iron as a lead element, added in excess to all others. Literature

has shown that taking into account (Li, Na, Mg, Al, Zn, Si, K, Ca, Ti, Sr, Y, Nb, Mo, Cd, Sn, Ba, Pb) about 50 compounds were found to show magnetic ordering above 25 °C.

As the yield of magnetic particles in SSC samples was fairly high (~ 75 %; N = 17), the number of phases collected by magnets may be seemingly high. While, sorting/identification of new phase is still in process, we look here for another perspective: We are considering metallic elements for which literature data are missing or do not provide details on ferromagnetic properties (Fe-compounds,  $T_c > 25$  °C). The following elements were identified to fall into this class: Ga, Ge, Te, Zr, La, Hf, W, Re.

At first, SSC syntheses were performed using these elements and 15 wt. % Fe<sub>2</sub>O<sub>3</sub> (reaction temperature  $T$ : 850 - 1000 °C; oxygen flow 1.6 l/h at 1 atmosphere; temperature: heating rate 150 °C/h; 850-1000 °C for 2 h, cooling rate 100 °C/h up to 500 °C then 150 °C/h up to 25 °C; for further details, see Ref. [8]). The effect of magnetic separation by the horizontal equipment is shown in Figure 3. Qualitative energy dispersive x-ray (EDX) microscopy analysis performed on a series of single grains indicated a preference for the following elements : Fe > La > Ga > W > Ge , Hf , Zr , Te , Re.

For a second series of SSC syntheses, we ignored Re and Te. At this stage, after separation of magnetic grains, preferably, Fe > La  $\approx$  Ga, and Zr, W, Ge, Hf were present. In a third series, we used Fe, La, W, Ga, Zr, Ge and found La > Fe > W > Ga , Zr. In this case, the elemental composition involving Fe, La, W, and Zr varied about ~ 1 atomic % for each element by selecting independently 5 different grains. There is strong evidence for magnetic phases in the system Fe / La / W / Zr oxides. For a last series, Zr and W were omitted. Up to this point, a preference for e.g. Fe, La as compared to other elements became evident. A classical preparation using, thus only La<sub>2</sub>O<sub>3</sub> : Fe<sub>2</sub>O<sub>3</sub> (molar ratio : 1:1, 3:1, 5:1 and 6:1) has yielded magnetic materials in significant amounts. Application of magnetic chromatography showed clearly an extraction of magnetic particles (see Figure 4, groove b). For the system La / Fe, reports on LaFeO<sub>3</sub> [12] and Fe<sub>12</sub>LaO<sub>19</sub> [13] were found. LaFeO<sub>3</sub> [12] is described as a typical perovskite type anti-ferromagnetic material (Neel temperature of 465 - 477 °C). Fe<sub>12</sub>LaO<sub>19</sub> shows magnetoplumbite structure and is ferromagnetic. According to a phase analysis, Fe<sub>12</sub>LaO<sub>19</sub> seems only to be stable in a small temperature range of 1380 – 1421 °C [13]. Present preparation was limited to 1000

°C. A detailed chemical/structural analysis exceeding the scope of this work will be necessary to identify possible new ferromagnetic phases in the system Fe / La and Fe / La / W / Zr oxides.

## 5.6. Conclusions

Combinatorial reasoning has initiated new perspectives for finding inorganic materials by locally occurring solid-state reactions. In principle, all configurations present in a single powder sample of 1 cm<sup>3</sup> represent starting conditions that may provide access to stable and metastable phases within a tremendous phase space. In this respect the SSC is more efficient than established combinatorial procedures.

Property oriented explorations of the phase space of e.g. oxides seems possible, because knowledge on existing phases, particularly mineralogy lets us anticipate that high- $q$  ( $q > 6$ ) compounds do not represent a field from which improvement for established property will result. All interesting solid-state properties we know so far were obtained for compounds with  $q < 6$ , generally 1 to 4. This is considered an optimistic perspective for solid-state chemistry, i.e. to explore the space  $q \leq 6$  by most efficient strategies. However, the present approach will need further improvement in the step of separation and fast analysis of single grains. To be faster than mineralogy, automatization will be required. Present separators represent a first step for extracting those grains showing the highest magnetization. Within a particular sample among these grains new phases may be retrieved. The present application bears evidence for ferromagnetic materials in the system Fe / La and Fe / La / W / Zr oxides.

## 5.7. Acknowledgements

We thank the Portland cement foundation for financial support. The experimental work was carried out partially by cooperation with students of the “Praktikum Anorganische Chemie II”, 2004.

## 5.7. References

- [1] J. Hulliger, M. A. Awan, B. Trusch, *Z. Anorg. Allg. Chem.*, 2004, 630, 1689; extended abstract, GDCH conference, Struktur-Eigenschafts-Beziehungen, plenary lecture, Marburg, 2004.
- [2] F. J. DeSalvo, *Pure. Appl. Chem.* 2000, 72, 1799.
- [3] I. D. Brown, *Acta Cryst.*, 1992, B48, 553.
- [4] M. Jansen, *Angew. Chem. Int. Ed.*, 2002, 41, 3746.
- [5] H. Strunz, E. H. Nickel, *Strunz Mineralogical Tables*, E. Schweizerbart'sche Verlagsbuchhandlung, Stuttgart, 2001.
- [6] W. F. Maier, G. Kirsten, M. Orschel, P.-A. Weiss, A. Holzwarth, Klein, *J. Comb. Chem.* (ACS Symposium Series), 2002, 814, 1.
- [7] B. Jandeleit, D. J. Schaefer, T. S. Powers, H. W. Turner, W. H. Weinberg, *Angew. Chem. Int. Ed.* 1999, 38, 2494.
- [8] J. Hulliger, M. A. Awan, *Chem. Eur. J.*, 2004, 10, 4694.
- [9] J. Hulliger, M. A. Awan, *J. Comb. Chem.*, 2005, 7, 73.
- [10] T. Ohara, S. Mori, Y. Oda, Y. Wada, O. Tsukamoto, *Trans. IEE Jap.*, 1996, 166 B, 979.
- [11] T. Nomizu, K. Yamamoto, M. Watanabe, *Ana. Sci.* (supplementary edition), 2001, 17, i177.
- [12] a) T. Karnki, H. Tanaka, T. Kawai, *J. Appl. Phys.*, 2003, 93, 4718; b) W. C. Koehler, E. O. Wollan, *J. Phys. Chem. Solids*, 1957, 2, 100.
- [13] V.I. Moruzzi, M.W. Shafer, *J. Am. Ceram. Soc.*, 1960, 43, 367.

## 6. Magnetic Chromatography and Ceramic Synthesis : a New Combinatorial Approach for Finding Ferri-/Ferromagnetic Materials

J. Hulliger, M. A. Awan, B. Trusch, *Z. Anorg. Allg. Chem.* **2004**, *630*, 1689.

**Keywords:** Combinatorial Chemistry; Magnetic Separation Chromatography; Ferri-/ferromagnetic and Superconducting Materials

Given a mixture of different solid phases obtained from geological origin or by a ceramic synthesis, ferri- and ferromagnetic materials can be extracted by application of magnetic field gradient techniques [1, 2]: After ball milling and addition of a surfactant, a suspension of  $\mu\text{m}$  sized particles is passed through a column (Figure 1), containing  $s$  ferromagnetic sieves being surrounded by cylindrical permanent magnets.

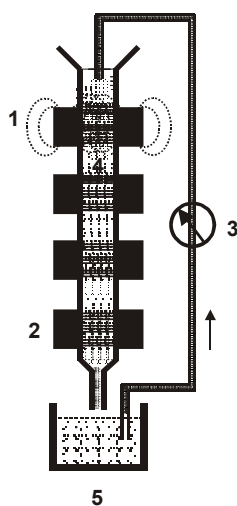


**Figure 1.** Principle of a magnetic separation column: (1) Magnetic field of  $\text{B}_8\text{Fe}_{77}\text{Nd}_{15}$  permanent magnets (2). Suspension (5) is pumped (3) into the column to pass over sieves (4) which generate a strongly inhomogeneous field. For releasing magnetic particles, magnets are removed and solvent is pumped through.

Because of attractive forces between ferri- or ferromagnetic particles and the wires making up the sieves, the probability  $P_{i, i+1}$  for passing a magnetic particle from sieve  $i$  to sieve  $i + 1$  (Figure 2) may be quite small. When using a large number of sieves ( $s = 500 - 1000$ ), even for a  $P_{i, i+1} = 0.99$ , nearly all magnetic particles will be retained as the probability  $P_s = (P_{i, i+1})^s$  for leaving the column can get very small. Confirmed by experimental work using  $\text{BaFe}_{12}\text{O}_{19}$  mixed up with nonmagnetic oxides, magnetic chromatography proved to be extremely effective for extracting *traces* of magnetic particles.

For superconductive materials, a similar effect is predicted: However, in this case particles are deflected from sieves, i.e. they refuse to enter a column.

In view of a property specific separation technique, we can think of a new combinatorial synthesis based on *ceramic bulk samples*: By mixing  $N$  different starting materials, followed by pressing powder into pellets, we obtain a particular starting situation for solid state reactions. Due to mechanical densification, particles undergo all kind of close contact arrangements. Local arrangements (configurations) of grains may be characterized by a number  $n$  accounting for grains in a configuration and a number  $q$  for different elements present in attempted compounds. If grains within configurations undergo local solid-state reactions, a manifold of possible compounds is predicted by combinatorial functions.

Among these many compounds there might be traces of new ferri-/ferromagnetic or superconducting compounds, which may be extracted by magnetic chromatography.

Combinatorial estimations show that the present *single sample concept* [3] (SSC; as compared to J. J. Hanak's "multiple sample concept" MSC [4]) can give access to a reasonable estimate for an upper limit of e.g. possible oxide compounds, starting by  $N$  oxides ( $q = 1$ ) and assuming a limited number of necessary metallic elements ( $q$ ) per compound to be obtained. An upper limit of metallic elements per compound of about 6 [5] seems reasonable, because known ferri-/ferromagnetic, superconducting and other interesting materials have been obtained for  $q$  up to 4.

The single sample concept was explored for obtaining ferri-/ferromagnetic iron oxides using  $N = 17, 24, 30$  nonmagnetic elements. For setting up configurations as discussed above, we have applied two routes: (I) Ceramic samples, and (II) use of a supporting

material, where oxide grains were dispersed onto them to form spatially isolated configurations. Sodium chloride crystallites being much larger than the average size of oxide particles were used (90 wt. % NaCl, 10 wt. % oxides mixture). Relatively high and comparable yields up to 75 wt. % of magnetic particles (I, II) were obtained for  $N = 17$ . Measured hysteresis loops have confirmed a magnetically ordered state for grains passed through columns. Elemental analysis by scanning electron microscopy has provided preliminary information on the elements present in individual grains.

For other 3d transition metals the yield of magnetic particles was much lower, confirming literature data, showing that ferri-/ferromagnetic compounds other than Fe-based are less frequent. In the case of copper oxides ( $N = 9$ ) the SSC has produced ceramic samples showing superconductivity up to about 100 K.

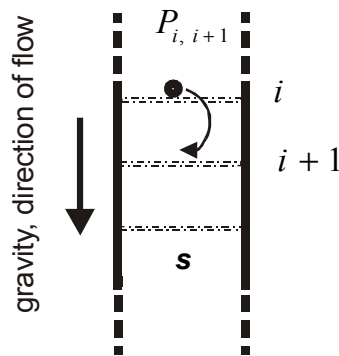


**Figure 2.** Schematic view for explaining the movement of grains (●) from sieve to sieve (s).

## 6.1. References

- [1] G. Gillet, F. Diot, *Miner. Metall. Process.* **1999**, *16*, 1 - 7.
- [2] T. Ohara, S. Mori, Y. Oda, Y. Wada, O. Tsukamoto, *Trans. IEE Jap.*, **1996**, *166 B*, 979 - 986.
- [3] J. Hulliger, M. A. Awan, *Chem. Eur. J.*, in press.
- [4] J. J. Hanak, *J. Mater. Sci.* **1970**, *5*, 964 - 971.
- [5] F. J. DeSalvo, *Pure. Appl. Chem.* **2000**, *72*, 1799 - 1807.



## 7. An Itinerary Report to the Synthesis of New Mg-Co and Zn-Co-oxides Ferromagnetic Materials

### 7.1. Introduction

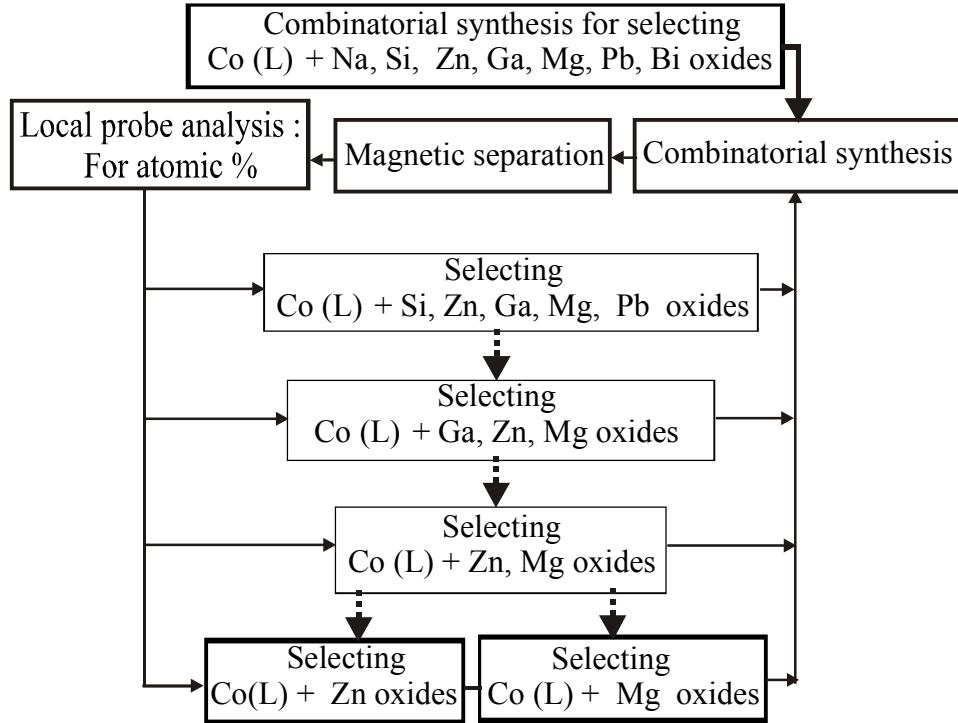
There is an interest to find new magneto-resistant and ferromagnetic materials and considerations have been given to the lattices of diamagnetic oxides. [1 - 11] Masking combinatorial technique was recently applied to find magneto-resistant materials, [3] where developments for generating libraries of solid-state compounds were made through 2D combinatorial approach. A 2-D combinatorial technique was applied for  $\text{Ln}_x\text{M}_y\text{CoO}_z$ , (Ln is Y and M is Pb, Ca, Sr, Ba). A library of 128 members for  $\text{Ln}_x\text{M}_y\text{CoO}_z$  was generated by using sequential radio-frequency sputtering deposition of thin films with a series of physical masking steps designed to produce Y, La, Ba, Sr, Ca and Co containing films with different compositions and stoichiometries. In this library a number of films showed a magneto-resistant effect.

The elemental stoichiometric combinations via 2-D combinatorial methods are not sufficient to provide the desired chemical diversity for new oxide phases. [12] Therefore, there is a possibility to find new oxides phases by providing further chemical diversity within a system. Here, the *single sample concept* (SSC) [13] was applied to find new ferromagnetic cobalt oxides phases because SSC provides large chemical diversity within a system.

### 7.2. Combinatorial Synthesis for New Ferromagnetic Cobalt Oxides

The present SSC combinatorial synthesis was performed by solid-state thermal activation in the presence of oxygen. Magnetic chromatography technique was used for product isolation, and energy dispersive X-ray (EDX) spectroscopic analysis technique was applied for the reduction of elements, which were absent after the reaction (magnetic separation) or in low atomic composition in the system. Thereafter, X-ray powder diffraction spectroscopic technique was used to identify magnetic oxide phases. For X-ray powder diffraction (XPD), a Stoe Powder Diffractometer was used. A process

overview for finding new magnetic cobalt oxides phases with the combinations of nonmagnetic oxides is shown in scheme 1.



**Scheme 1.** A systematic reduction of elements to find new ferromagnetic Co oxides.

The SSC combinatorial experimental procedure is as follows :

- i) In a first experiment, we selected Co-oxide (15 vol. %) and oxides of Na, Si, Zn, Ga, Mg, Pb, Bi (85 vol. %). These oxides were ball-milled in excess (70 – 90 vol. %) of isooctane slurry to improve homogenization. The ball-mill was rotated at speed ~ 400 rpm for 1 – 1.30 h and achat spherical balls of about 5 – 10 (diameter 1 – 3 mm) were used. Thereafter, ball-milled mixtures were filtered, dried and then pressed into single pellets. Ceramic pellets were made at about 7 – 9 t pressure for about 1 – 2 min by using hydrostatic pressure machine (Perkin : 2445). Ceramic pellets were placed in an aluminum ( $Al_2O_3$ ) crucible and heat-treated within a quartz glass tube (diameter ~ 3 cm) in a

furnace. A temperature controller (Tecon : 232) was used for heating and cooling cycles. Combinatorial reactions were performed by applying a maximum temperature ( $T$ ) of about 930 °C for a period of about 2 – 4 h. A heating rate  $\sim 150$  °C h<sup>-1</sup> and cooling rate  $\sim 100$  °C h<sup>-1</sup> was used. Oxygen gas (1 – 2 L h<sup>-1</sup>) during the annealing process was continuously flowed at  $P(O_2)$  of about 1 atm. After reaction, ceramic pellets were ball-milled again in excess isooctane slurry  $\sim 0.40$  – 1 h for down sizing of intergrown grains into the micrometer size range.

A magnetic chromatography technique was used to extract magnetic grains by passing a suspension of reacted combinatorial mixture through a magnetic column separator. In the magnetic column separator, iron spherical balls (diameter 0.5 – 2 mm) were used to produce magnetic field gradients within a magnetic column. For magnetic separator instrumental detail, see Chapter 2. EDX analysis showed that Na and Bi were almost not present in the magnetic grains

- ii) A second experiment was performed by selecting Co oxide and oxides of Si, Zn, Ga, Mg, Pb. The same experimental procedure as described above for i) was applied with a reaction temperature  $\sim 980$  °C.
- iii) In the same way a third experiment was performed by selecting Co oxide and oxides of Zn, Ga, Mg at a reaction temperature  $\sim 1000$  °C.
- iv) A final experimental series were carried out for oxides of Co, Zn and Co, Mg using a classical synthesis.

Optical microscopic analysis showed that reacted ceramic pellets of Zn/Co oxides were changed color from black to green and for Mg/Co oxides from black to pink-gray. After magnetic separation significant magnetic yields were obtained.

### 7.3. Ferromagnetism in the System of Zn/Co Oxides

A number of SSC samples were prepared for the identification of possibly new ferromagnetic Zn/CO oxides phases by taking different molar ratios of ZnO : CoO such as 0.95 : 0.05, 0.90 : 0.10, 0.80 : 0.2, 0.70 : 0.30 and 0.60 : 0.40 respectively.

These SSC samples were examined via X-ray powder diffraction (XPD). Here, let us consider the SSC sample a) of ZnO : CoO with mole ratio 0.90 : 0.10. X-ray powder diffraction for this SSC sample a) prior to reaction and after reaction showed deviation in a few weak lines (see Figure 1 and for d-values see Table 1). These scattered weak lines appeared after the reaction. When the XPD data for the reacted SSC sample a) was compared with the known data for the spinels, i.e.  $\text{ZnCo}_2\text{O}_4$ , many deviations in lines were observed (see Figure 2 and for d-values see Table 2). Moreover, new weak lines for the SSC sample a) were very closet to the lines of the known spinels, i.e.  $\text{ZnCo}_2\text{O}_4$  (see Figure 3).

This difference in the weak lines could be explained that this anomaly might come from the difference in the molar ratios between the known compounds and the reacted SSC sample a). It could also be possible that this difference is from ZnO phase dominance over CoO.

Additionally, optical microscopic observations showed that the color of the SSC sample a), prior to reaction and after reaction changed. It was black before the reaction and brown thereafter. The reacted SSC sample a) produced significant magnetic yield for a low molar ratio of CoO, i.e. 0.10. Hence, it might be possible that Co was present in the system according to percolation theoretical bases<sup>[4]</sup> and a solid solution could be formed. XPD lines deviation between the reacted SSC sample a) and the known spinels, i.e.  $\text{ZnCo}_2\text{O}_4$  could be used to argue that these differences are indicative of new phase. Consequently, new ferromagnetic oxides might be present due to weak lines.

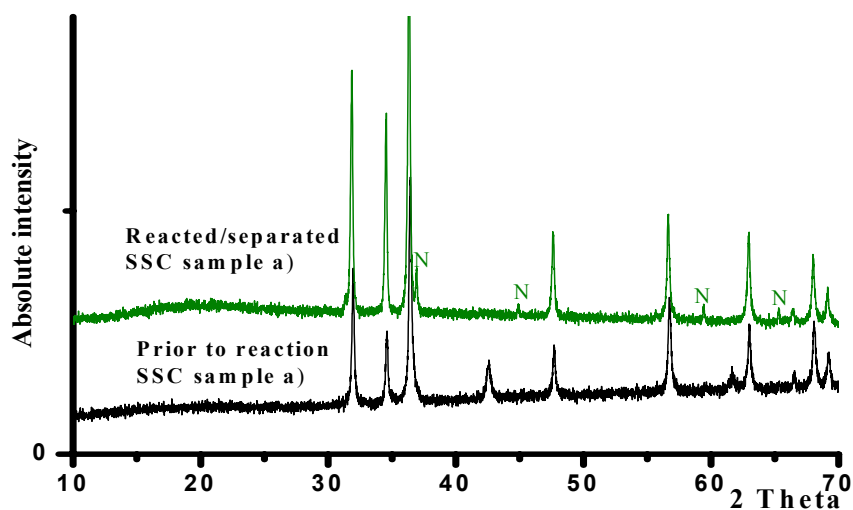


**Figure 1.** Comparison X-ray diffraction patterns for the SSC sample a) Zn : Co (mole ratio 0.90 : 0.10) prior to reaction and after reaction/separation. N : New lines.

**Table 1.** The d-values of X-ray powder diffraction of Figure 1, for the SSC sample a) Zn : Co (mole ratio 0.90 : 0.10), prior to reaction and after reaction.

d-values for the SSC sample a) prior to reaction	d-values for the SSC sample a) after reaction	d-values for the SSC sample a) prior to reaction	d-values for the SSC sample a) after reaction
2.800*	2.807*	1.503	1.554
2.590*	2.595*	1.474*	1.475*
2.464*	2.470*	1.404	1.406
	2.431	1.375*	1.377
2.121	2.016	1.356	1.357
1.904	1.908	1.299	
1.621*	1.623*	1.235	1.236

\* Represents intense lines. Bold numbers represent d-values matching.

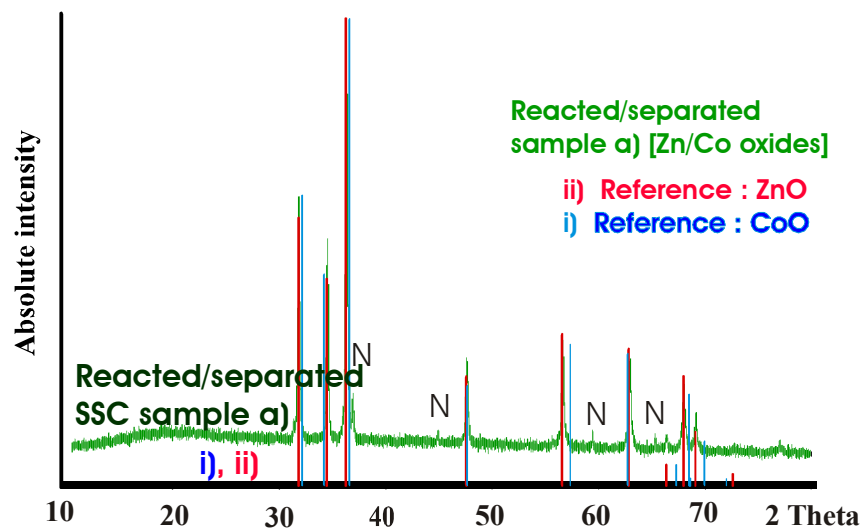


**Figure 2.** X-ray diffraction patterns for the reacted/separated SSC sample a) Zn : Co (mole ratio 0.9 : 0.1) compare with the known compounds i) ZnO and ii) CoO (X-ray powder diffraction PDF reference files number for i) is 89 – 280 and for ii) is 36 – 1451). N : New lines.

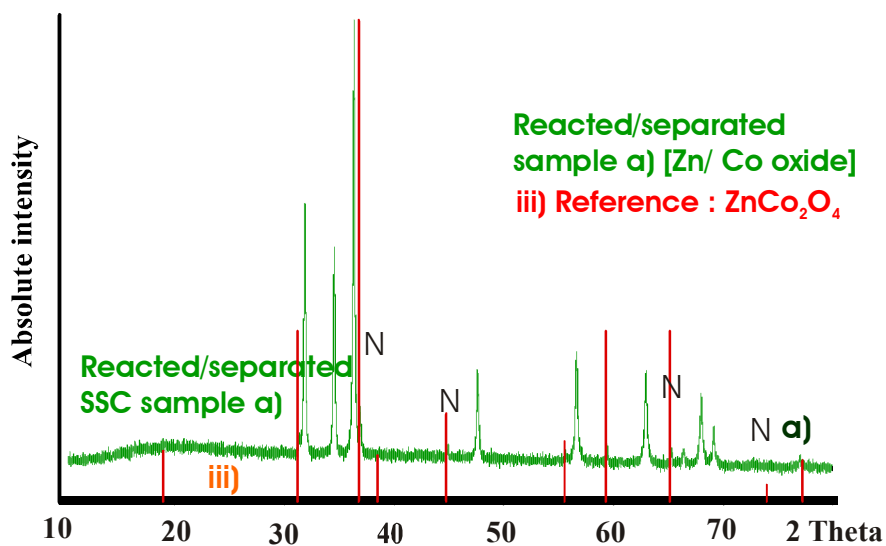


**Figure 3.** X-ray diffraction patterns for the reacted/separated SSC sample a) Zn : Co (mole ratio 0.9 : 0.10) compare with the known spinels iii) ZnCo<sub>2</sub>O<sub>4</sub> (X-ray diffraction PDF file No. 23 – 1390).

N : New lines.

**Table 2.** The d-values of X-ray powder diffraction of Figure 2 and 3, for the SSC sample a) Zn : Co (mole ratio 0.9 : 0.1) prior to reaction, after reaction/separated and for the known compounds CoO, ZnO and ZnCo<sub>2</sub>O<sub>4</sub>.

d-values for the SSC sample <i>a)</i> prior to reaction	d-values for the SSC sample <i>a)</i> after reaction/separated	CoO *	ZnO **	ZnCo <sub>2</sub> O <sub>4</sub> ***
<b>2.800*</b>	<b>2.807*</b>		<b>2.807*</b>	2.863*
<b>2.590</b>	<b>2.595</b>		<b>2.593*</b>	2.440*
<b>2.464*</b>	<b>2.470*</b>	<b>2.459*</b>	<b>2.469*</b>	
	2.431			2.337
2.121	2.016	2.130*		2.024
<b>1.904</b>	<b>1.908</b>		<b>1.905*</b>	1.858
<b>1.621*</b>	<b>1.623*</b>		<b>1.620*</b>	1.652
<b>1.503</b>	<b>1.554</b>	<b>1.506*</b>		<b>1.557*</b>
<b>1.474*</b>	<b>1.475*</b>		<b>1.472*</b>	
<b>1.404</b>	1.427			
<b>1.375</b>	1.405		1.403	
<b>1.356</b>	1.377			1.368*
1.299	1.357	1.284	1.335	

\* Represents intense lines. Bold numbers represent d-values matching.

X-ray powder diffraction PDF file reference No. \* 43 – 1004, \*\* 79 – 205, \*\*\* 23 – 1390.

#### 7.4. Ferromagnetism in the System of Mg/Co Oxides

A number of SSC samples were prepared for the identification of new ferromagnetic Mg/Co oxides by taking different molar ratios of MgO : CoO such as 1.0 : 1.0, 1.0 : 4.0 and 2.0 : 1.0 respectively. These SSC samples were examined via X-ray powder diffraction (XPD) (see Figure 4). Here, for the comparison let us consider the SSC sample c) MgO : CoO (molar ratio 2.0 : 1.0). It showed a few lines scattered, prior to

reaction and after reaction (see Figure 4 and for XPD d-values see Table 3). The d-values of XPD for the known compounds CoO, MgO, MgCo<sub>2</sub>O<sub>4</sub> and for the SSC sample c) are shown in Table 4. A comparison of the d-values data of XPD for the SSC sample c) between the known compounds MgO and CoO showed deviations in a few lines (see Table 4).

Further, X-ray powder diffraction showed deviation in many lines between the SSC sample c) and the known spinels, i.e. MgCo<sub>2</sub>O<sub>4</sub> (see Figure 5 and for XPD d-values see Table 4). However, we did not find these lines in agreement with any of the known spinels (Mg<sub>x</sub>Co<sub>2-x</sub>O<sub>4</sub>). Here, one may expect such differences in the diffractograms might be due to starting compositions MgO : CoO (molar ratio 2.0 : 1.0) and for the known spinels, i.e. MgCo<sub>2</sub>O<sub>4</sub>.

An optical microscopic analysis showed that ferromagnetic grains of the SSC sample c), prior to reaction and after reaction changed color from black to pink-gray. The known spinels, i.e. MgCo<sub>2</sub>O<sub>4</sub> showed blackish color and no color change was discussed in the literature. One may expect the change in color (during annealing process) might be due to grains size variation in the ceramic pellets. In such a case the surface of a pellet and grains should produce different colors due to different sizes and shapes. However, reacted pellets were homogenous and reflected uniform pink-gray color.

For the system of Mg/Co oxides, there could be a new ferromagnetic oxides phase.



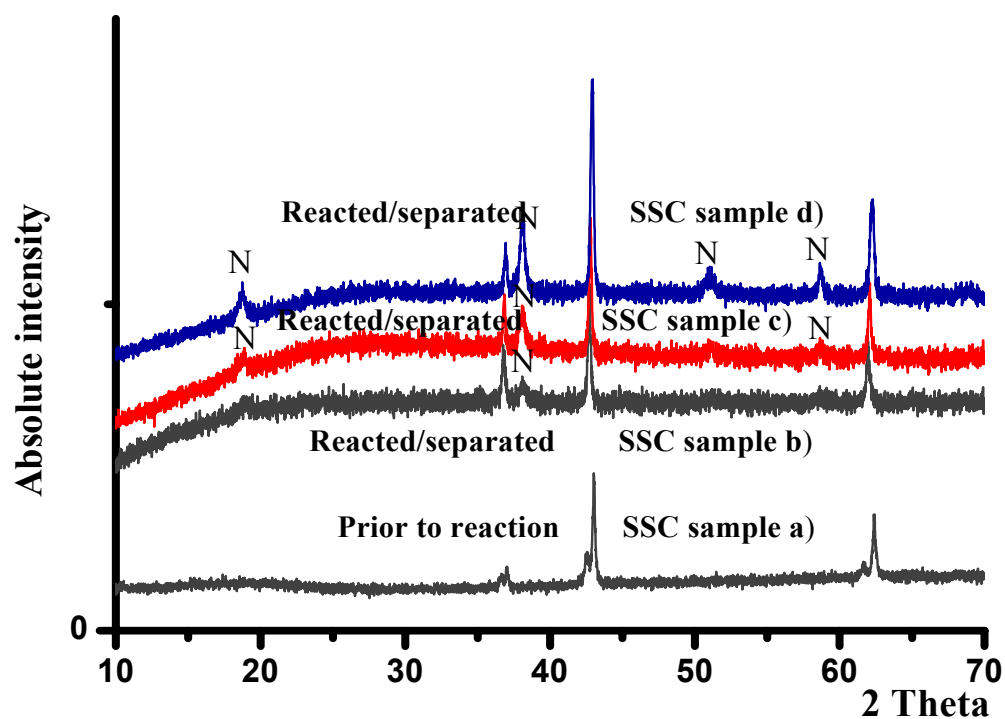


**Figure 4.** Comparison X-ray diffraction patterns for the SSC samples *a)* MgO : CoO (mole ratio 1.0 : 4.0), prior to reaction and for the reacted/separated SSC samples : molar ratios of MgO : CoO for *b)* is 1.0 : 1.0, for *c)* is 2.0 : 1.0 and for *d)* is 1.0 : 4.0. N represents deviated/new lines.

**Table. 3.** The d-values of X-ray powder diffraction for the SSC sample *c)* MgO : CoO (mole ratio 2 : 1), prior to reaction and after reaction.

d-values for the SSC sample <i>c)</i> prior to reaction	d-values for the SSC sample <i>c)</i> after reacted	d-values for the SSC sample <i>c)</i> prior to reaction	d-values for the SSC sample <i>c)</i> after reacted
2.432	2.432		1.572
	2.359*	1.490*	1.490*
2.106*	2.106*		1.358
1.506	1.789	1.272	1.272

\* Represents intense lines. Bold numbers represent d-values matching.

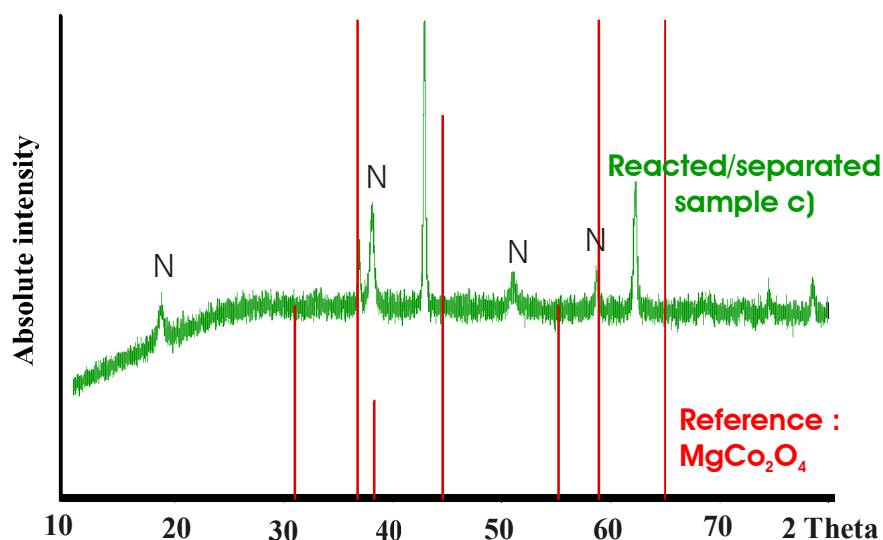


**Figure 5.** X-ray diffraction patterns for the reacted/separated SSC sample *c)* MgO : CoO (mole ratio 2.0 : 1.0) compare with the known spinels, i.e. MgCo<sub>2</sub>O<sub>4</sub> (X-ray powder diffraction PDF file No. 2 - 1073). N represents deviated/new lines.

**Table 4.** The d-values of X-ray powder diffraction of Figure 4, for the known compounds CoO, MgO and MgCo<sub>2</sub>O<sub>4</sub> and for the SSC sample *c)* \* MgO : CoO (mole ratio 2.0 : 1.0).

Observed d-values * for the SSC sample <i>c)</i> prior to reaction	CoO **	MgO ***	Observed d-values * for the SSC sample <i>c)</i> after reaction	MgCo <sub>2</sub> O <sub>4</sub> #
2.432	2.436*	2.432*	2.432	2.880, 2.440 *
2.106*	2.110*	2.106*	2.106*, 2.359*	2.350
1.506	1.492*		1.789	2.030, 1.663
1.490*		1.489*	1.572, 1.490*	1.567*
1.272	1.272*	1.270	1.358, 1.272	

\* Represents intense lines. Bold numbers represent d-values matching.

X-ray powder diffraction PDF files No. \*\* 70 – 2855, \*\*\* 78 – 430, # 2 – 1073.

## 7.5. Reference

- [1] F. J. DiSalvo, *Science* **1990**, 247, 649.
- [2] X. -D. Xiang, X. Sun, G. Briceño, Y. Lou, K-An Wang, H. Chang, W. G. W-Freeman, S-W. Chen, P. G. Schultz, *Science* **1995**, 268, 1738.
- [3] G. Briceño, H. Chang, P. G. Schultz, X. -D. Xiang, *Science* **1995**, 270, 273.
- [4] R. Zallen, *The Physics of Amorphous Solids* J. Wiley and Sons, New York, **1983**.
- [5] K. Petrov, L. Markov, *J. Mater. Sci.* **1985**, 20, 1211.
- [6] K. Krezhov, P. Konstantinov, *J. Phys. Condens. Matter*, **1992**, 4, L543.
- [7] Natl. Bur. Stand. (U.S.) Monogr. **1972**, 25, 60.
- [8] S. Holgersson, A. Karlsson, *Z. Anorg. Chem.* **1929**, 183, 384.
- [9] K. Krezhov, P. Konstantinov, *J. Phys. Condens. Matter*, **1993**, 5, 9287.
- [10] K. Petrov, L. Markov, P. Konstantinov, *J. Phys. chem. Solids* **1989**, 50, 577.
- [11] T. V. Andrushkevich, G. K. Bpreskov, V. V. Popovskil, L. M. Plyasona, L. G. Karacheiev, A. A. Ostankovich, *Kinet. Kat.* **1968**, 9, 1244 (in Russian).
- [12] See Chapter 2.
- [13] See Chapter 3.

## 8. A First Attempt to Obtain Superconductivity by the SSC

### 8.1. Introduction

Superconductivity is a fascinating and challenging field. In order to understand this remarkable phenomenon, significant efforts are in progress to develop materials that could offer superconductivity. A superconductor is a material that exhibits a strong diamagnetism and also exhibits a Meissner effect. This property of superconductors is often demonstrated experimentally by the levitation of a magnet over a superconducting material, as shown in Figure 1.

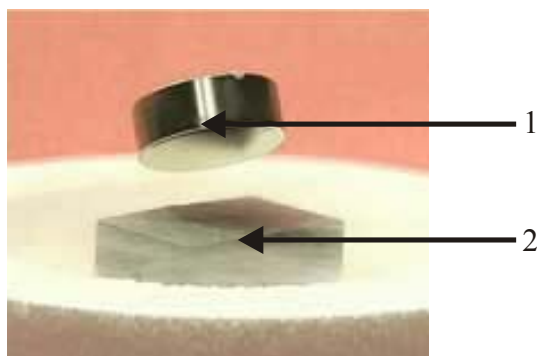


**Figure 1.** A magnet (1) levitates above a ceramic superconducting material (2).

All substances exhibit a *weak* diamagnetism but as a rule of thumb, the onset of a strong diamagnetism in a material is one of the most reliable criteria to ascertain that the material has become superconductive. For last couple of decades several families of superconductors have been discovered with critical temperatures ( $T_c$ ) ranging from 30 – 135 K. However, none of these approaches enabled to achieve a room temperature superconductor. Combinatorial <sup>[1]</sup> approaches have been applied to discover high temperature superconductors (HTS), although the efforts for finding high  $T_c$  superconductors has not yet succeeded. Presently, we are applying a *single sample concept* (SSC): <sup>[2]</sup> a new combinatorial approach to discover high  $T_c$  superconductors.

## 8.2. Diamagnetism of Ceramic Materials

It is commonly difficult to separate and identify strong and weak diamagnetic grains in ceramic materials. However, one still needs a clarification. <sup>[3]</sup> In this case different diamagnetic grains of different sizes and shapes might show a different Meissner effect as well as different diamagnetic properties, which correspond to different chemical properties of the materials.

For the diamagnetic properties identification, different techniques are commonly employed such as a four-probe electrical resistance measurements, diamagnetic susceptibility, electron-spin resonance spectroscopy, tunneling and neutron scattering measurements.

The diamagnetic behavior of powder and bulk samples was discussed in the literature <sup>[3 - 6]</sup> and the data with high resolution were reported <sup>[3]</sup> for powdered  $\text{YBa}_2\text{Cu}_3\text{O}_{7-x}$ . In these measurements, <sup>[3]</sup> a sensitive magnetometer was used which succeeded to some extent to distinguish good from poor diamagnetic grains at  $\sim 77$  K. The magnetic field  $B_y$  at the position of levitation, generated with an electromagnet, could be changed continuously (from  $\sim 0$  G to 1200 G).

In addition to above ones, the following characterize of the magnetometer :

- 1) A vertical gradient  $\frac{\partial B}{\partial z}$  could be adjusted by variation the magnetic field ( $B_y$ ) from 0 – 30 kG/cm. Two gradients as low as 7 and 4.7 kG/cm could be obtained simply by changing the distance between the pole caps of the electromagnets. In this way it was possible to levitate the same piece of a bulk diamagnetic material at different values of the magnetic field.
- 2) The operation in a high field gradient and changing the current in the electromagnet, the levitometer is acting as a spectrometer, i. e. selecting grains of a different magnetization.
- 3) The levitation was taken place in a region (the “levitation chamber”, kept at liquid  $\text{N}_2$  temperature) in which the levitating object was in contact only with He (g), the thermal exchange gas.

Diamagnetic grains of about 4  $\mu\text{m}$  in diameter showed levitation effects under strong magnetic field gradients. Stable levitation conditions for a diamagnetic piece of matter were calculated by applying following Equation <sup>[3]</sup> :

$$mg = \mu \frac{\partial B}{\partial z}$$

Here,  $m$  is the mass of the object,  $g$  is the gravity acceleration,  $\mu$  is the magnetic moment of the levitating grains,  $\frac{\partial B}{\partial z}$  is a vertical magnetic field gradients at the position of levitation.

On the bases of these experimental observations it was reported that also smaller size (1 – 3  $\mu\text{m}$ ) superconducting grains were found within the collection of levitated grains. <sup>[3]</sup> However, magnetic field effects showed a little influence on diamagnetic grains with the size larger than 5  $\mu\text{m}$ . In case when different sizes and shapes of grains are present in a bulk sample, it may be possible that some non-diamagnetic grains are also collected along with the levitated diamagnetic grains.

A number of different elements (oxides/carbonates) are normally considered for the SSC syntheses. These different elements might be possible to produce different grains of different sizes and shapes within a system. These grains might show different chemical and diamagnetic properties. Hence, it is also more difficult to separate strong diamagnetic particles from weak ones.

### **8.3. Superconducting Critical Behavior**

Why do some materials show superconductivity? The Bardeen-Cooper-Schrieffer (BCS) <sup>[7]</sup> microscopic theory suggests that electrons team up in a “Cooper pairs” in order to help each other to overcome molecular obstacles, such as phonon mediated coupling due to the generation of wave packets by flexing of the crystal lattice. At below  $T_c$  a macroscopic condensation (quantum state) take place where paired electrons are formed that move without resistance. However, only a small fraction of the electrons are paired-up and the bulk does not qualify as being a "Bose-Einstein condensate" <sup>[8]</sup> (collapse of the

atoms into a single quantum state). BCS theory assumes that superconductivity is associated only with the electron-phonon interactions. But, BCS theory seems unsuitable to predict high temperature superconductivity in the class of HTS oxide materials.

Recently, hole theory<sup>[9]</sup> describes the fundamental mechanism of superconductivity from the interaction of a hole within the outer electrons in an atom. The hole theory asserts that superconductivity only occurs when hole carriers exist in the normal state of a metal. A hole exists in the absence of an electron and hole carriers exist when an electronic energy band of an atom is almost full. In a full band a hole has a difficulty to propagate due to disruption that it causes in its environment. Thus, superconductivity occurs due to the pairing of hole carriers, and is driven by the fact that paired holes can propagate more easily having a smaller effective mass than single hole.

Further more, the hole theory predicts that when a metal enters into a superconducting state, a negative charge is expelled from its interior to the surface. A superconductor at ground state is predicted to have a non-homogeneous charge distribution than an electric field in its interior. As a consequence their kinetic energy is lowered. So, single electrons can move easily and they don't pair-up. The “dynamic Hubbard model” describes the different physics of electron and hole carriers in a metal. The different mobility of holes and electrons can be illustrated by a garage analogy. The reason for the increase mobility of holes upon pairing is that they undress during pairing up and turn into electrons. This new understanding of superconductivity is that a superconductor is a giant atom. If hole theory would be correct, then it implies that the electron-phonon interaction is irrelevant to superconducting behavior. However, there are experiments clearly showing that phonons play a significant role in superconductivity.

### **8.3.1. Critical Parameters for Superconductivity**

A critical behavior of the superconducting state is defined by three parameters, such as critical temperature ( $T_c$ ), critical field ( $H_c$ ) and critical current density ( $J_c$ ). Each one of them is dependant on the other two properties present in the superconducting materials. The superconducting states  $T_c$ ,  $H_c$  and  $J_c$  should remain below such critical values. These critical values depend on the characteristic of superconducting material.

Higher  $H_c$  and  $J_c$  values are affected through the magnetic penetration ( $\lambda$ ) and coherence length ( $\xi_0$ ). The magnetic penetration refers to an exponential decay of the magnetic field at the surface of superconducting material. In conventional superconductors magnetic penetration related with transition temperature, and in case of high transition temperature the magnetic penetration decrease in the superconducting materials. <sup>[10]</sup>

In case of conventional superconductors the magnetic penetration is related to the transitional temperature and if the transitional temperature is large enough, then the magnetic penetration will be lower. <sup>[10]</sup> On the other hand, if magnetic penetration is infinite, then the material will be in a non-superconducting state (normal state). Thus, applied magnetic field will penetrate into the material that means high magnetic penetration can destroy the superconducting behavior of the superconducting materials.

The coherence length ( $\xi_0$ ) is related to the Fermi velocity of the material and the energy gap with the condensation to the superconducting state. It is a fact that electron density cannot change quickly when there is a minimum change in the coherence length. For example, transition from the superconducting state to a normal state will have a transition layer of infinite thickness, which is related to coherence length. The ratio of the magnetic penetration ( $\lambda$ ) and coherence length ( $\xi_0$ ) is known as the Ginzburg-Landau parameter. If this value is greater than 0.7, then complete flux exclusion is no longer favorable and flux is allowed to penetrate into the superconductor through cores known as vortices. The current is swirling around the normal cores and generates a magnetic field parallel to the applied field. The magnetic moments repel each other and move to arrange themselves in an order known as a fluxon lattice. This kind of mixed phase helps to preserve superconductivity in between higher critical field ( $H_{c2}$ ) and lower critical field ( $H_{c1}$ ), see Figure 2. It is important to note that these vortices do not move in response to magnetic field if superconductors are carrying a large current. The field penetration causes normal metallic regions within the superconductor known as vortexes. There are wide regions of magnetic field strengths where the superconductivity and vortexes coexist (mixed state) in the superconducting materials and zero resistance continues to be displayed as long as vortexes are not moved.



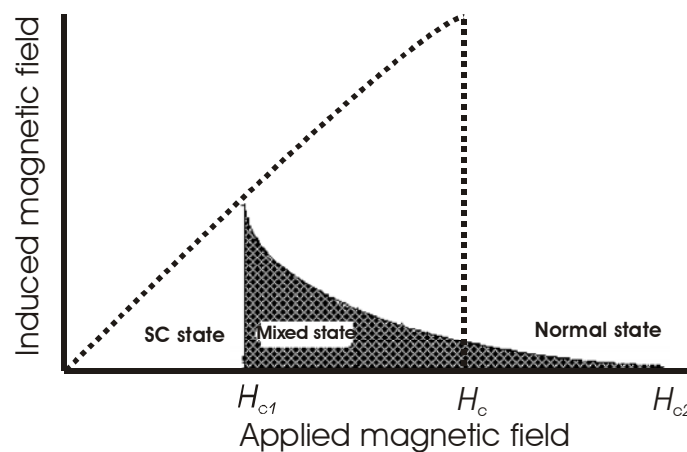


**Figure 2.** Superconducting behavior (normal state, mixed state and superconducting state) of oxide materials with respect to critical magnetic field.

#### 8.4. Four-Probe Technique for Electrical Resistance Measurements

The four-probe electrical resistance measurement is a most common method to determine  $T_c$  of a superconducting ceramic material; where four wires are connected to a material at four points with a conductive adhesive such as silver paste. A voltage is applied through two of connected points and if the material is conductive, then current will flow through the material. If any resistance exists in the material a voltage will appear across the other two points in accordance with Ohm's law. When the material enters into a superconductive state, its resistance drops to zero and no voltage can be measured across the second set of points. By applying four-points method resistance in the adhesive and wires can be neglected. As the second set of points does not conduct any current and therefore only show the voltage, that appear across the bulk surface of a material.

### 8.5. Cryostat (Leybold : RGS 20) : Instrumentation

The cryostat is a major part of the equipment for four-probe electrical resistance measurements to provide a variable temperature range. In our laboratory we have instrumented a cryostat (Figure 3), which has the ability to attain temperature down to 10 K.

A ceramic sample (diameter  $\sim 0.75 - 1.50$  cm, thickness  $\sim 0.1 - 0.25$  cm) could be connected directly with four vertical sharp needles (rhodium/nickel material coated with gold, Figure 3). Gold prohibits oxidation between contacts and no need to apply large force for good contact formation. The needles were adjusted vertically within a hard insulating spherical plate (Glass Epoxy : FR 4) and connected to the surface of a ceramic sample. To avoid resistance of the conductive adhesive, four vertical needles might be the best choice for four-points electrical resistance measurements.

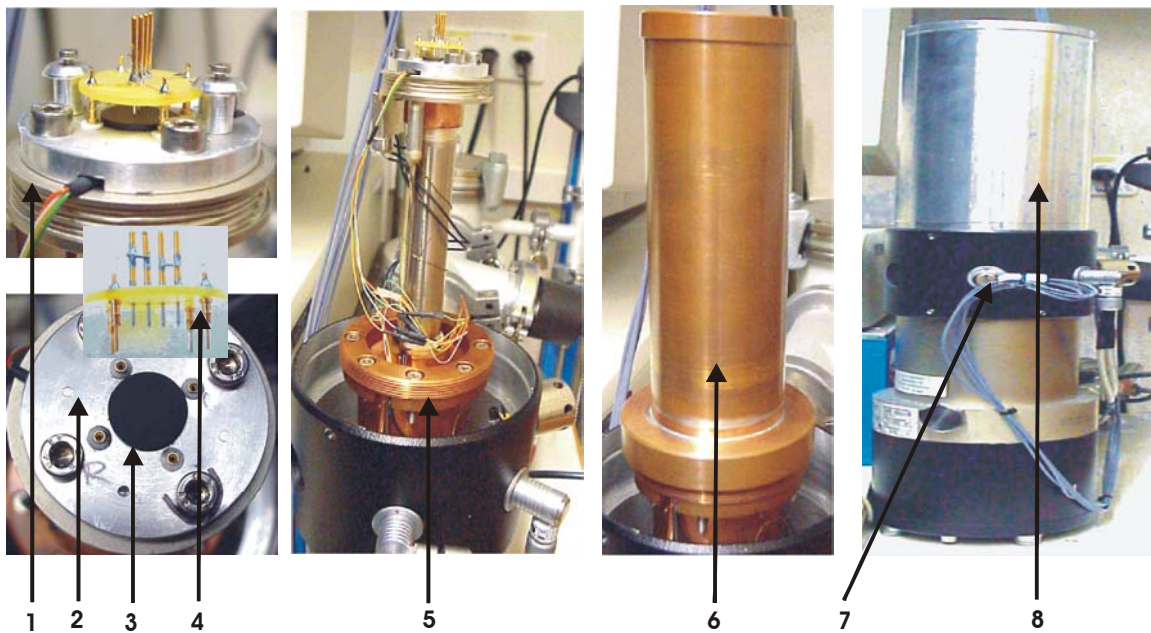


**Figure 3.** Different connections parts such as 1) is a cryostat (Leybold : RGS 20) cooling head, 2) silver plate for adjustment of a ceramic sample, 3) ceramic sample, 4) needles (i.e. Glass Epoxy FR 4), 5) cryostat lower part, 6) primary column, 7) four-wire connections and 8) is a secondary column.

The cryostat cooling head was made of aluminum. A silver plate was tightly adjusted on the top of the cooling head. An insulator material of sapphire plate (diameter  $\sim 1.5$  cm, thickness  $\sim 0.01$  cm) was used to prevent thermal conductivity and was placed between the ceramic sample and the cooling head. Further, connections were made to the source meter (Keithley : Series 2400), for four-probe electrical resistance measurements. The cryostat head was covered with a primary column of copper (internal diameter  $\sim 5$  cm) and a secondary column of aluminum (internal diameter  $\sim 5.0$  cm) for vacuum system. A vacuum of  $10^{-5}$  m bar should create in the cryostat before operation through primary and secondary vacuum pumps. (A radial seal ensures *vacuum-tight* connections were applied.)

The compressor (Leybold : RW 2, RW 3) should require a pressure of about 16 bar before and 22 bar during operation for best operation. A continuous flow of water within the compressor was created to cool the engine. [The cryogenerator operates in a closed pure helium gas cycle according to Gifford-McMahon principle.] A computer was connected to the ohmmeter and also with a low temperature controller (Leyold : LTC 60). The overall instrumental adjustment is shown in Figure 4.

The data was recorded automatically by using Lab-view program, which was installed in the computer (Dell Optiplex : GX 200) and the Lab-view diagram, as shown in Figure 5. A superconducting sample of a nominal starting composition of  $0.5\text{Y}_2\text{O}_3$ ,  $2.0\text{BaO}_2$ ,  $3.0\text{CuO}$  (YBCO) was synthesized by using the same experimental procedure as described in section 8.6. A sample pellet (diameter  $\sim 1.0$  cm, thickness  $\sim 0.2$  cm) was adjusted for four-probe electrical resistance measurements. The electrical resistance data was recorded, as shown in Figure 6. Various samples of YBCO with different diameter and thickness were tested and showed approximately the same resistance impact. The present instrumented cryostat equipment has an ability to measure an electrical resistance through four-probe technique for the superconducting samples having diameter  $\sim 0.75 - 1.50$  cm and thickness  $\sim 0.1 - 0.25$  cm.

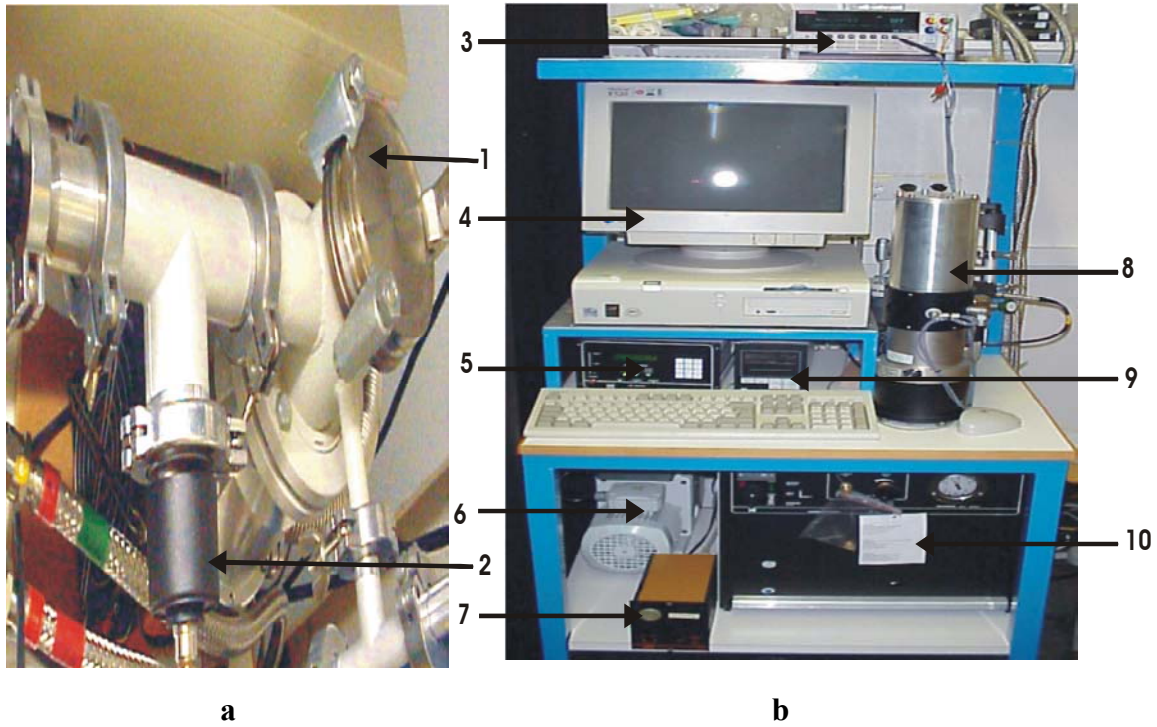


**Figure 4.** An overall cryostat connection is represented by *a)* and *b)*. Here, 1) is a secondary vacuum pump, 2) primary and secondary gage for vacuum reading, 3) source meter (Keithley : 2400), 4) computer, 5) low temperature controller (Leyold : LTC 60), 6) primary vacuum pump (Edwards : 12), 7) CIT aktatel : CFF 100 (for secondary pump operation), 8) cryostat, 9) vacuum reader LH combivac : CM 31 and 10) is a compressor (Leybold : RW 2, RW 3).

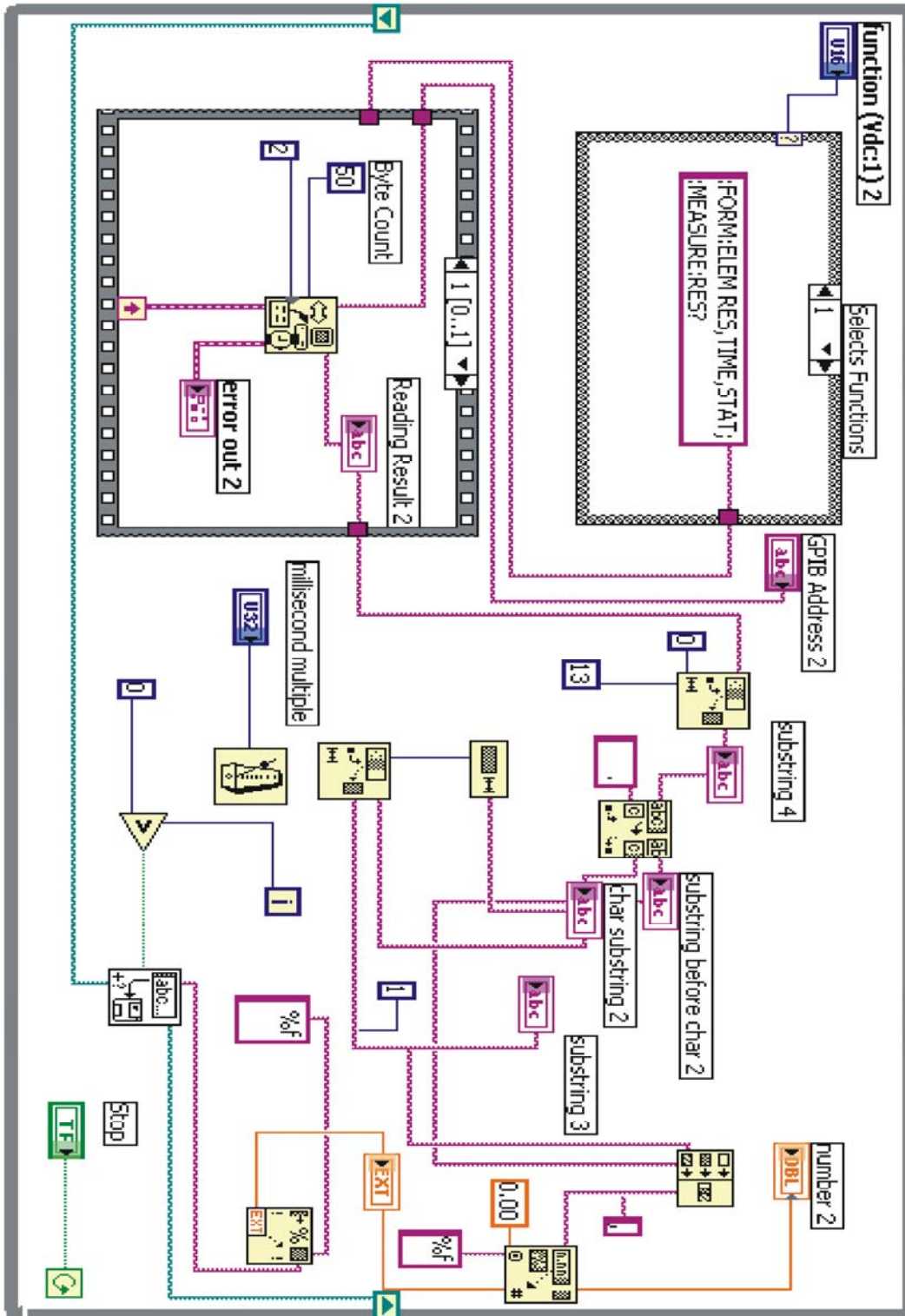


**Diagram 5.** Schematic view of a Lab-view program for automatic resistance measurement control through Keithley source meter (series 2400).

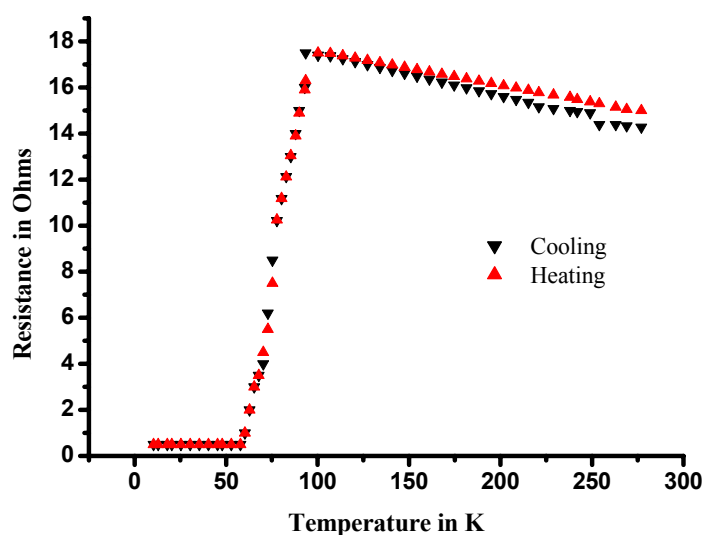


**Figure 6.** Electrical resistance curve (up and down measurements) obtained for test sample  $\text{YBa}_2\text{Cu}_3\text{O}_x$  by using four-probe technique with present cryostat set up.

## 8.6. Combinatorial Synthesis for Oxide Superconductive Materials

In the present combinatorial synthesis emphasis was placed on elements that commonly occur in cuprate superconductors: Oxides /carbonates of B, Ca, Cu, Sr, Y, Ba, La Tl, Pb and Bi were used. Copper was selected as a *lead* element because of its dominant role<sup>[11-12]</sup> for high  $T_c$  compounds.

The SSC experimental procedure is as follows:

- a) A nominal starting composition of  $0.125\text{Y}_2\text{O}_3$ ,  $1.0\text{BaO}_2$ ,  $0.25\text{PbCO}_3$ ,  $1.81\text{SrCO}_3$ ,  $1.36\text{CaCO}_3$ ,  $0.125\text{Tl}_2\text{O}_3$ ,  $0.175\text{La}_2\text{O}_3$ ,  $\text{Bi}_2\text{O}_3$ ,  $4\text{CuO}$  was ball-milled for 1 – 2 h in an excess (70 – 90 vol. %) of isooctane slurry for providing local coordination among oxides. The ball-milled mixture was filtered and dried at room temperature. Ceramic pellets were made at pressure of 7 – 9 t and this pressure was used for 1 – 2 min. by using hydrostatic pressure machine (Perkin : 2445). These ceramic pellets were placed in an aluminum crucible and heat-treated within a quartz glass tube of diameter ~ 3 cm using a furnace (Heraeus : Ro 4/25). A temperature controller (Tecon : 232) was used for

controlling heating and cooling cycles. Combinatorial reactions were performed by applying a maximum temperature ( $T$ ) of about 850 °C for a period of about 4 – 8 h. A heating rate of 150 °C h<sup>-1</sup> and cooling rate of 100 °C h<sup>-1</sup> was used. During annealing, oxygen gas 1 – 2 L h<sup>-1</sup> was continuously flowed at  $P(O_2)$  of about 1 atm.

- b) A second experiment was carried out by selecting a nominal starting composition of 0.12Y<sub>2</sub>O<sub>3</sub>, 0.33B<sub>2</sub>O<sub>3</sub>, 0.10PbCO<sub>3</sub>, 0.50Ti<sub>2</sub>O<sub>3</sub>, 2.0BaO<sub>2</sub>, 1.36CaCO<sub>3</sub>, 4CuO and the same experimental procedure and reaction conditions were applied as described for above a).

Optical microscopy showed that these reacted pellets for both the SSC samples a) and b) were homogenous, hard, brittle and dark black in appearance. A four-probe electrical resistance, a magnetic susceptibility and a low field microwave absorption (LFMA) measurements were recorded.

## **8.7. Results and Discussion**

### **8.7.1. Four-probe Electrical Resistance and SQUID Measurements**

The four-probe electrical resistance and a magnetic susceptibility for the SSC samples a) and b) (see details of these samples in the above Section 8.6) were measured. These measurements were performed at the MPI Stuttgart (group of Prof. A. Simon). Both of these samples a) and b) showed an onset  $T_c$  at about 100 K (see Figures 7a and 8a). The super quantum interference device (SQUID) magnetometer was applied for diamagnetic susceptibility measurements that showing a negative susceptibility for the sample a) which is predominately diamagnetic (see Figure 7b). Contrary, the SCC sample b) showed a positive susceptibility (see Figure 8b). A positive susceptibility in a SCC sample b) confirms a predominant phase being paramagnetism.

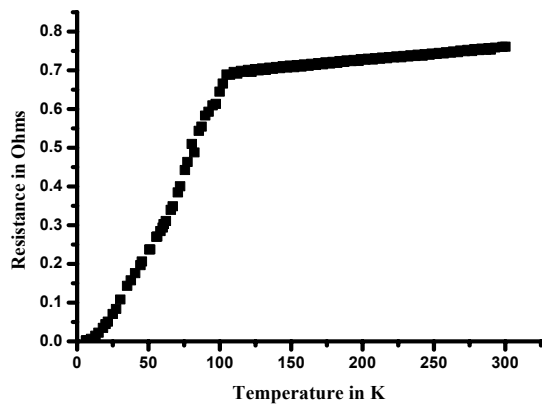


**Figure 7 a.** Electrical resistance curve for a combinatorial mixture of a nominal starting composition of 9 oxides, i.e.  $0.125\text{Y}_2\text{O}_3$ ,  $1.0\text{BaO}_2$ ,  $0.25\text{PbCO}_3$ ,  $1.81\text{SrCO}_3$ ,  $1.36\text{CaCO}_3$ ,  $0.125\text{Tl}_2\text{O}_3$ ,  $0.175\text{La}_2\text{O}_3$ ,  $1.0\text{Bi}_2\text{O}_3$ ,  $4\text{CuO}$ .

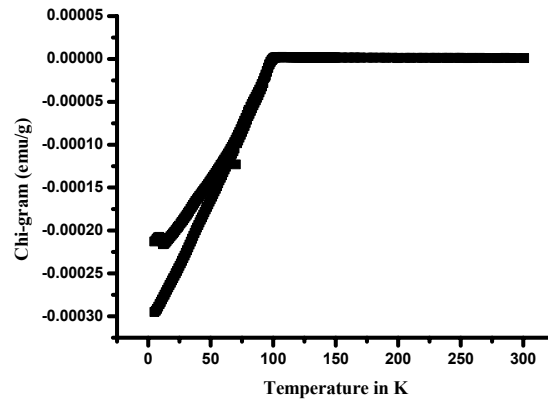


**Figure 7 b.** Diamagnetic susceptibility curve for a combinatorial mixture of a nominal starting composition of 9 oxides, i.e.  $0.125\text{Y}_2\text{O}_3$ ,  $1.0\text{BaO}_2$ ,  $0.25\text{PbCO}_3$ ,  $1.81\text{SrCO}_3$ ,  $1.36\text{CaCO}_3$ ,  $0.125\text{Tl}_2\text{O}_3$ ,  $0.175\text{La}_2\text{O}_3$ ,  $1.0\text{Bi}_2\text{O}_3$ ,  $4\text{CuO}$ .

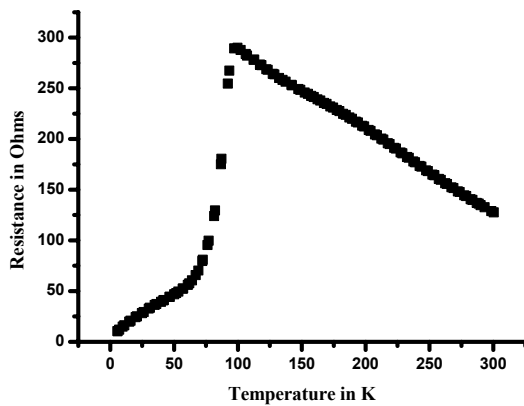


**Figure 8 a.** Electrical resistance curve for a combinatorial mixture of a nominal starting composition of 7 oxides, i.e.  $0.12\text{Y}_2\text{O}_3$ ,  $0.33\text{B}_2\text{O}_3$ ,  $0.10\text{PbCO}_3$ ,  $0.50\text{Tl}_2\text{O}_3$ ,  $2\text{BaO}_2$ ,  $1.36\text{CaCO}_3$ ,  $4\text{CuO}$ .

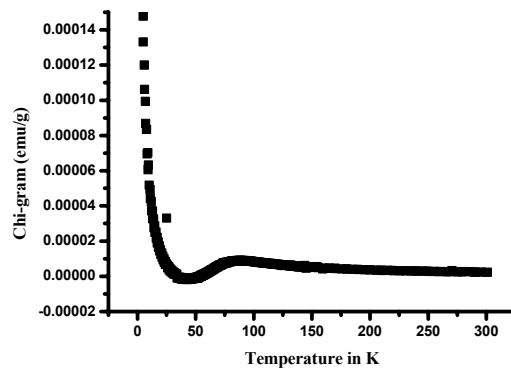


**Figure 8 b.** Magnetic susceptibility curve for a combinatorial mixture of a nominal starting composition of 7 oxides, i.e.  $0.12\text{Y}_2\text{O}_3$ ,  $0.33\text{B}_2\text{O}_3$ ,  $0.10\text{PbCO}_3$ ,  $0.50\text{Tl}_2\text{O}_3$ ,  $2\text{BaO}_2$ ,  $1.36\text{CaCO}_3$ ,  $4\text{CuO}$ .



In our group, A. Gaschen (diploma student, 2001) has synthesized superconducting materials by applying the same combinatorial procedure. In her experiments, she selected the same elements as we were taken for the sample a) but with other nominal starting compositions, e.g.  $0.5\text{Y}_2\text{O}_3$ ,  $2.0\text{BaO}_2$ ,  $1.0\text{PbCO}_3$ ,  $1.0\text{SrCO}_3$ ,  $3.0\text{CaCO}_3$ ,  $1.0\text{Tl}_2\text{O}_3$ ,  $1.0\text{La}_2\text{O}_3$ ,  $0.5\text{Bi}_2\text{O}_3$ ,  $5\text{CuO}$  etc. and found superconductivity at an onset  $T_c$  near about 100 K.

X-rays powder diffraction (XPD) was performed for the sample a) prior to reaction and after reaction. A comparison of the d-values of XPD for the sample a) prior to reaction and those of the known compounds allowed to see that all elements which were present in the diagram (see Figure 7 C and for the d-values see Table 1). A comparison of XPD for the sample a) prior to reaction and after reaction the d-values of XPD for these samples showed deviations in many lines (see Table 1). Inspection of d-values of XPD between the unreacted and reacted sample a) revealed that starting materials were consumed.

We selected these elements by considering different combinations between them and compared with the known compounds, which were available in X-powder diffraction PDF files. We did not find any known compound (superconductors or non-superconductors), which fully or partially agreed with intense lines for the reacted sample a). However, there were a few superconducting compounds, which showed agreement for some lines (see Table 2).

Here, one might be able to say that starting materials were consumed and all elements of the starting materials were present in the product showing superconductivity. A comparison of the d-values of XPD revealed that there might be a presence of some known or new superconducting oxide phases.

In the same way, we selected elements of the sample b) in different combinations and did not yet find any related compound (available in X-powder diffraction PDF files). For the d-values of XPD for the combinatorial sample b) (after reaction), see Table 3.

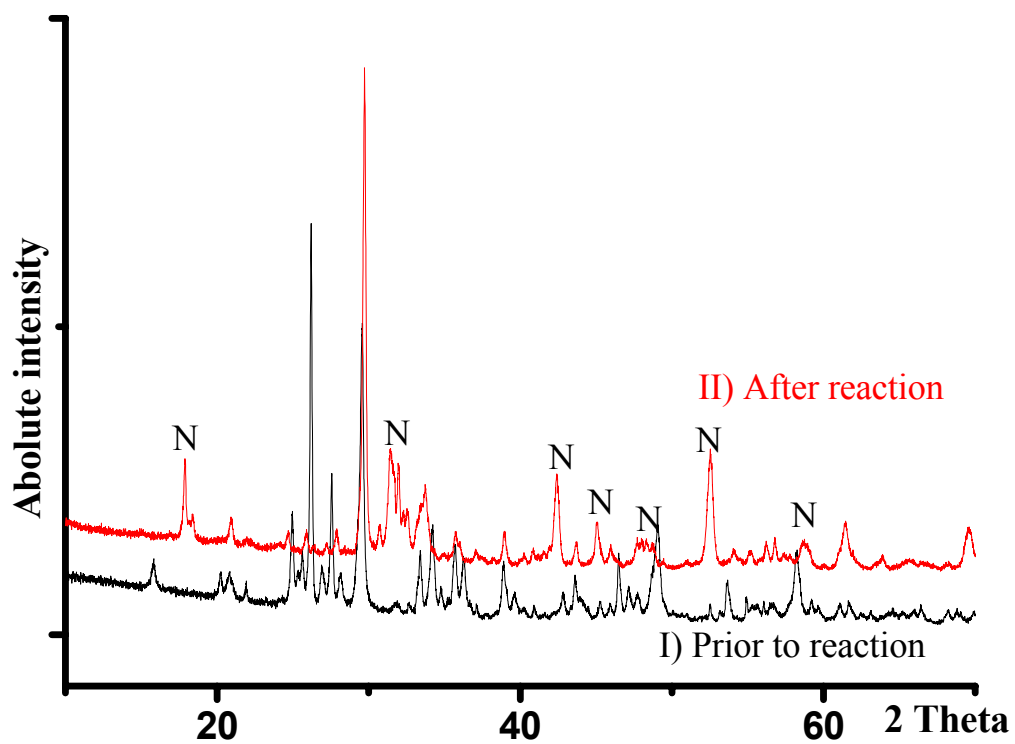


**Figure 7 C.** Comparison X-ray diffraction patterns for the sample a) 9 oxides/carbonates of  $0.125\text{Y}_2\text{O}_3$ ,  $1.0\text{BaO}_2$ ,  $0.25\text{PbCO}_3$ ,  $1.81\text{SrCO}_3$ ,  $1.36\text{CaCO}_3$ ,  $0.125\text{Tl}_2\text{O}_3$ ,  $0.175\text{La}_2\text{O}_3$ ,  $1.0\text{Bi}_2\text{O}_3$ ,  $4\text{CuO}$  I) prior to reaction and II) after reaction. N : New lines.

**Table 1.** The d-values of XPD of Figure 7 C, for the sample a) 9 oxides/carbonates of  $0.125\text{Y}_2\text{O}_3$ ,  $1.0\text{BaO}_2$ ,  $0.25\text{PbCO}_3$ ,  $1.81\text{SrCO}_3$ ,  $1.36\text{CaCO}_3$ ,  $0.125\text{Tl}_2\text{O}_3$ ,  $0.175\text{La}_2\text{O}_3$ ,  $1.0\text{Bi}_2\text{O}_3$ ,  $4\text{CuO}$  prior to reaction and after reaction, and for CuO [PDF file No. 80 – 76],  $\text{La}_2\text{O}_3$  [PDF file No. 22 – 369],  $\text{Y}_2\text{O}_3$  [PDF file No. 43 – 661],  $\text{SrCO}_3$  [PDF file No. 71 – 2393],  $\text{CaCO}_3$  [PDF file No. 86 – 2339],  $\text{Tl}_2\text{O}_3$  [PDF file No. 33 – 14041],  $\text{Bi}_2\text{O}_3$  [PDF file No. 65 – 3319].

d-values for the sample a) prior to reaction	d- values for CuO	d- values for $\text{La}_2\text{O}_3$	d- values for $\text{SrCO}_3$	d- values for $\text{CaCO}_3$	d- values for $\text{Tl}_2\text{O}_3$	d- values for $\text{Bi}_2\text{O}_3$	d-values for the sample a) after reaction
5.967							4.955*
4.386			4.347		4.304		4.238
4.050				3.854*		3.719	
3.563*							3.603
<b>3.513</b>			<b>3.519*</b>				3.437
3.397*							
3.308		<b>3.270*</b>					
3.233*							
3.167				3.039*			3.201
3.018*			2.998*		3.042*	3.036	3.002*
		2.830	2.843	2.853	2.816		2.842*
	2.754		2.822*				2.796
2.744	2.534*						2.769
2.618*			2.583		2.635*	2.630	
<b>2.544</b>	<b>2.540*</b>		<b>2.545*</b>				
2.513	2.524*						2.507
2.475			2.468*	2.492*	2.484		
2.420		2.413	2.436*				2.425
<b>2.313</b>	<b>2.309*</b>						<b>2.310</b>

2.272		2.220		<b>2.283*</b>	2.248		
2.110						2.147	2.129
<b>2.069</b>			2.043*	2.092	<b>2.068</b>		<b>2.069</b>
<b>2.002</b>		<b>2.003*</b>					2.010
<b>1.975</b>			<b>1.973*</b>				<b>1.973</b>
<b>1.926</b>				<b>1.927*</b>			
				1.877	1.863*		1.866
<b>1.855*</b>	<b>1.862*</b>	1.836	1.839		1.808	<b>1.859</b>	1.842
<b>1.740</b>		<b>1.747</b>			1.758	1.753	<b>1.740*</b>
<b>1.722</b>	1.715*						
<b>1.706</b>		<b>1.702*</b>			<b>1.710</b>		
<b>1.670</b>					<b>1.668</b>	1.663	1.662
<b>1.638</b>					1.628		<b>1.634</b>
<b>1.623</b>				<b>1.624</b>			1.619
<b>1.591</b>				<b>1.591</b>			
<b>1.583*</b>	<b>1.583*</b>					1.586	1.571
<b>1.559</b>			<b>1.559*</b>		<b>1.554*</b>		
<b>1.515</b>				<b>1.512</b>	1.522		
<b>1.503</b>	<b>1.506*</b>						<b>1.508</b>
<b>1.471</b>		1.266		<b>1.472</b>	1.491		1.455

---

\* Represents intense lines. Bold numbers represent d-values matching.

**Table 1.** The d-values of XPD for the sample a) 9 oxides/carbonates of  $0.125\text{Y}_2\text{O}_3$ ,  $1.0\text{BaO}_2$ ,  $0.25\text{PbCO}_3$ ,  $1.81\text{SrCO}_3$ ,  $1.36\text{CaCO}_3$ ,  $0.125\text{Tl}_2\text{O}_3$ ,  $0.175\text{La}_2\text{O}_3$ ,  $1.0\text{Bi}_2\text{O}_3$ ,  $4\text{CuO}$  after reaction and for the known compounds I)  $(\text{Tl}_{0.535}\text{Ca}_{0.4})_2\text{Ba}_2(\text{Ca}_{0.9}\text{Tl}_{0.1})(\text{Ca}_{0.85}\text{Tl}_{0.15})_2\text{Cu}_4\text{O}_{11.8}$  [PDF file No. 82 – 1679], for II)  $\text{LaBa}_{1.6}\text{Ca}_{0.4}\text{Cu}_3\text{O}_{6.8}$  [PDF file No. 44 – 303], for III)  $(\text{Tl}_{0.6}\text{Pb}_{0.2}\text{Bi}_{0.2})(\text{Sr}_{1.8}\text{Ba}_{0.2})\text{Ca}_2\text{Cu}_3\text{O}_{9.8}$  [PDF file No. 87 – 1413].

<b>d-values for the sample a) after reaction</b>	<b>d-values for the known compound I)</b>	<b>d-values for the known compound II)</b>	<b>d-values for the known compound III)</b>
<b>3.002*</b>	<b>3.003</b>	3.243	3.058*
2.907	2.970*		
2.842*			
<b>2.769</b>	2.722*	<b>2.761*</b>	
	2.712*		2.704*
<b>2.607</b>	2.627		<b>2.658*</b>
2.507	2.476*		2.553*
2.425	2.335	2.345	2.389*
2.310	2.285		
<b>2.205</b>		2.251	<b>2.206</b>
<b>2.153</b>	<b>2.149</b>		2.188
<b>2.129</b>			<b>2.122</b>
1.973	1.924*	1.961	1.909*
1.866	1.918	1.943*	1.899
1.842	1.890		1.855
<b>1.740*</b>	<b>1.750</b>	<b>1.737</b>	1.788
<b>1.662</b>			<b>1.666</b>
<b>1.619</b>	<b>1.615*</b>	1.595	
1.571	<b>1.569*</b>		1.554*

\* Represents intense lines. Bold numbers represent d-values matching.

**Table 3.** The d-values of XPD for the reacted sample b) 7 oxides/carbonates of  $0.12\text{Y}_2\text{O}_3$ ,  $0.33\text{B}_2\text{O}_3$ ,  $0.10\text{PbCO}_3$ ,  $0.50\text{Tl}_2\text{O}_3$ ,  $2\text{BaO}_2$ ,  $1.36\text{CaCO}_3$ ,  $4\text{CuO}$ .

4.711	4.265*	3.771	3.353*	3.191	3.094	3.028*	2.938*	2.882*	2.772
2.560*	2.401	2.352*	2.271	2.173	1.949	1.888	1.861	1.762	1.696

\* Represents intense lines.

### 8.7.2. EPR Measurements Through Low Field Microwave Absorption

In the literature, <sup>[13 - 16]</sup> electron paramagnetic resonance (EPR) at low microwave field absorption (LFMA) showed signals for a superconducting phase. <sup>[16]</sup>

Portis et al. <sup>[17]</sup> have experimentally observed that there is a convincing evidence for a linear relationship between the signal intensity and the sample surface area if the sample is cooled down to liquid helium temperature near to zero magnetic fields. A resolved low-field microwave absorption line spectrum was reported <sup>[18]</sup> for a single crystal of  $\text{YBa}_2\text{Cu}_3\text{O}_{7-x}$  (see Figure 9).

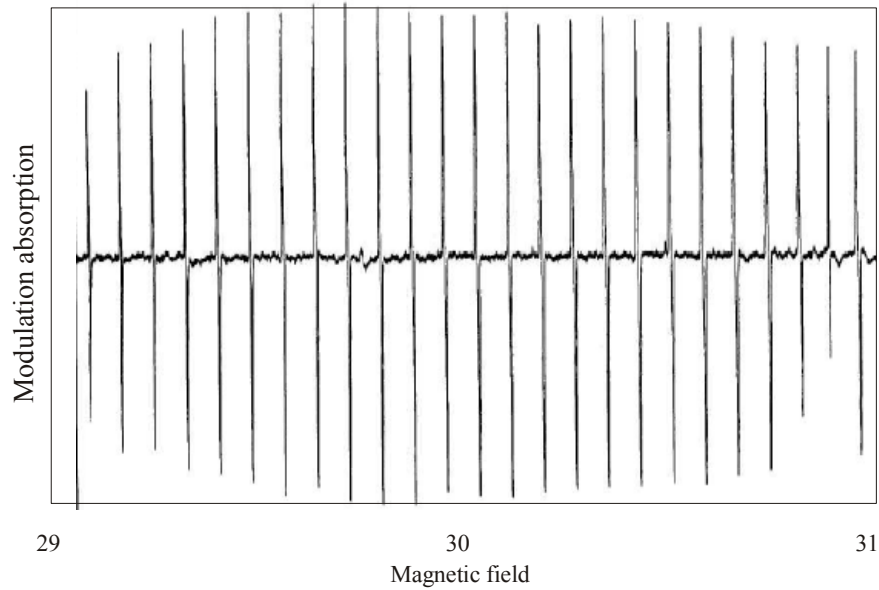


**Figure 9.** A segment of the 9.44 GHz microwave absorption line spectrum of a  $\text{YBa}_2\text{Cu}_3\text{O}_{7.8}$  single crystal between 29 and 31 gauss at 4.31 K. The applied magnetic field is  $\perp \langle c \rangle$  and  $\parallel \langle 110 \rangle$ , and the microwave field  $\parallel \langle c \rangle$ .

The reason for the LFMA signal of a superconducting material is that when a sample is at the normal state ( $T > T_c$ ) it absorbs some of the energy from the electromagnetic field due to the skin effect. In this case the loss of absorption is independent of the applied magnetic field.

Thereafter, no signal can be detected because the signal recorded by the EPR spectrometer is a derivative of  $d\chi/dH$ . However, the superconducting state is affected by the applied external magnetic field and therefore signals can be observed.

A fairly linear region of the microwave response with respect to the modulating field amplitude and the absorption derivative may be interpreted as the number of fluxoids trapped as a function of temperature. When the dc field (H) is swept while the modulation field ( $h_m$ ) direction is parallel (parallel configuration)<sup>[19]</sup> to it, the nature of the absorption below  $T_c$  is simply understood from the fact at above  $T_c$  that there are no fluxoids and maximum absorption occurs. At below  $T_c$  there is decrease in the absorption. Thus, by varying temperature (from above to below  $T_c$ ) one would indeed expect a change in the magnetically modulated microwave absorption signal. The difference in absorption depends on the anisotropy of fluxoid formations. When the dc field (H) is swept while the microwave field ( $h_{rf}$ ) direction is perpendicular (perpendicular configuration)<sup>[19]</sup> to it, the microwave absorption occurs in a superconducting region rather than in the fluxoid region. In the superconducting state, due to a Meissner effect, the loss of absorption decreases obviously when the applied field H approaches to zero, and absorption increases with the increase of H. Therefore, a low field microwave absorption signal is detected near H to zero. The LFMA showed negative sign of the EPR signal, which might also be the indication for the presence of superconducting materials in a sample (see Figures 10 – 12). However, this negative derivative of the EPR signal may not appear for the normal or non-superconducting materials.

Here, the LFMA measurements were recorded by using a spectrometer (Bruker : E 500) at X-band within a super high-Q (SHQ) cavity of parallel arrangement. For each of the LFMA measurements, the EPR tubes were filled with the He(g) and sealed with grains powder of a few milligrams. Liquid helium gas was supplied throughout the experiments for high to low temperature. Thereafter, an EPR tube was adjusted vertically in the center of the SHQ cavity.

Strong LFMA signals were recorded for the samples of YBCO, i.e. a) and b) around zero fields as shown in Figures 10 – 12. The strong LFMA signals for YBCO at 90 – 100 K may be an indication of the presence of large amount of the superconductive phase. The indication of weak signals at about 300 K might be due to the presence of low percentage of diamagnetic phases having very less diamagnetic susceptibility. Strong LFMA signals appeared for the sample a) at  $\sim 100$  K (see Figure 11) and comparatively a weak signals for the sample b) around 100 K (see Figure 12). This comparatively weak signal might be due to the dominant diamagnetic phase in the bulk sample b). Anyhow, on the other hand, the SQUID magnetometer did not show the presence of the diamagnetic phases for the sample b) (see the above Section 8.7.1). This means, the EPR by considering LFMA is considered a sensitive technique for the detection of low percentages of superconducting phases in a ceramic materials.



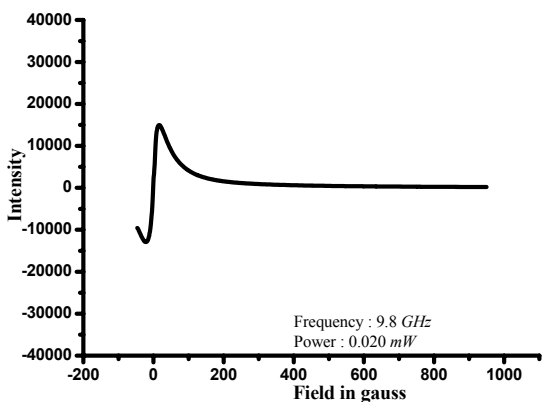


Figure 10 a. EPR signal at 90 K for a sample  $\text{YBa}_2\text{Cu}_3\text{O}_x$ .

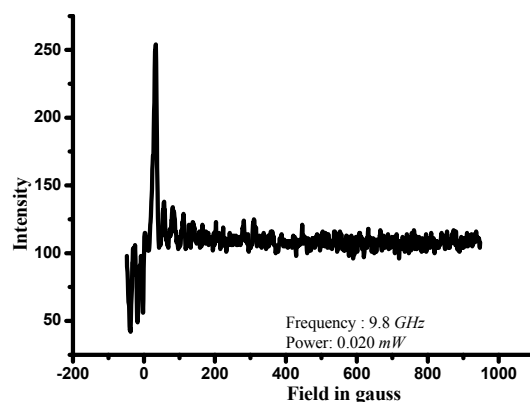


Figure 10 b. EPR signal at 100 K for a sample  $\text{YBa}_2\text{Cu}_3\text{O}_x$ .

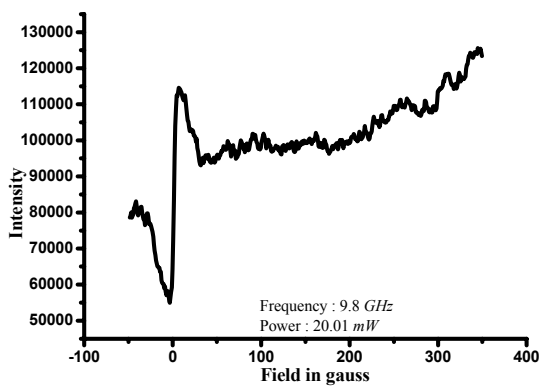


Figure 10 c. EPR signal at 125 K for a sample  $\text{YBa}_2\text{Cu}_3\text{O}_x$ .

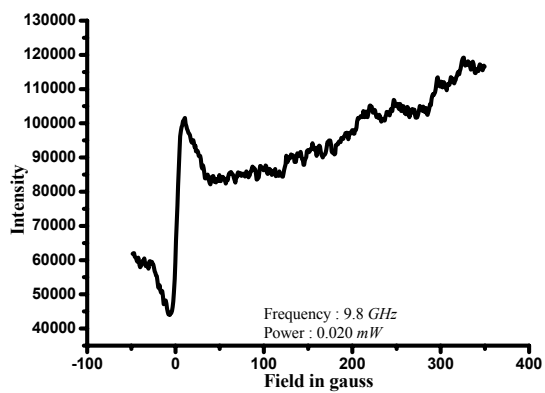
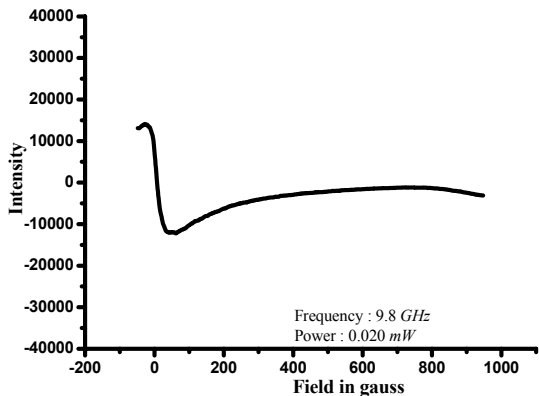
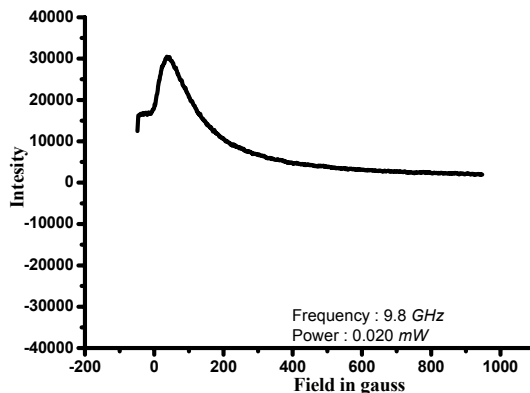


Figure 10 d. EPR signal at 295 K for a sample  $\text{YBa}_2\text{Cu}_3\text{O}_x$ .



**Figure 11 a.** EPR signal at **90 K** for a nominal starting composition of 9 oxides, i.e.  $0.125\text{Y}_2\text{O}_3$ ,  $1.0\text{BaO}_2$ ,  $0.25\text{PbCO}_3$ ,  $1.81\text{SrCO}_3$ ,  $1.36\text{CaCO}_3$ ,  $0.125\text{Tl}_2\text{O}_3$ ,  $0.175\text{La}_2\text{O}_3$ ,  $1.0\text{Bi}_2\text{O}_3$ ,  $4\text{CuO}$ .



**Figure 11 b.** EPR signal at **100 K** for a nominal starting composition of 9 oxides, i.e.  $0.125\text{Y}_2\text{O}_3$ ,  $1.0\text{BaO}_2$ ,  $0.25\text{PbCO}_3$ ,  $1.81\text{SrCO}_3$ ,  $1.36\text{CaCO}_3$ ,  $0.125\text{Tl}_2\text{O}_3$ ,  $0.175\text{La}_2\text{O}_3$ ,  $1.0\text{Bi}_2\text{O}_3$ ,  $4\text{CuO}$ .

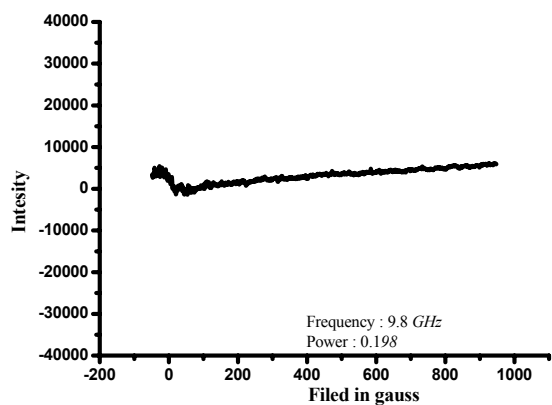


**Figure 12 a.** EPR signal at **90 K** for a combinatorial mixture of a nominal starting composition of 7 oxides, i.e.  $0.12\text{Y}_2\text{O}_3$ ,  $0.33\text{B}_2\text{O}_3$ ,  $0.10\text{PbCO}_3$ ,  $0.50\text{Tl}_2\text{O}_3$ ,  $2\text{BaO}_2$ ,  $1.36\text{CaCO}_3$ ,  $4\text{CuO}$ .

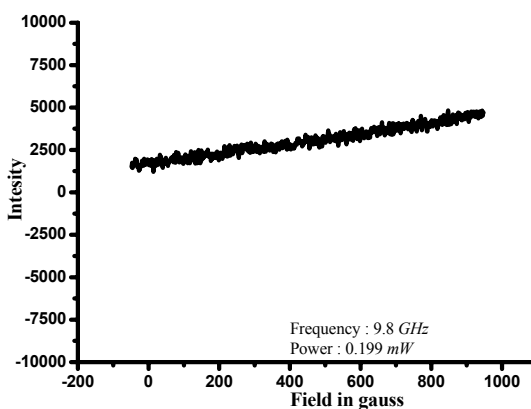


**Figure 12 b.** EPR signal at **110 K** for a combinatorial mixture of a nominal starting composition of 7 oxides, i.e.  $0.12\text{Y}_2\text{O}_3$ ,  $0.33\text{B}_2\text{O}_3$ ,  $0.10\text{PbCO}_3$ ,  $0.50\text{Tl}_2\text{O}_3$ ,  $2\text{BaO}_2$ ,  $1.36\text{CaCO}_3$ ,  $4\text{CuO}$ .

## 8.8. Conclusions

The SSC combinatorial approach was applied by taking *seven* and *nine* metal oxides/carbonates, where copper was selected as a *lead* element. The nominal starting compositions of  $0.12\text{Y}_2\text{O}_3$ ,  $0.33\text{B}_2\text{O}_3$ ,  $0.10\text{PbCO}_3$ ,  $0.50\text{Tl}_2\text{O}_3$ ,  $2.0\text{BaO}_2$ ,  $1.36\text{CaCO}_3$ ,  $4\text{CuO}$  and  $0.125\text{Y}_2\text{O}_3$ ,  $1.0\text{BaO}_2$ ,  $0.25\text{PbCO}_3$ ,  $1.81\text{SrCO}_3$ ,  $1.36\text{CaCO}_3$ ,  $0.125\text{Tl}_2\text{O}_3$ ,  $0.175\text{La}_2\text{O}_3$ ,  $1.0\text{Bi}_2\text{O}_3$ ,  $4\text{CuO}$  showed onset  $T_c$  of about 100 K.

Superconductivity measurement techniques such as the four-probe electrical resistance method, the superconducting interference device (SQUID) magnetometer and the electron spin/pair resonance (ESR/EPR) spectrometer were used for the identification of superconductivity. The EPR by considering LFMA was found a sensitive analysis technique for the detection of a low percentage of superconducting phases in the ceramic materials containing many phases.

## 8.9. References

- [1] X. -D. Xiang, X. Sun, G. Briceno, Y. Lou, K. -A. Wang, H. Chang, W. G. W. - Freedman, S. -W. Chen, P. G. Schultz, *Science*, **1995**, 268, 1738.
- [2] See Chapter 3.
- [3] M. Marinelli, G. Morpurgo, G. L. Olcese, *Physica C*, **1989**, 157, 149.
- [4] M. Barsoum, D. Patten, S. Tyagi, *Appl. Phys. Lett.* **1987**, 51, 1987.
- [5] S. Viera, A. Aguilo, M. Hortal, M. Pazo, *J. Phys. E.* **1987**, 20, 1292.
- [6] S. Labroo, Y. Ebrahimi, J. Y. Park, W. J. Yeh, *IEEE Trans. Magn.* **1992**, 28, 1895.
- [7] J. Bardeen, L. N. Cooper, J. R. Schrieffer, *Phys. Rev B.* **1957**, 122, 124.
- [8] A. S. Alexandrov, N. F. Mott, *Rep. Prog. Phys.* **1994**, 57, 1197.
- [9] a) A. S. Davydov, *Phys. Rep.* **1990**, 190, 191; b) J. E. Hirsch *Phys. Lett. A.* **1989**, 134, 451.
- [10] W. Buckel, *Supraleitung*, VCH, New York, **1990**, P. 123.
- [11] R. Hazen, *Sci. Am.* **1988**, 258, 74.
- [12] V. Emery, K. Kivelson, O. Zachar, *Phys. Rev. B.* **1997**, 56, 1197.
- [13] A. Pöpll, L. Kevan, *J. Chem. Soc. Faraday Trans.* **1993**, 89, 2063.
- [14] F. J. Owens, Z. Iqbal, *Solid State Commun.* **1988**, 68, 523.
- [15] S. V. Bhat, P. Ganguly, C. N. R. Rao, *Pramana -J. Phys.* **1987**, 28, L 425.
- [16] K. W. Blazey, K. A. Muller, J. G. Bednorz, W. Berlinger, G. Amoretti, E. Buluggiu, A. Vera, F. C. Maticotta, *Phys. Rev. B.* **1987**, 36, 7241.
- [17] A. M. Protis, K. W. Balzey, K. A. Mueller, J. G. Bednorz, *Europhys. Lett.* **1988**, 5, 467.
- [18] K. W. Blazey, F. H. Holtzberg, *J. Res. Develop.* **1989**, 33, 324.
- [19] R. Karim, S. A. Oliver, C. Vittoria, A. Widom, G. Balestrino, S. Barbanera, P. Paroli, *Phys. Rev. B.* **1989**, 39, 797.

## 9. Resume

Name : Muhammad Aslam Awan

Place of Birth : Lahore (Pakistan)

### Educational Career

---

Title	Years	Education
<b>Ph.D.</b>		
“Thesis Project”		<b>A New Combinatorial Approach to the Synthesis and Isolation of Ferromagnetic and Superconductor Oxides Materials</b>
	2001 – 2005	Ph.D. Supervisor : <b>Prof. Dr. J. Hulliger</b> , Department of Chemistry and Biochemistry, University of Berne, Switzerland.
<b>M.Sc.</b>		
“Thesis” Project		“Formation of Transparent Thin Film of Metal Oxides on Glass Substrates” Research Supervisor : <b>Prof. Dr. Istiaq Hussain</b>
	1993 – 1996	M. Sc in Chemistry, Major Subjects : Inorganic, Organic, Physical, and Applied Chemistry. Institute of Chemistry, University of the Punjab, Pakistan.
<b>B.SC</b>		
	1991 – 1992	Major Subjects : Inorganic, Organic and Physical Chemistry, Modern Physics, Mechanics Physics, Thermodynamics, Wave and Oscillations Physics, Mathematics (Calculus, Trigonometry, etc.). Government F. C. College, Lahore, Pakistan.

---

## Academic Courses

- 1) Attend *MaNEP course on Materials with Novel Electronic Properties*, from 6 – 11 Sept. **2004**, Saas-Fee, Switzerland.

## Experience

- 1) Teaching assistant in the group of Prof. Hulliger, from **2001 – 2005**, Department of Chemistry and Biochemistry, University Berne, Switzerland.
  - Practical of Combinatorial Chemistry, Magnetic Chromatography and Phase Diagrams etc. for AC-II (advance undergraduate) Students.
- 2) Internship at “Research Development & Quality Control” Department of Packages, Lahore, from **1995**, Pakistan.
- 3) Teaching the undergraduate students, from **1997 – 1998**, Lahore, Pakistan.

## Administration Position

President “*Speers Chemical Society*”, from **1991 – 1992**, Government Forman Christian College, Lahore, Pakistan.

## Publications

- 1) Chemical Diversity in View of Property Generation by a New Combinatorial Approach.  
J. Hulliger, M. A. Awan, B. Trusch, T. A. Samtlebe, *Z. Anorg. Allg. Chem.* **2005**, 631, 1255 - 1260.
- 2) “Single Sample Concept” (SSC) :  
Theoretical Model for a New Combinatorial Approach to Solid-State Materials.  
J. Hulliger, M. A. Awan, *J. Comb. Chem.* **2005**, 7, 73 - 77.
- 3) A “Single Sample Concept” (SSC) :  
New Combinatorial Chemistry of Inorganic Materials.  
J. Hulliger, M. A. Awan, *Chem. Eur. J.* **2004**, 10, 4694 - 4702.

- 4) Magnetic Chromatography and Ceramic Synthesis :  
a New Combinatorial Approach for Finding Ferri-/Ferromagnetic Materials.  
J. Hulliger, M. A. Awan, B. Trusch, *Z. Anorg. Allg. Chem.* **2004**, 630, 1689.

### **Presentations and Posters**

- 1) Presented at *Inorganic Combinatorial Workshop*, Downing College, Cambridge, UK.  
J. Hulliger, M. A. Awan, B. Trusch, 3 – 4 March. **2005**.
- 2) Presented at 12. Fachgruppentagung zum Thema “*Festkörperchemie and Materialforschung*”, Philipps-University, Marburg, Germany  
J. Hulliger, M. A. Awan, B. Trusch, 13 – 15 Sept. **2004**.
- 3) Presented at *1st BENEFRi Material Day*, Fribourg, Switzerland  
J. Hulliger, M. A. Awan, 27 June **2003**.
- 4) Poster at *1st BENEFRi Material Day*, Fribourg, Switzerland  
M. A. Awan, J. Hulliger, 27 June **2003**.
- 5) Presented at *Third International Conference Inorganic Material*, Konstanz, Germany  
J. Hulliger, A. Gaschen, M. A. Awan, 7 – 10 Sept. **2002**, abstract, p. O 40.